

Morphological and Structural Analysis of
Cellulose Microfibrils Using Enzymatic Treatment

(酵素処理を用いたセルロースマイクロフィブリルの
形態および構造の解析)

林 徳子

**Morphological and Structural Analysis
of Cellulose Microfibrils
Using Enzymatic Treatment**

(酵素処理を用いたセルロースマイクロフィブリルの形態および構造の
解析)

林 徳子

General Introduction1
----------------------	--------

Chapter 1. Features of cell walls in the xylem developing zone of hardwood and softwood after enzymatic hydrolysis

1. Introduction7
2. Materials and Methods	
(1) Samples8
(2) Microscopic observation8
(3) Enzymatic hydrolysis of ultrathin sections9
3. Results	
(1) Tracheid walls of Sugi and Akamatsu 10
(2) Shirakamba	
1) Wood fiber walls13
2) Vessel walls16
(3) Buna17
4. Discussion19
5. Summary21

Chapter 2. Enzymatic hydrolysis of autohydrolyzed softwood followed by ozone treatment

1. Introduction22
2. Experimental	
(1) Pretreatment of samples23
(2) Treatment with ozone24
(3) Enzymatic hydrolysis24
(4) General analysis25

3. Results	
(1) Treatment of wood-meals with ozone26
(2) Treatment of autohydrolyzed woods with ozone29
(3) Characterization of the samples treated with ozone before and after enzymatic treatment31
4. Discussion35
5. Summary39

Chapter 3. Influence of aggregation of microfibrils on enzymatic hydrolysis of crystalline cellulose of cotton-ramie type

1. Introduction40
2. Experimental	
(1) Substrates42
(2) Enzymatic hydrolysis42
(3) Observation by TEM43
(4) X-ray diffraction and electron diffraction43
(5) Solid-state CP-MAS ¹³ C-NMR43
3. Results	
(1) Features of Avicel residues after treatment with large quantity of cellulase44
(2) Features of Avicel residues after cellulase treatment over a long period of time47
(3) Features of <i>Halocynthia</i> cellulose and cotton linter pulp residues after cellulase treatment over a long period of time48
4. Discussion51
5. Summary54

Chapter 4. Enzymatic susceptibility of cellulose microfibrils of the algal-bacterial type and the cotton-ramie type

1. Introduction55
2. Experimental	
(1) Substrates57
(2) Enzymatic hydrolysis57
(3) Hydrothermal treatment58
(4) Observation by TEM58
(5) FTIR spectral analysis59
(6) X-ray diffraction and electron diffraction59
3. Results60
4. Discussion61
5. Summary69

Chapter 5. Selective degradation of cellulose I_α component in some *Cladophora* cellulose with *Trichoderma viride* cellulase

1. Introduction70
2. Experimental	
(1) Substrates72
(2) Enzymatic hydrolysis72
(3) Observation by TEM73
(4) FTIR spectral analysis73
3. Results74
4. Discussion83
5. Summary86

Chapter 6. Characterization of short microfibrils in native *Cladophora* cellulose produced by enzymatic hydrolysis

1. Introduction87
-----------------	---------

2. Experimental	
(1) Substrates88
(2) Enzymatic hydrolysis88
(3) Acid hydrolysis89
(4) Determination of molecular weight90
(5) General analysis90
3. Results91
4. Discussion96
5. Summary 100

Chapter 7. Characterization of I β crystalline domain in native *Halocynthia* cellulose by analyzing the enzymatically hydrolyzed residues

1. Introduction 101
2. Experimental	
(1) Substrates103
(2) Enzymatic hydrolysis103
(3) Observation by TEM104
(4) FTIR spectral analysis104
3. Results104
4. Discussion109
5. Summary111
General Conclusion112
Acknowledgment117
References119

General Introduction

Cellulose is one of the most famous polymer in the world because it has intimately been connected with the history of man. Furthermore, cellulose is the most abundant biopolymer on earth. It is estimated that at least 10^9 tons [Coughlan, 1985] or 10^{11} tons [Hess, 1928] of cellulose are produced and destroyed annually. Therefore, it is worthwhile to clarify the cellulose degradation in the global carbon cycle in which microorganisms play an important role.

In catalyzing the digestion of crystalline cellulose, cellulolytic fungi such as *Aspergillus* sp., *Penicillium* sp., *Schizophyllum* sp., *Trichoderma* sp. *Phanerochaete chrysosporium* and *Humicola*, possess their individual and excellent cellulase systems. *Trichoderma reesei* in particular has been exploited for cellulase production. It is well characterized that *Trichoderma* cellulase is a complex mixture of three main types of enzymes with different specificity in hydrolyzing glycosidic bonds. The three main cellulase enzymes are: endo-cellulase (1,4- β -D-glucan-4-glucanohydrolase, endo-1,4- β -glucanase, EG), exo-cellulase (1,4- β -D-glucan-cellobiohydrolase, CBH) and β -glucosidase (β -D-glucosidoglucohydrolase, cellobiase). The predominant enzyme component is an exo-cellulase (CBH I) which amounts to 60% of the secreted cellulase protein [For example, Goyal et al., 1991].

The enzymatic hydrolysis of cellulose, particularly hydrogen-bonded and ordered crystalline cellulose, is a very complex process. As the cellulose is insoluble, the cellulases must diffuse and fit themselves to the structural feature of the substrate. The mechanism of the enzymatic degradation of crystalline cellulose has been investigated by many researchers. Historically, Reese et al. [1950] assumed the existence of C1 and Cx components and supposed that the C1 component acts on cellulose to shorten linear poly-anhydroglucose chains, and then Cx component

degrades them to soluble small molecules and finally the small molecules are degraded to glucose by β -glucosidase. The hydrogen bondase and swelling factor were also considered as one of the C1-cellulase reactions [Marsh et al., 1953; Reese & Gilligan, 1954; King & Lee, 1967]. The findings that cellobiohydrolases acted synergistically with Cx enzymes led to the formulation of the endo/exo cooperation to degrade the crystalline cellulose [Wood & McCrae, 1972]. Thus, the current consensus on the cellulolysis by enzymes is as follows: endo-1,4- β -glucanase (EGs) initially attack the amorphous region of cellulose microfibril to generate multiple sites for attack by CBHs, and continue to act synergistically with exo-, and endo-type enzymes to split polysaccharides, and then soluble oligomers are hydrolyzed to glucose by EGs and cellobiase [Goyal et al., 1991]. Furthermore, Chanzy et al. [1984] and Enari et al. [1987] suggested that CBH I and CBH II had a mode of action of endo-type as well as exo-type.

A number of investigators regarded the crystallinity, the surface accessibility and the particle size of cellulosic substrates as the major factors affecting enzyme hydrolysis [Walker & Wilson, 1991]. The relationship between the fine structural features and the digestibility in cellulosic materials should be clarified, not only for achieving effective glucose production, but also for better understanding of the reaction mechanism. It has not been completely clarified yet how the cellulase degrade the cellulose crystallite. Cowling and Kirk [1976] first pointed out the importance of following eight substrate's characteristics associated with the substrate's "accessibility to extracellular enzymes": (1) moisture content, (2) size of enzyme in relation to capillary diameters, (3) the degree of crystallinity, (4) the unit dimensions, (5) conformation and steric rigidity of the anhydroglucose units, (6) the degree of polymerization, (7) the presence of associated substances and (8) the type of substituent groups on the cellulose. The physical contact between

enzyme and a cellulose chain is usually restricted, because of the structure of cellulose crystallite. Furthermore, in the plant cell walls cellulose is encrusted by lignin and hemicellulose and the microfibrils in commercially available cellulosic materials are re-crystallized and/or aggregated [Akishima et al., 1992]. Thus, the contact of cellulase to a cellulose chain seems to become more difficult. To improve the accessibility of substrate, the effective pretreatments have been investigated by many researchers. It was reasonable that Cowling and Kirk [1976] and Sinitsyn et al. [1991] considered that the milling and chemical treatment caused the increase in the specific surface area accessible to protein molecules and decreased the crystallinity index. These discussions are some examples of the trends to consider the importance of the conditions of surface area on the cellulose crystallite to degrade with enzyme. Woodcock et al. [1995] investigated the docking of congo red to the surface of cellulose crystallite using molecular mechanics, which showed a new way of investigation on the surface structure of crystalline cellulose. Concerning the exo-exo synergy of CBH I and CBH II, it is now considered that a CBH acting processively along the cellulose surface and peeling off single surface chains could induce disorder on the next layer of the chains on the cellulose crystal, and processive enzyme can uncover new chain ends previously hidden under the surface and these caused the cellulose chain on the crystallite to become short and more susceptible to the enzyme [Divne et al., 1994; Samejima, 1995; Teeri, 1997].

More recently, through a combination of biochemical and molecular biological approaches the amino acid sequences of cellulases from different species have been reported and the relationship between the structure of the enzymes and the function was clarified [Henrissat et al., 1989; Gilkes et al., 1991; Henrissat, 1992; Henrissat & Bairoch, 1993].

Comparison of the deduced amino acid sequences of cellulases from different series revealed a common structural organization of enzymes with two distinct domains [Knowles et al., 1987; Teeri et al., 1987], the larger domain, "core", and the smaller domain, "tail", namely the catalytic domain and the cellulose binding domain (CBD), respectively [Bhikhabai & Petterson, 1984; Schumuck et al., 1986; Abuja et al., 1988a, 1988b; Tilbeurgh et al., 1986; Tomme et al., 1988; Ståhlberg et al., 1991], and these domains are connected with flexible "hinge" [Knowles et al., 1987]. Several investigators have determined the three-dimensional structures of CBH I, CBH II from *T. reesei* [Johansson et al., 1989; Kraulis et al., 1989; Rouvinen et al., 1990; Divne et al., 1994]. On the basis of the studies of the structure of the enzymes, it is estimated that the catalytic domain of CBH are like a doughnut or a cleft, through which a cellulose chain is drawn being chopped into cellobiose unit as it goes, and the CBD has one flat face, which contributes to the binding onto cellulose and contains at least two tyrosine residues and a glutamine residue being essential for tight binding of the CBD to cellulose [Linder et al., 1995]. From this view point, Converse [1993] suggested that a free cellulose chain end, "waving in the breeze", ought to be very reactive and the adsorption region on enzyme acts like a plough to loosen the cellulose chain from the fiber, so that the concentration of cellulose chain ends available at the surface of cellulose crystallite is important. The actions of many enzymes, which are contained in a crude cellulase, are considered to be different owing to the design of active-site tunnels [Teeri, 1997].

Chanzy et al. [1985] suggested that CBH I from *T. reesei* could affect some disaggregation of cellulose into microfibrils from observation by TEM of the residual cellulose. From the observation of the adsorption of cellulases to cellulose, it is illustrated that the CBD could prevent flocculation of the cellulose crystallite suspension. Henrissat [1994]

suggested that the CBD could promote dispersion of complex cellulosic substrates and release embedded substances such as hemicellulose.

These previous investigations tend to be focused on the function of cellulases to degrade crystalline cellulose. The author thinks that it must be equally important to investigate the structural feature of crystalline cellulose hydrolyzed with cellulase to completely explain the enzymatic hydrolysis of cellulose crystallite, because not only the surface structure of cellulose crystallite but the three-dimensional structure, which is not completely clarified yet, should have an important relation to the enzymatic attack. In recent years, fortunately, the development of the instruments has accelerated the study on the structure of cellulose crystallites. Therefore, the aim of this thesis was to examine how the characteristics of the crystalline cellulose, such as aggregation of cellulose microfibril and encrustation with lignin, influenced the enzymatic susceptibility. Another aim of this thesis was to be that the morphological changes of cellulosic substrates caused by mild hydrolysis with enzyme might give an information about the supermolecular structure of cellulose crystallite.

This study is composed of seven chapters. In Chapter 1, the enzymatic susceptibility was compared in the xylem differentiating zone in tracheid of gymnosperm and in the wood fibers of angiosperm. In the xylem differentiating zone the depositing stages of cellulose, hemicellulose, and lignin have been clarified by Fujita et al. [1979; 1987] and Takabe et al. [1981a; 1983; 1984; 1986a]. In the differentiating tracheid and wood fiber, the intact cellulose microfibrils are completely accessible to enzyme before lignification, on the other hand, after lignification the accessibility of the cellulose microfibrils in the tracheid are different from those in the wood fiber. In Chapter 2, the author examined the changes of enzymatically hydrolyzed bundle of tracheids of

autohydrolyzed and ozone-treated softwood and discussed the influence of delignification in the cell wall and the aggregation of cellulose microfibrils on enzymatic attack. In Chapters 3, 4 and 5, the enzymatic susceptibilities in the various cellulose samples were compared. In Chapter 3, the features of the enzymatically hydrolyzed Avicel, cotton linter pulp and *Halocynthia* cellulose were compared under various conditions. In Chapter 4, the enzymatic susceptibilities of cellulose microfibrils of the algal-bacterial type were compared with those of the cotton-ramie type. In Chapter 5, the enzymatic susceptibility of the microcrystalline cellulose in *Cladophora* sp., the algal-bacterial type, was compared with that of *Halocynthia* sp. In Chapters 6 and 7, the structures of cellulose microfibrils were speculated from the observations of the enzymatic hydrolysis residues. The supermolecular structure of the algal-bacterial type cellulose was referred to in Chapter 6, and that of *Halocynthia* cellulose, the cotton-ramie type, in Chapter 7.

Chapter 1. Features of cell walls in xylem developing zone of gymnosperm and angiosperm after enzymatic hydrolysis.

1. Introduction

For enhancing the susceptibility of lignified cell walls to cellulolytic enzyme, pretreatments such as steaming, mechanical milling, X-ray irradiation, delignification with white-rot fungi, cooking with organic solvents, and so forth, have been studied because intact wood meal is hardly degraded by the enzyme [Sudo et al., 1976; Shimizu et al., 1983; Hayashi et al., 1989]. The enzymatic susceptibility of steamed wood chips is different among wood species [Shimizu et al., 1983], and it is related closely to the residual lignin content after autohydrolysis and successive extractions [Fujii et al., 1985]. It has been assumed that the enzymatic susceptibilities of polysaccharides in cell walls depend on the lignin encrusting structure. Guaiacyl lignin forms in more rigid networks and masks polysaccharides more tightly than syringyl lignin does [Fujii et al., 1985; Terashima et al., 1986; Fujii et al., 1987; Terashima et al., 1988a].

Tree xylem cells differentiate and mature after the origination from the fusiform initials in the cambium. In the tracheids of gymnosperm and the wood fiber in angiosperm, occupying a large part of xylem tissue, the whole differentiating process can be visualized by tracing the successive differentiating cells being lined up in a radial file from cambium to mature as following: primary wall (P) deposition, S₁ layer deposition, S₂ layer thickening, S₃ layer deposition and warty layer (W) deposition [Fujita et al., 1979; Araki et al., 1982; Araki et al., 1983; Fujita et al., 1987]. It is more complicated in the differentiation process of angiosperm than in gymnosperm because in the differentiating zone enormous expanding of vessel elements and remarkable elongation of wood fibers affect the arrangement and differentiation of other cells. However the

maturing process can be followed approximately in the xylem differentiative zone of angiosperm.

Cellulose microfibrils are deposited first, and then hemicellulose is added mainly in intermicrofibrillar spaces [Takabe et al., 1981a]. Deposition of lignin follows that of polysaccharides with time [Terashima et al., 1988a]. The most inner parts of developing cell walls are free of lignin as indicated by ultraviolet (UV) microscopy [Takabe et al., 1981b] and hydrofluoric acid (HF) lignin skeleton method [Takabe et al., 1986b].

The focus of this chapter was on the changes of the enzymatic susceptibility of cell walls during their formation in some wood species. The masking effect of lignin on cellulose microfibrils was discussed in relationship to the differences among cell types and cell wall layers.

2. Materials and Methods

(1) Samples

The stems of the following species grown in the experimental nursery of the Forestry and Forest Products Research Institute were cut into sample blocks containing differentiating xylem in early June; Shirakamba (*Betula platyphylla* Sukachev var. *japonica* Hara, 3 years-old), Buna (*Fagus crenata* Blume, 8 years-old), Sugi (*Cryptomeria japonica* D. Don, 6 years-old), and Akamatsu (*Pinus densiflora* Sieb. and Zucc., 6 years-old). These blocks were immediately fixed with 2.5% glutaraldehyde and embedded in epoxy resin through a graded series of ethanol and propylene-oxide.

(2) Microscopic observation

Transverse sections of 2.5, 1.0, and 0.1 μm thickness were cut serially from the epoxy embedded blocks using an ultramicrotome (LKB

IV 2128). The sections of 2.5 μm in thick stained with 1% safranin sol. were observed with the outline of the differentiating zone by a conventional light microscope and with the cell wall structure a polarizing light microscope.

The sections of 1.0 μm in thick were observed under an ultraviolet (UV) microscope with a micro-spectrophotometer (Carl Zeiss MPM-O3), which was controlled by a desk top computer. It is well known that lignin absorbs specifically the UV ray of about 280 nm wave length and the lignin distribution can be examined without any staining procedures. UV microphotographs were taken at 280 nm with a band width of 5 nm to visualize the difference between guaiacyl and syringyl lignin. UV absorption spectra were measured in a range from 260 to 290 nm by 1 nm steps. Measuring spot diameter was 0.5 nm, and the band width at each measuring wavelength was 5 nm. The measurements were repeated at least 30 times at every step using the program "Lambda-scan."

(3) Enzymatic hydrolysis of ultrathin sections

According to the method reported in a previous paper [Fujii et al., 1987], ultra-thin sections (0.1 μm thickness) were treated with sodium methylate (CH_3ONa) solution for 20 to 30 min to remove the embedding resin. First set of the sections was shadowed by Pt-Pd to observe the deposition of cell wall layers using a transmission electron microscope (TEM; JEM-2000EX, JEOL). Second set was immersed in an 0.5% enzyme solution in 0.1 M acetate buffer, pH 5 (a commercial cellulase preparation, "Meicelase," Meiji Seika Co. LTD., derived from *Trichoderma viride* pers. ex Fr.) without stirring at 40-45 $^\circ\text{C}$ for 1-4 h. When lignified wood fibers of shirakamba and buna were treated with the enzyme for more than 2 h, the S_2 layers were eroded significantly. Therefore, the enzymatic hydrolysis was performed within 1 h for the

study of the effect of lignin-encrusting structures on enzymatic susceptibilities. The second set was rinsed with distilled water and shadowed by Pt-Pd. On the remaining two sets of the sections, one was treated with 55% hydrofluoric acid (HF) at room temperature for more than 8 h to learn the ultra-structural distribution of lignin and the other with 5% KOH at room temperature for 1 h to learn that of hemicellulose according to the method described in a previous paper [Fujii et al., 1981].

3. Results

(1) Tracheid walls of Sugi and Akamatsu

The tracheid walls in the xylem developing zones, both of Sugi and Akamatsu, had the same behavior, so that the focus was put on the behavior of Akamatsu thereafter.

Fig. 1-1a shows the differentiating zone of Akamatsu xylem. In the deposition stage of the S₁ layers, the compound middle lamellae (CML) were lignified mostly and they were not affected by the enzyme. S₁ layers were susceptible to the enzyme at this stage. In the early stage of S₂ layer deposition the outer parts of S₁ layers were lignified, and the S₁ and S₂ layers in this stage were degraded completely by the enzyme except for the lignified parts of the S₁ layer (Fig. 1-1b). In the stage of S₃ layer deposition most parts of S₂ layers were susceptible to enzymatic attack and only a narrow part of S₂ resisted (Fig. 1-1c upper tracheid). As lignification progressed in the S₂ layer, the insusceptible part of S₂ layer became wider gradually from the outer part (Fig. 1-1c right-hand tracheid). The secondary wall layer quickly became insusceptible to the enzyme when warts were formed as shown in Fig. 1-1c (left hand side and lower tracheids), although the layer were not lignified completely (Fig. 1-2).

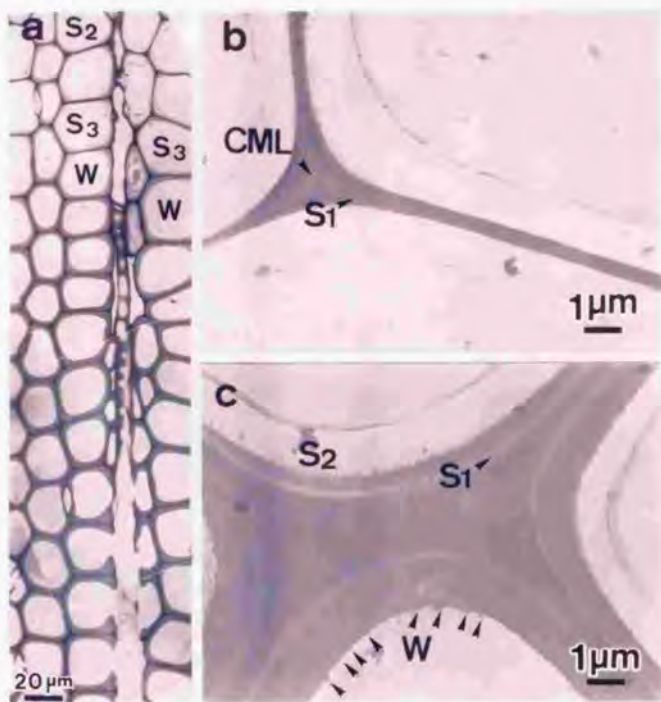


Figure 1-1. UV photograph (a) and electron micrographs of ultrathin cross-sections (b, c) treated with cellulase for 1h of a developing zone of Akamatsu.

Notes: a: S₂, S₃ and W mean the tracheid in the stage of S₂, S₃ and warty-layer deposition stage, respectively. b: tracheids in early stage of the S₂ layer deposition. c: upper and right-side tracheids are in the S₃ layer deposition stage, and the lower and left side ones are in the warty-layer deposition stage.

During the S₂ formation, UV absorption was firstly detected at the outer portion of the S₁ layer at the early stage of S₂ layer deposition, and gradually spread toward the lumen side. Unlignified parts of secondary walls were transparent in UV photographs and were bounded by cytoplasm (Fig. 1-1a). Before the formation of warty layers, UV absorbance of secondary walls in the tracheids was less than those of mature tracheids (Fig. 1-2). The inner parts of these secondary walls were degraded by the enzyme. After the warty layer formation, UV absorbance of secondary walls at 280 nm increased gradually and reached about 0.4 when tracheids matured.

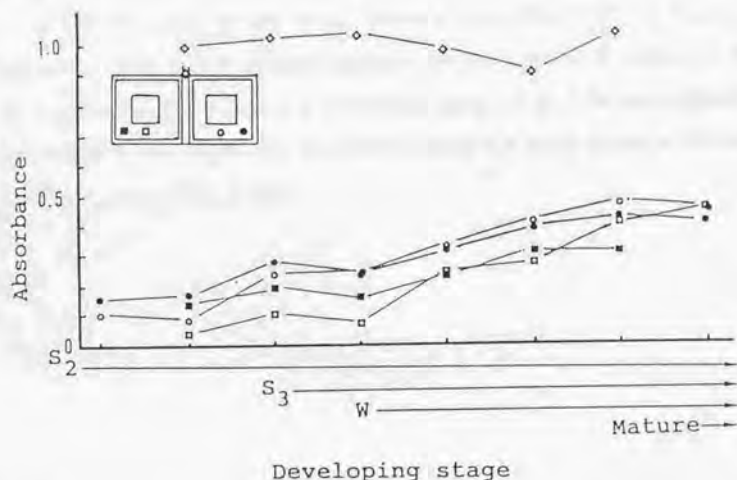


Figure 1-2. UV absorbances at 280 nm of developing secondary walls of Akamatsu tracheids.

Legend: S₂, S₃ and W are similar to those in Fig. 1-1.

Notes: Samples were tracheids in two radial files. The measuring positions were CC regions of CML and two different part of secondary walls as illustrated within the figure.

(2) Shirakamba

1) Wood fiber walls

The CML in the fibers were also degraded by the enzyme remarkably in the stage just before the deposition of S₁ layers, whereas the triangles of CML, which were the only portions lignified at this stage, remained intact (Fig. 1-3a, the upper arrowhead). In the early stage of S₁ layer deposition stage, the CML and cell corner (CC) were lignified and remained almost intact after the enzymatic hydrolysis (Fig. 1-3a, the lower two arrowheads). The S₁ layer, at least the inner-most part, was susceptible to the enzyme during the S₁ layer deposition stage, (Fig. 1-3a, the lower two arrowheads). The S₁ layer became resistant against the enzymatic attack in the S₂ layer deposition stage.

The S₂ layers in the wood fibers in the early stage of S₂ layer deposition were almost eroded, and the outer parts of the S₂ layers in the CC regions became resistant to enzymatic attack (Fig. 1-3b arrowheads). Insusceptible area of the S₂ layers increased as the lignification of the cell walls progressed (Fig. 1-3c).

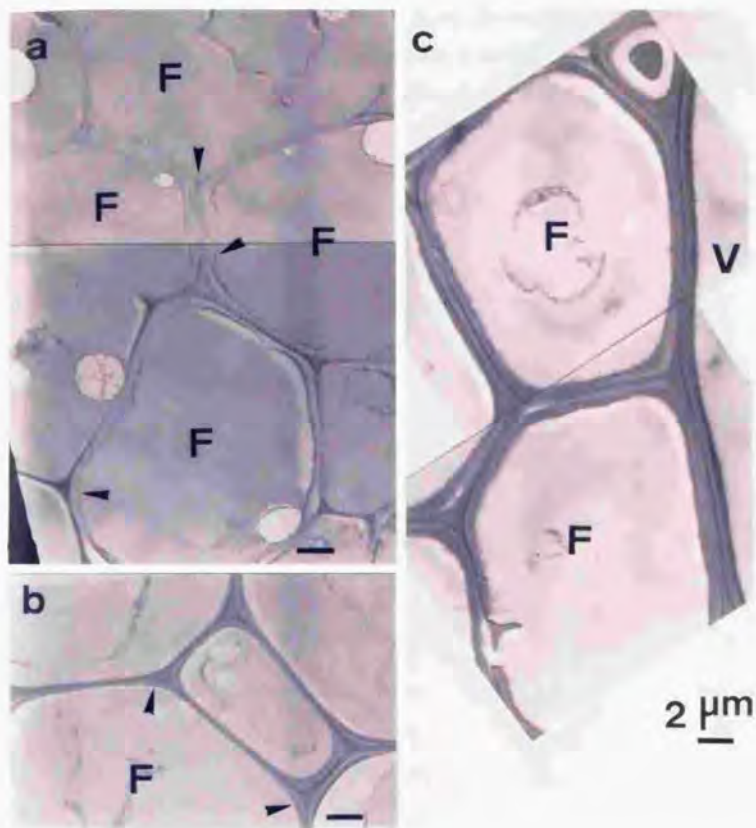


Figure 1-3. Electron micrographs of ultrathin cross-sections of developing xylem elements of Shirakamba, after the treatment with cellulase for 1 h. Notes: a: fibers (F) from the S1 layer deposition stage (upper ones) and the beginning of S2 layer deposition (lower ones). (Arrow-heads: CC insusceptible to enzymatic attack.) b: fibers in the early stage of S2 layer deposition. (Arrow-heads: insusceptible S2 layer portions at CC regions). c: fibers in the late stage of S2 layer deposition and a vessel (V) in the early stage of S3 layer deposition.

The S2 layer in the middle stage of the S2 layer deposition was disintegrated by a 5% KOH treatment (Fig. 1-4a). Fig. 1-4b shows the lignin skeleton of the same area of Fig. 1-4a. Note that the cellulose microfibril and the hemicellulose of the S2 layer in cell walls of mature fiber were degraded by treating with enzyme more than 1 h.

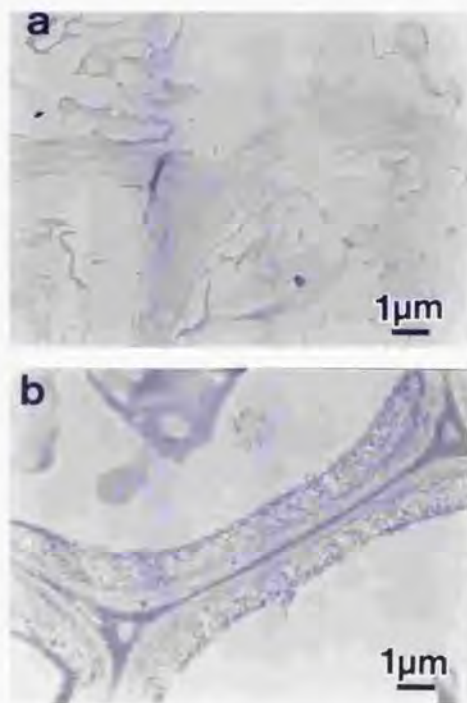


Figure 1-4. Electron micrographs of ultrathin cross-sections of Shirakamba treated with 5% KOH (a) and treated with 55% hydrofluoric acid (HF) (b). Note: The fibers in a and b are in the middle stage of S2 layer deposition.

2) Vessel walls

Fig. 1-5 shows UV spectra of vessel secondary walls during secondary wall formations. The UV absorption of vessel secondary walls in the early stage of S₃ layer deposition are shown in Fig. 1-5-B. The vessel spectrum in this stage showed less UV absorption than that of mature vessel elements (Fig. 1-5-F). These spectra had absorption maxima at about 280 nm despite the different developing stages. UV absorbance increased with the developments of the secondary walls (Fig. 1-5-B, C, D, and E).

Secondary walls of vessel were not attacked with the enzyme except for the innermost part. Secondary walls just formed but not lignified yet were hydrolyzed by the enzyme (Fig. 1-3c).

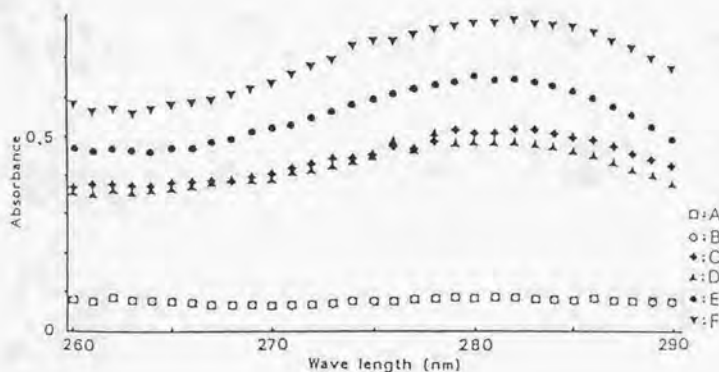


Figure 1-5 UV absorption spectra of vessel secondary walls of Shirakamba in various developing stages; A: in early S₂ layer deposition stage; B-D: in stages of S₂-S₃ layer deposition; E: in mature stage.

(3) Buna

Cell walls of wood fibers and vessels of Buna in the developing stages showed similar behavior to those of Shirakamba with the enzyme and the KOH treatments. The cell wall of upper vessel in Fig. 1-6a was in the course of lignification, and the unlignified area was hydrolyzed by the enzyme. The cell wall of the lower vessel had been lignified completely and was insusceptible to enzymatic attack. Fibers in Fig. 1-6a were in the S3 layer deposition stage. As shown in Fig. 1-6b, S2 layers of fibers had been lignified, but they were quite susceptible to enzymatic attack (Fig. 1-6a). By extraction with 5% KOH, a fibrillated structure was visualized because of the removal of hemicellulose. Most of the S2 layer of wood fibers were degraded upon incubation for more than 1h with the enzyme even if they had been lignified. The enzymatic susceptibility of fibers coincided with the results of Fujii et al [1987].

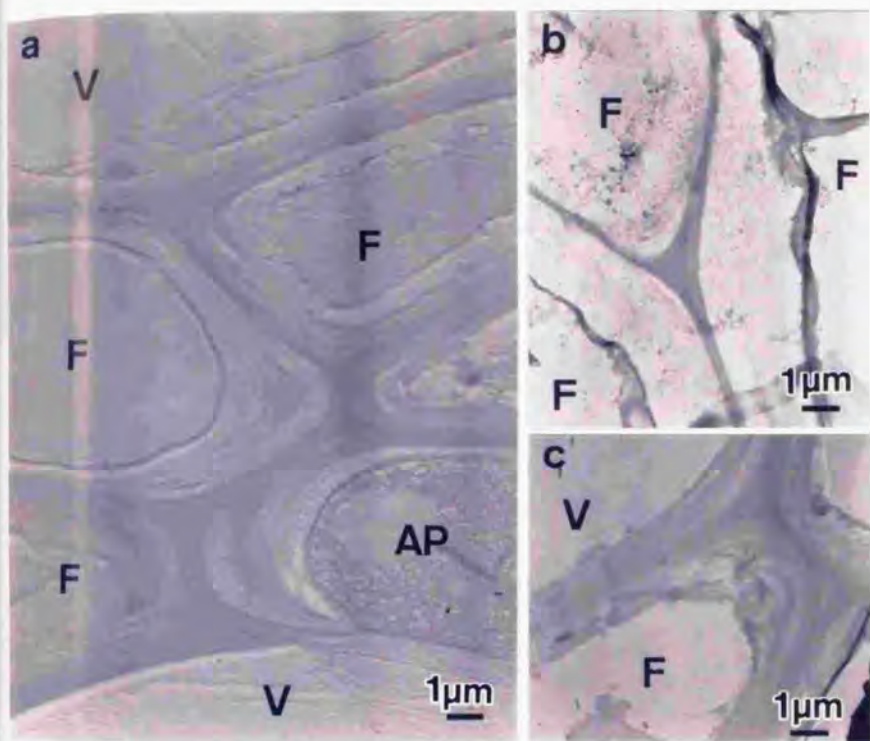


Figure 1-6. Electron micrographs of ultrathin cross-sections of developing xylem elements of Buna treated with cellulase for 1 h (a), 55% hydrofluoric acid (HF) (b) and 5% KOH (c).

Legend: F: fiber; V: vessel; AP: axial parenchyma.

Notes: a: Lignification is in progress in the cell wall of the upper vessel. The lower vessel wall is completely lignified. Fibers are in the S3 deposition stage. b: Lignin skeleton of fibers in the same stage as a. The inner part of the upper fiber walls on the right side is not lignified yet. The other two fiber walls are lignified uniformly. c: Fibers treated with 5% KOH in the same stage as a. Fibrillated structure appears by removal of the hemicellulose.

4. Discussion

The results obtained showed that tracheids, wood fibers and vessels in various differentiating stages had different susceptibility for enzymatic attack. The unligified part of cell walls consisting of cellulose microfibril and hemicellulose was susceptible to enzymatic attacks without any exceptions. It is known that the *T. viride* cellulase used in this study includes not only cellulases but also hemicellulases [For example, Senior & Saddler, 1990]. It was observed that the hemicellulose in the S₂ layers of lignified wood fibers of Shirakamba and Buna were able to be removed more easily than that in the S₂ layers of lignified vessels with 5% KOH. This behavior was almost same as the attack of the enzyme to those cell walls. The alkali-soluble hemicellulose in secondary walls (SWs) of the fiber from Shirakamba and Buna might not be linked physically or chemically (except for ester linkage) to lignin. The hemicellulose may be associated entirely with the cellulose microfibrils as proposed by Kerr and Goring [1975].

As lignification progressed, insusceptible part of secondary walls of the tracheid increased. From the results of Sugi and Akamatsu, the S₂ and S₃ layers of tracheids became insusceptible to enzymatic attack after the stage of warty layer formation. The UV absorption suggested that lignification was almost accomplished in this stage. It is considered that the insusceptibility of cellulose in these walls is attributed to more densely deposited lignin and to the nature of lignin consisting predominantly of guaiacyl residues [Fujii et al., 1987]. Terashima et al. have investigated the distribution of lignin in secondary wall, CML and CC of tracheid, wood fiber and vessel during formation of cell wall. According to their studies, secondary walls (SWs) of coniferous tracheid and vessel contain guaiacyl lignin with high degree of condensation, whereas SW of wood fiber

contains mostly syringyl lignin. Guaiacyl lignin contains more condensed unit than that formed during later stages in the SW [Terashima, 1988a; Terashima *et al.*, 1988b]. This may explain the different behavior on the enzymatic hydrolysis between softwood and hardwood. Fig. 1-1c shows that even the SWs of tracheids was susceptible to enzymatic attacks unless accomplished lignification and also lignification proceeded quite promptly.

In spite of the completion of lignification, the fiber SWs of Shirakamba and Buna were susceptible to enzymatic attack. The cellulose microfibrils and hemicellulose of the S₂ layers in the mature cell walls of Shirakamba and Buna were hydrolyzed completely by prolonged enzymatic treatment. Fujii *et al.* [1987] proved that the SWs of these woods have relatively low lignin contents and their lignins are rich in the syringyl type. This suggests that the cellulose microfibril and hemicellulose are encrusted loosely enough with lignin to be attacked by the enzyme. The vessel walls contained guaiacyl type lignin as well as the tracheid walls and at the same time lignification brought the difficulty for enzymatic hydrolysis. This is given as an interpretation for the difference of enzymatic susceptibility between the tracheids and wood fibers.

The difference of the lignin encrusting structure between the tracheids, wood fiber and vessels was observed after the enzymatic hydrolysis of xylem differentiating zone of wood. The condensed units of the guaiacyl lignin was considered to cause the enzymatic insusceptibility of cellulose microfibril.

5. Summary

Lignified cell walls are hardly attacked by cellulolytic enzymes without any pretreatments, because the cellulose is encrusted with lignin. In this chapter, the effects of lignification on enzymatic susceptibilities of cell wall polysaccharides were studied. The xylem developing zones of Shirakamba (*Betula platyphylla* Sukat. var. *japonica* Hara), Buna (*Fagus crenata* Blume), Sugi (*Cryptomeria japonica* D. Don), and Akamatsu (*Pinus densiflora* Sieb. and Zucc.) were cut into ultra-thin sections and treated with cellulolytic enzymes.

Cell walls of fibers, vessels and tracheids were first lignified at the cell corner regions of compound middle lamellae (CML) in the S₁ layer deposition stage. Then lignification was successively extended in the entire CML, S₁, S₂ and S₃ layers. Cell walls before lignification were completely degraded by the enzyme. CML became resistant against enzymatic attacks in the early stages of S₁ layer deposition. S₁, S₂ and S₃ layers became successively resistant in the following lignification stages. The behavior of the cell walls to the cellulolytic enzyme was determined by the kind of lignin which is contained in the cell walls of hardwood and softwood. Furthermore, unless accomplished lignification, SWs of tracheids was susceptible to enzymatic attacks and also lignification proceeded quite promptly.

Keywords: Lignification, Enzymatic susceptibility, Xylem differentiation, TEM, UV microscopy.

Chapter 2. Enzymatic susceptibility of autohydrolyzed and ozone-treated softwood.

1. Introduction

Enzymatic susceptibility of autohydrolyzed woods has been comparatively investigated among 44 species of angiosperm and 6 species of gymnosperm [Shimizu *et al.*, 1983]. The susceptibility of some species of angiosperm was improved remarkably by autohydrolysis, but almost no effect was obtained on the susceptibility of softwood. In chapter 1, it is described that the lignin in the tracheid of gymnosperm prevents the cellulolytic enzymes from attacking to the cellulose microfibrils more persistently than that in the wood fiber of angiosperm. This was explained partly by the fact that the tracheid of gymnosperm has a greater lignin content and smaller amounts of hemicelluloses and acetyl groups than wood fiber. The difference of the chemical structures of lignin in gymnosperm and angiosperm was also be more important factor of enzymatic susceptibility [Fujii *et al.*, 1985; 1987]. Upon steaming, an appreciable amount of lignin in angiosperm becomes soluble in dilute aqueous-alkali and in organic solvents such as methanol and dioxane, but in gymnosperm, lignin becomes only slightly soluble. For enhancing the enzymatic susceptibility of autohydrolyzed softwoods lignin must be modified or degraded by methods other than steaming.

Ozone treatment has been investigated as a non-polluting agent for bleaching pulps. The degradation mechanism of lignin with ozone has been made clear by Kaneko *et al.* [1979; 1980; 1981; 1983] and by Hosoya [1985]. There are a few reports on ozone pretreatments of lignocellulosics for enhancing the enzymatic saccharification [Puri, 1983; Neely, 1984; Joseleau & Martini, 1981]. In these papers, many lignocelluloses, such as wheat straw, bagasse, peanut shells, green hey, shaving (poplar, pine),

sawdust (red oak) and wood meals (*Eucalyptus regnans*, *Pinus radiata*) has been studied. After treatment with ozone, all the lignocelluloses become susceptible to enzymatic saccharification. Neely [1984] has expressed the enzymatic digestibility as a percentage of the amounts in pure cellulose. Puri [1983] has estimated *in vitro* digestibility by the weight loss of organic matter. Although they have gotten rather high digestibility, almost all the polysaccharides in the lignocelluloses have not always been digested. Mizumoto and Shimizu [1986] have investigated the enzymatic susceptibility (increase in reducing sugar) of Karamatsu (*Larix leptolepis*) wood meal and Ezomatsu (*Picea jezoensis*) wood meal after 8 hr treatment with ozone. The enzymatic susceptibility (weight loss) before and after treatment with ozone was 9.4% and 33.7% for Karamatsu, and 9.7% and 63.2% for Ezomatsu, respectively.

Cellulose and hemicellulose do not become susceptible enough to enzymatic attack upon only the treatment with ozone. Thus, we investigated the effects of ozonization on enzymatic hydrolysis of previously autohydrolyzed softwood by using Sugi (*Cryptomeria japonica* D. Don) which is one of the samples of difficult to degrade with *Trichoderma* cellulase.

2. Experimental

(1) Pretreatment of samples

Chips of Sugi (*Cryptomeria japonica* D. Don) were autohydrolyzed with saturated steam at 200 °C equivalent to 1.5 MPa for 10 min and defiberized in a refiner with a clearance of 0.2 mm. The fiber was extracted with water at 70 °C for 1 h to remove the partly hydrolyzed hemicelluloses. For ozonization, the moisture content of the fiber was adjusted to 50%.

Sugi wood meal was prepared with a Wiley mill. The 40-80 mesh fraction was collected by sieving. A part of the sample was autohydrolyzed with steam at 200 °C for 10 min and extracted with water at 70 °C for 1 h. For ozonization, the moisture contents of the untreated wood meal, the steamed wood meal to 30% and 50%, respectively. Osawa et al. [1963] have stated that the ozonization reaction is most rapid and homogeneous if done in the gas phase on wood containing moisture at fiber saturation point. Neely [1984] has found that the optimum range for moisture content is present around 25-35% of the dry weight of the lignocellulose.

(2) Treatment with ozone

Ozone was produced by passing pure oxygen at a flow rate of 250 mL/min through a laboratory ozonizer (Chiyoda Seisakusho; type BH-2). The ozone concentration was estimated to be 3% by the conventional titration method.

The moisture-adjusted samples (5-10 g as dry weight) were treated with ozone in 200 mL flasks, fitted to a rotary evaporator and rotated under ambient temperature for 15-102 min. The unreacted ozone was collected in a 30% KI solution, and the concentration was determined. At the maximum, 3 moles of ozone were supplied per guaiacyl propane unit (C₉ unit, molecular weight 200) in lignin.

(3) Enzymatic hydrolysis

The ozone treated samples were hydrolyzed with a commercial enzyme preparation, "Meicelase" (Meiji Seika Co., Japan), derived from *Trichoderma viride*. Samples of 200 mg (dry weight) were incubated in 10 mL of a 0.1 M acetate buffer at pH 4.8 including 50 mg of enzyme in water bath at 40 °C for 2 days. After 2 days' incubation, the reaction

mixture was filtered by suction funnel and the residue was separated from the hydrolyzate. The residue was freeze-dried. The relative sugar composition in the enzymatic hydrolyzate was analyzed by ion-exchange chromatography as described below.

(4) General analysis

A part of the ozonized samples was extracted with 90 % dioxane at 70 °C for 1 h (wood to liquor ratio, 1: 20) and/or with a 0.1 M acetate buffer at pH 5 at 40 °C for 48 h. The dioxane extracts were characterized by spectrophotometrical analyses and gel permeation chromatography (GPC) [Sudo et al., 1985]. The residue, after extraction with dioxane, was analyzed for Klason lignin and neutral sugars. The lignin in the residue was characterized by alkaline nitrobenzene oxidation [Sudo et al., 1985]. Ultraviolet (UV) absorption spectra were recorded on a Shimadzu UV-250 spectrophotometer. Infrared (IR) absorption spectra were recorded on a JASCO FT/IR 3 spectrophotometer using the KBr disk method. Klason lignin was determined according to JIS P 8008-1961. Neutral monosaccharide composition was determined by borate complex ion-exchange chromatography [Sinner et al., 1975; Honda et al., 1981]. The oligosaccharides were analyzed by high performance liquid chromatography (HPLC) with a Shodex Ionpak KS-802 (300 mm x 8 mm x 2, Showa Denko, Tokyo, Japan) and a 5 cm KS 800P guard column connected in series [Sudo et al., 1986].

Microscopic observations. — Samples were embedded in epoxy resin by the usual method. Transverse sections (1-2.5 µm in thickness) were cut by a LKB ultramicrotome. The thin sections (2.5 µm thick) were observed after staining with 1% safranin under a conventional and polarizing light microscopes same as described in chapter 1. Other sections (1-2 µm) were used for observation under UV micro-photometer (Carl Zeiss MPM-O3).

UV absorption spectra were measured on these sections in the same way as described in Chapter 1.

X-ray diffraction analysis — X-ray diffractograms were measured by a Rigaku Denki X-ray diffractometer employing Cu-K α radiation operated at a tube voltage of 30 kV and at a tube current of 15 mA. The sample was scanned over the range $2\theta = 30^\circ$ to 6° at a rate of $1^\circ/\text{min}$. The width of micelle was calculated according to Sherrer's equation [1918].

Electron microscopy — Electron microscopy was performed with a JEOL JEM-100 CX electron microscope, being operated at 100 kV for imaging purposes and for electron diffraction. The samples were collected on a carbon coated microgrid.

3. Results

(1) Treatment of wood-meals with ozone

Table 2-1 shows the results of analysis of ozone-treated Sugi wood meals.

Table 2-1 Analysis of ozone-treated Sugi wood meals.

Ozone consumed		Klason lignin (%)	Reducing sugars ^{a)} (%)	Relative sugar composition (%)					Klason lignin in residue ^{b)} (%)
(by weight) (%)	(mole/C ₉ unit)			Man	Ara	Gal	Xyl	Gluc	
	untreated	34.7	52.2	14.2	1.9	2.9	8.1	72.9	34.6
4.1	0.5	31.2	(48.4)	14.1	1.8	2.5	8.3	73.2	24.2
8.7	1.0	34.4	53.1	13.5	2.1	2.5	8.5	73.5	-
13.3	1.5	22.0	51.7	13.5	1.6	2.4	7.7	74.8	16.4
15.4	2.0	20.6	50.5	13.2	1.6	2.3	7.2	75.6	14.2
19.2	2.4	17.3	49.6	13.4	1.5	2.3	7.3	75.5	12.4
21.1	2.6	17.7	49.0	13.5	1.7	2.3	7.6	75.0	12.7

a) Amount of reducing sugars in the acid hydrolysate.

b) Amount of Klason lignin remaining after dioxane extraction based on original samples.

The Klason lignin content decreased progressively with increasing ozone consumption. After 2.6 moles of ozone consumption per C₉ unit of lignin, almost half of the lignin was degraded with ozone and became undetectable as Klason lignin. The ozonized lignin was soluble in 90% dioxane. The amount of dioxane extracts increased with increasing ozone

consumption. The UV spectra of the dioxane extracts of ozone-treated wood meals show that the maximum absorptivity around 280 nm decreased with increasing ozone consumption, whereas the peak around 260-270 nm increased relatively (Fig. 2-1). The IR absorption spectrum shows that the peaks at 1514 and 1610 cm^{-1} , attributed to the lignin aromatic nuclei, decreased upon ozonization, whereas the peaks near 1640 and 1743 cm^{-1} , attributed to conjugated carbonyl and carboxyl groups, increased (Fig. 2-2).

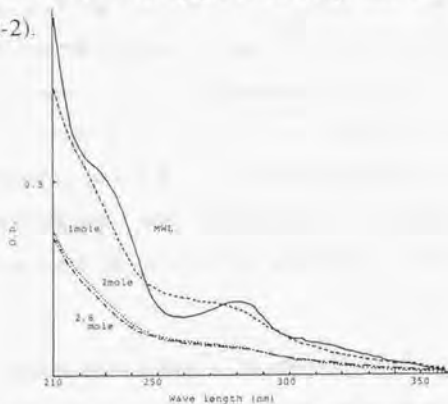


Figure 2-1. UV absorption spectra of 90% dioxane extracts obtained from Sugi wood-meals with various degrees of ozonization.

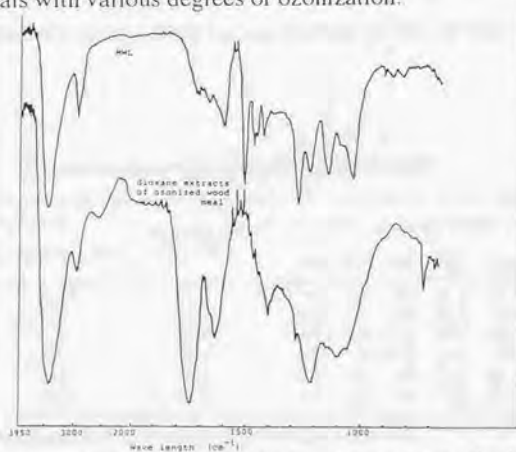


Figure 2-2. IR absorption spectra of 90% dioxane extracts obtained from Sugi wood-meal after ozone treatment and MWL of Sugi.

The content of polysaccharides decreased only slightly with even prolonged ozonization time (Table 2-1). The sugar composition shows that the polysaccharides in the cell walls were not affected by the treatment with ozone.

The reducing sugar yield of ozone-treated wood meals increased with decreasing Klason lignin content and leveled off after 2 moles of ozone consumption (Table 2-2). After 2.6 moles of ozone consumption, the hydrolysis extent of the polysaccharides in the wood meals reached 46%. The sugar composition of the enzymatic hydrolyzates revealed that the proportion of mannose was considerably small compared with the amount of the starting materials. The little susceptibility of mannan to enzymatic hydrolysis also was observed in the wood meal partly delignified with acid chlorite as reported in a previous paper [Sudo et al., 1976].

To attain a substantial extent of the reducing sugar yield of the Sugi wood meal, the amount of ozone required was more than 20%, based on the weight of the sample (Table 2-2). This large requirement of ozone can be explained simply by the high lignin content (35%) of the Sugi wood meal.

Table 2-2 Enzymatic susceptibility of ozonized wood meals.

Ozone consumed		Reducing sugar ^{a)} yield (%)	Relative sugar composition (%)				
(by weight) (%)	(mole/C ₉ unit)		Man	Ara	Gal	Xyl	Gluc
4.1	0.5	23.3	9.5	2.4	3.0	11.4	73.7
8.7	1.0	36.8	9.1	2.0	1.9	12.5	76.4
13.3	1.5	39.2	6.7	1.9	2.4	10.1	78.9
15.4	2.0	45.8	7.3	1.8	1.7	9.6	79.6
19.2	2.4	48.9	6.1	1.6	1.4	9.3	81.6
21.1	2.6	46.1	5.9	1.5	1.6	9.5	81.5

a) Reducing sugar yield. Based on polysaccharides in wood meal.

(2) Treatment of autohydrolyzed woods with ozone

As reported previously, upon autohydrolysis with saturated steam (180-230 °C), most of hemicelluloses were hydrolyzed partially and became soluble in water [Shimizu et al., 1983]. The yield of autohydrolyzed wood meal was 87.3%, and the yield of water extracts was 13.7%, based on the original wood meal. The sugar composition of the water extract was Man: Ara: Gal: Xyl: Glc = 30: 8: 16: 41: 10. The sugar composition of the residual wood meal indicated that most of the hemicelluloses were removed (Table 2-3). The water extract was separated into neutral and acidic sugars in the usual way [Shimizu et al., 1983]. The fragments of hemicelluloses, glucomannan, and xylan, were present as monosaccharides and oligosaccharides (degree of polymerization (dp) = 2-10) as shown in Fig. 2-3.

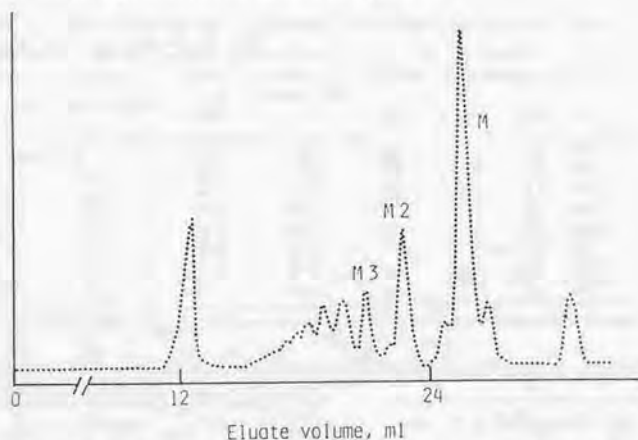


Figure 2-3. GPC of neutral sugars of water extract of Sugi steamed at 200°C for 10 min. M: monosaccharides; M2, M3: oligosaccharides.

When the autohydrolyzed and water-extracted wood meals were subjected to ozonization, the Klason lignin content decreased more progressively than untreated wood meals with increasing ozone

consumption (Table 2-3). After 3.3 moles of ozone consumption per C₉ unit, about 71% of the lignin was degraded and became undetectable as Klason lignin. The extent of enzymatic hydrolysis also increased with the increasing extent of lignin degradation. Finally, the susceptibility of polysaccharides, mainly consisting of cellulose, reached 59%. This value is greater than that of the untreated wood meal described above.

Subsequently, the Sugi chips were steamed at 200 °C for 10 min, defiberized with the refiner having a clearance 0.2 mm, and then extracted with water. The yield of the extract was 13% based on the autohydrolyzed sugi chips. About 70% of the hemicelluloses were solubilized upon autohydrolysis and were removed by extraction with water (Table 2-4) as well as in the case of autohydrolyzed wood meal.

Table 2-3 Effect of ozonization on chemical composition and enzymatic susceptibility of autohydrolyzed Sugi wood meal.

Ozone consumed (by weight) (mole/C ₉ unit) (%)		Klason lignin (%)	Reducing ^{a)} sugar yield (%)	Relative sugar composition (%)				
				Man	Ara	Gal	Xyl	Gluc
untreated		41.2	2.8	4.9	-	0	2.4	94.2
3.2	0.3	36.0	18.0	5.3	-	0	2.9	93.2
9.7	1.0	31.3	33.4	4.8	-	0	2.9	93.2
13.1	1.3	27.2	40.3	4.7	-	0	2.9	93.3
18.1	1.8	23.2	45.9	5.2	-	0	2.8	92.8
21.5	2.1	20.3	50.5	4.4	-	0	2.8	93.7
27.3	2.7	17.4	59.3	4.8	-	0	2.4	94.7
33.0	3.3	11.9	50.5	4.0	-	0	2.0	95.3

a) Amount of reducing sugars in the enzymatic hydrolyzate. Based on polysaccharides in wood meal.

Table 2-4 Effect of ozonization on chemical composition and enzymatic susceptibility of autohydrolyzed Sugi chips

Ozone consumed (by weight) (mole/C ₉ unit) (%)		Klason lignin (%)	Reducing ^{a)} sugar yield (%)	Relative sugar composition (%)				
				Man	Ara	Gal	Xyl	Gluc
untreated		40.2	11.1	6.3	-	0.8	5.0	88.0
4.4	0.5	35.1	30.0	6.0	-	0.7	4.5	89.5
9.8	1.0	29.0	44.5	3.1	-	-	4.6	92.3
16.8	1.7	20.9	58.5	5.0	-	-	4.5	90.5
18.7	2.0	20.2	58.2	5.6	-	0.6	4.8	90.3
24.1	2.5	17.4	61.7	4.7	-	-	4.2	91.0
30.4	3.0	12.1	67.2	4.9	-	0.5	3.7	91.4

a) Amount of reducing sugars in the enzymatic hydrolyzate. Based on polysaccharides in chip.

The results of the ozonization of autohydrolyzed chip followed by enzymatic hydrolysis are presented in Table 2-4. The results were quite similar to those with the autohydrolyzed and ozone-treated wood meals. After 3 moles of ozone consumption, the Klason lignin content decreased by 70%, and the enzymatic susceptibility of the polysaccharides in the fiber reached 67%; although the fiber had much larger dimension than the autohydrolyzed wood meal.

(3) Characterization of the samples treated with ozone before and after enzymatic hydrolysis.

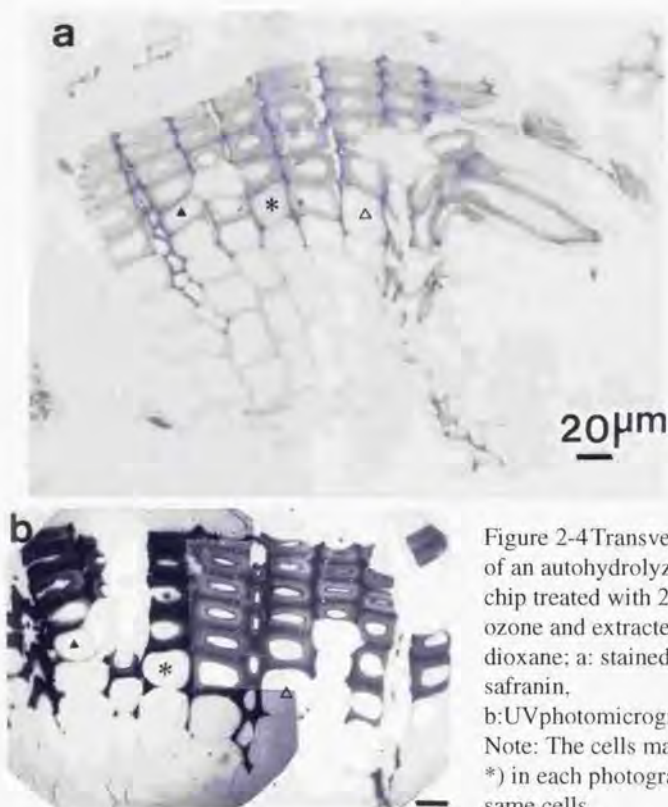


Figure 2-4 Transverse sections of an autohydrolyzed Sugi wood chip treated with 2.5 moles of ozone and extracted with 90% dioxane; a: stained with 1% safranin, b: UV photomicrograph. Note: The cells marked (, and *) in each photograph are the same cells.

Fig. 2-4 shows transverse sections of an autohydrolyzed Sugi wood chip, which contained a bundle of tracheids, treated with 2.5 moles of ozone and extracted with 90% dioxane; Fig. 2-4a was observed under the light microscope after staining with 1% safranin, and Fig. 2-4b is observed under the UV microscope. The stained region agreed well with a strong UV absorption region. The outer part of the bundles had no UV absorption (and also unstained with 1% safranin sol.). In the inner part of the bundles, the early wood with large lumens and the thin cell walls had no UV absorption (unstained, either). In addition, in the transitional tracheids from early wood to late wood, the inner sides of the cell walls had no UV absorption (unstained), but the outer sides of the cell walls and the late wood showed strong absorption of UV and was stained (marked in Fig. 2-4; Δ , \blacktriangle and $*$). In some of the transitional tracheids, concentric circles within the secondary wall were observed. The polarizing light micrograph shows that cellulose existed in both the early wood cell walls and the late wood cell walls to same extent.

Fig. 2-5 shows the three kind of the enzymatic hydrolyzed residues of autohydrolyzed wood chip treated with 2.5 moles of ozone. (a) is dark brown colored residue which maintained the bundle structure. The unstained region of the cell walls was not observed after 2 days' enzymatic hydrolysis in the area of early wood and transitional tracheids. (b) is brown colored residue, and (c) is white residue with fibrous structure. This white material (Fig. 2-5c) appeared as hydrolysis residues in addition to the colored residues containing lignin (Fig. 2-5a, b). The amount of the white material was larger in the samples treated with ozone for longer time. Since the white material had a slower sedimentation velocity than the colored residues, they were separated from each other by fractional sedimentation in an aqueous suspension. After a consumption of 3 moles of ozone per C₉ unit, the yield of the white material was about 10% on ozone treated sample. The white material stained well with chlor zinc iodine but not with phloroglucinol in

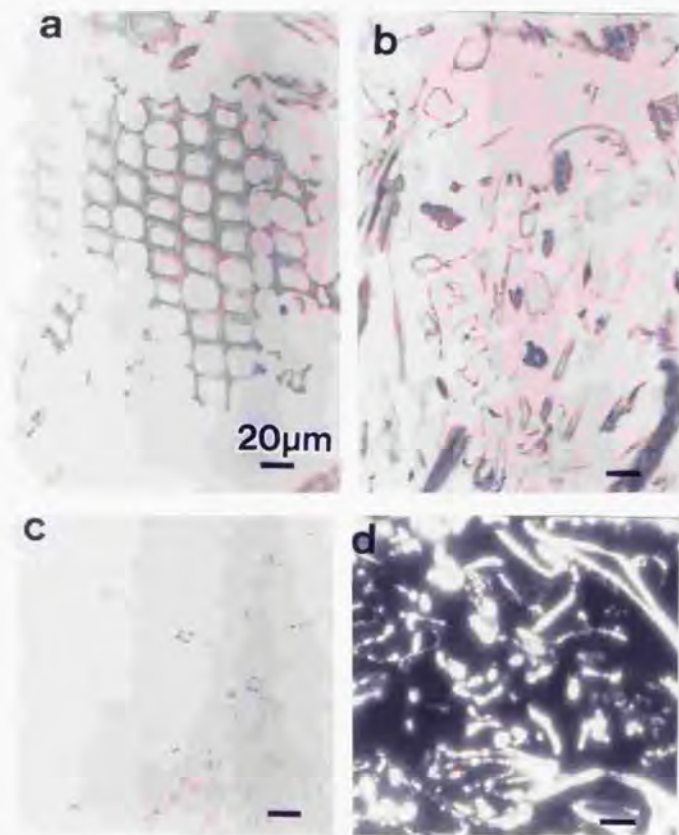


Figure 2-5. The three kinds of the enzymatic hydrolyzed residues of autohydrolyzed wood chip treated with 2.5 moles of ozone (a, b, c). c is white residue with fibrous structure (white material) and d is a polarizing light microphotograph of the white material.

hydrochloric acid, indicating that it was quite free of lignin, and proved to be crystalline by polarizing light microscopic observations. The X-ray diffractograms of Sugi wood meal, autohydrolyzed Sugi wood chip and the white material are shown in Fig. 2-6. The crystallinity index (CrI) increased upon autohydrolysis and ozonization. The observation with

TEM showed that the white material should be a piece of tracheid cell wall and microfibrils in the white material were aggregated tightly and partially fibrillated (Fig. 2-7). The diffractogram of the white material showed a typical pattern of cellulose I (Fig. 2-6, 7). The micelle width of the (200) plane of the white material calculated from X-ray diffractogram was about 1.2 times wider than that in Sugi wood meal.

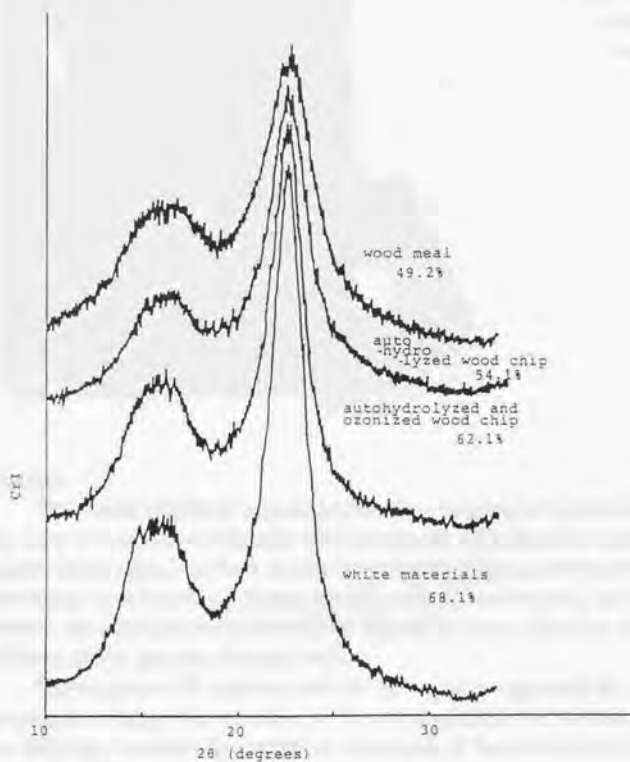


Figure 2-6. X-ray diffractograms of untreated Sugi wood-meal, autohydrolyzed wood-chip, autohydrolyzed and ozonized wood-chip, and white material appeared as enzymatic hydrolysis residues.



Figure 2-7. A bright field-image by diffraction of the white material and a corresponding electron-diffraction diagram (inset).

4. Discussion

The results obtained suggested that the treatment of ozone after the steaming were prominent combination for enzymatic hydrolysis of softwood. The microscopic observations made it clearer that the degradation of lignin in cell walls by the treatment with ozone contributed to the effective enzymatic hydrolysis. Furthermore, the fiberization by the refiner should be more effective for the penetration of ozone gas into the cell wall.

The results of IR analysis and UV absorption suggested the formation of dioxane-extractable lignin by treatment with ozone, namely the formation of a muconic-acid type structure by oxidative cleavages of lignin aromatic nuclei [Kaneko et al., 1979; 1980; 1981; 1983]. GPC of the dioxane extracts showed that the lignin was degraded to compounds having a number average molecular weight about 500. The results of

alkaline nitrobenzene oxidation of Sugi wood meal, 2.6 moles of ozone treated wood meal and autohydrolyzed Sugi wood chip treated with 2.7 moles ozone indicated that the remarkable chemical modification occurred in the lignin in the cell walls. Furthermore, the chemical modification of the residual lignin of the autohydrolyzed wood chips treated with ozone was larger than that of the wood meal treated with ozone only.

On the other hand, the sugar composition showed that the polysaccharides in the cell walls were not affected by the ozone treatment as observed in the wheat straw by Joseleau and Martini [1981]. Although β -glycosidic linkages were found to be cleaved with ozone forming gluconic acid or gluconate [Pan et al., 1981], the loss of polysaccharides by ozone oxidation could be disregarded under the ozonolysis condition used.

The chemical structure of lignin is modified by steaming and ozone treatment. Upon treatment with ozone, a part of the lignin becomes soluble in 90% dioxane. However, the lignin in the late wood tracheids that remains in the cell wall after 90% dioxane extraction might undergo chemical modifications to some extent. The alkaline nitrobenzene oxidation of untreated wood meals afforded vanillin and vanillic acid, in the joint yield of 20.6% on Klason lignin; whereas the wood meals oxidized with 2.6 moles of ozone per lignin unit and extracted with 90% dioxane yielded them at 8.4% on Klason lignin. This indicates that the aromatic nuclei of the residual lignin were cleaved partly. Upon autohydrolysis at 200 °C for 10 min, the yield of the alkaline nitrobenzene oxidation products decreased to 8.2% indicating that condensation reactions took place during autohydrolysis. When autohydrolyzed wood meal treated with 2.7 moles of ozone was subjected to alkaline nitrobenzene oxidation, the yield of the products was 4.3%

Water extraction after the autohydrolysis removed most hemicellulose, presumably resulting in the formation of porous cell wall structures of the tracheids. This might facilitate the penetration of ozone into cell walls and thus the reaction between ozone and lignin. Also, it has been reported that α - and β -aryl ether linkages in lignin are cleaved upon autohydrolysis, forming phenolic hydroxyl groups [Sudo et al., 1985]. According to Kaneko et al. [1979; 1980; 1981; 1983] and Hosoya [1985], guaiacyl nuclei are more reactive than veratryl nuclei. Therefore, autohydrolysis possibly enhances the reaction between the ozone and the lignin.

The microscopic observations illustrate the progress in reaction of lignin with ozone. Ozone's attack to the tracheid cell wall is topochemically heterogeneous. The early wood tracheid with large lumens and thin cell walls was ozonized much more rapidly than the late wood tracheid. The penetration of ozone into the late wood tracheids was strictly restricted. Puri and Anand [1986] have pointed out that the lignin content decreased progressively with increasing ozonization time, and that a small portion of lignin was resistant to ozonization. They have concluded that the degradation process in lignin followed a first order kinetics, but the lignin fraction, resistant to ozonolysis, may be degraded by different mechanisms. The appearance of the concentric circles in the cell wall of the transitional tracheid suggested the complex reaction between ozone and lignin. As Osawa et al. [1963] have stated, the course of reaction with ozone is considered to be affected greatly by the permeability of the wood structure. Osawa et al. have described that the differences on various wood species, tissues, and particle sizes primarily reflect the differences in gas permeability. In our case, the penetration of ozone was estimated from the microscopic observation. When the bundle of tracheids was exposed in ozone gas phase, in the outer part of the

bundle ozone started to erode the tracheids from the outside, even in the late wood. In the inner part of the bundle, ozone might penetrate through pits, and through cracks, which was formed during autohydrolysis or fiberization with a refiner. Then it diffused from the lumen so that the order of gas contacts might be secondary wall, compound middle lamella, and the cell corner area. The late wood tracheid has a thicker cell wall and a narrower lumen than the early wood tracheid, thus the penetration of ozone gas should remarkably be difficult.

The white material was considered to be a crystalline cellulose resistant to enzymatic hydrolysis. Its formation is estimated as the following: a compact aggregation of the cellulose microfibrils might occur in the cell wall, which was not influenced with ozone after the treatment by removal of lignin and hemicelluloses from the cell wall. Therefore, the surface of these cellulose microfibrils could not contact with the cellulase and this occurred the delay of the enzymatic attack to cellulose. The electron diffraction diagram and X-ray diffraction diagram confirmed that the material, which interrupted to obtain the clear cellulose diffraction, lignin and hemicellulose, were eliminated from the cell walls. Tanahashi et al. [1983] investigated physical properties of explosion wood and found that crystallinity and micelle width of explosion wood increased by explosion. They suggested that the amorphous region of cellulose was crystallized with the explosion. We think that when hemicellulose was eroded and lignin network became loose, cellulose microfibrils packed compactly through autohydrolysis and treatment with ozone. The microscopic observations of the autohydrolyzed softwood samples treated with ozone revealed that there are two problems to be solved; although ozone treatment after autohydrolysis is an effective pretreatment for enhancing the enzymatic susceptibility of softwood. The first problem is the poor permeability of ozone into the late wood, and the second is the

formation of the nonsusceptible crystalline cellulose through autohydrolysis and treatment with ozone.

5. Summary

Upon ozonization after autohydrolysis, the enzymatic susceptibility of the softwood (Sugi: *Cryptomeria japonica* D. Don) increased up to 67%. The susceptibility of individually treated Sugi wood meal was less than 3% for steaming, and 46% for ozonization. The solubilization of hemicellulose and the cracks owing to steaming followed by fiberization resulted in the generation of the porous structure of cell walls facilitating the penetration of ozone into the wood. Microscopic observations revealed that the permeability of ozone was different between cell walls in early wood and in late wood. Most of the lignin in the cell walls of early wood was oxidized with ozone, whereas the lignin in the cell walls of late wood was not accessible to ozone. Oxidation of lignin was restricted only in the inner part of the secondary walls in the tracheids of the area transitioning from early wood to late wood. When the ozonized samples were subjected to enzymatic hydrolysis, a white material appeared as a hydrolysis residue, which was quite free from lignin and was identified as cellulose I. This heterogeneity of ozonization and the aggregated cellulose microfibrils resistant to enzymatic attack prevented the complete hydrolysis of autohydrolyzed and ozonized Sugi wood.

Keywords: Ozone pretreatment, Enzymatic hydrolysis, Softwood, Autohydrolysis.

Chapter 3 Influence of aggregation of microfibrils on enzymatic hydrolysis of crystalline cellulose of cotton ramie type.

1. Introduction

Crystalline cellulose is degraded by the continuous synergistic action of exo-, and endo-type enzymes [Wood, 1989; Walker & Wilson, 1991]. Many researchers have investigated on the interrelation between crystalline cellulose and cellulases. Some factors influencing the enzymatic susceptibility of the crystalline cellulose have been studied crystallinity, particle size, degree of polymerization (dp), and specific surface area available to protein molecules. Among these factors it is accepted that the surface area is most important for the enzyme to attack crystalline cellulose [Shevale & Sanada, 1979; Rivers & Emert, 1988; Sinitsyn et al., 1991].

Wardrop and Jutte [1968], White and Brown [1981], White [1982] and Chanzy and Henrissat [1983a; 1983b; 1984; 1985; 1986] have investigated the morphology of the crystalline cellulose residue after cellulase treatment with transmission electron microscope (TEM) to clarify the mechanisms of enzymatic degradation of crystalline cellulose. *Valonia* cellulose and bacterial cellulose were used owing to large size of crystalline and high crystallinity in their studies. They have observed that the residual cellulose microfibrils are disaggregated, become thin and split to subfibrils. Both EG and CBH I from *Trichoderma reesei* bring fibrillation to the cellulose microfibrils [Sprey & Bochem, 1992]. Recently, the cellulose-binding domain isolated from EG of *T. reesei* on *Valonia* cellulose have been visualized on TEM by immunogold labeling [Gilkes et al., 1992]. The colloidal gold labeling of the intact cellulase and its isolated cellulose-binding domain has revealed that the proteins bind

preferentially onto certain faces or edges of the cellulose crystals. Gilkes et al. have also reported that the flocculation of microcrystalline cellulose inhibited by the surface coverage with the cellulose-binding domain. They have speculated that cellulose-binding domains increase the available surface area of cellulose and at the same time function to increase the local concentration of the catalytic domains. The hypothesis agrees with earlier understanding that the overall increase in digestibility of crystalline cellulose is apparently determined by decreasing particle size and generating more available surface, rather than reducing the crystallinity.

Recent investigations have revealed that native cellulose crystal is the composite of two different crystalline components, cellulose I α and I β , and that cellulose I α is rich in the algal-bacterial type celluloses, whereas cellulose I β is dominant in the cotton-ramie type celluloses [Atalla & VanderHart, 1984; VanderHart & Atalla, 1984, Horii et al., 1987; Horii, 1989] which exist in cotton, ramie and other higher plants. The cellulose from the tunic of *Halocynthia* sp. exists in a pure I β phase [Belton et al., 1989] and cellulose I β is a dominant component in wood cell walls [Wada et al., 1994]. The cotton-ramie type cellulose is usually used as substrate for the measurement of exo-cellulase activity.

The contact between enzymes and cellulose molecule is restricted because the cellulosic materials such as Avicel and pulp are not water-soluble. In addition, the microfibrils present in these substrates are always tightly aggregated and have many complex hydrogen-bonding. Therefore, the difficulty of the enzymatic hydrolysis of crystalline cellulose is not enough explained only by the morphological changes of the residual cellulose. In this chapter, the features of the residues of some crystalline cellulose of cotton-ramie type after severe degradation with the cellulase and discussed focusing on the influence of aggregation of microfibrils on the cellulase attack.

2. EXPERIMENTAL

(1) Substrates.

The following cotton-ramie type cellulose which is dominant in cellulose I β : Avicel (PH-101, Asahi Chemical Co.), cotton linter pulp (dp 3500), and tunic of *Halocynthia* sp. commercially obtained. The tunic of *Halocynthia* sp. was repeatedly bleached with 0.3% NaClO₂ in an acetate buffer at pH 4.9. This sample was soaked in 5% KOH overnight and washed thoroughly with distilled water [Sugiyama et al., 1990], and then defiberized in a refiner (FPI mill) with a clearance of 0.3 mm. Avicel was boiled with 2.5 N hydrochloric acid for 15 min in order to eliminate amorphous region and contamination. The neutral sugar composition of Avicel was performed with potassium borate buffer of pH 8.8 at 60 °C and was analyzed by ion-exchange chromatography [column: Sugar AXI (Toso Co. Ltd.), Length 0.46 x 15 cm] following by the method of Honda et al [1981].

(2) Enzymatic hydrolysis.

All the samples were hydrolyzed with a commercial enzyme preparation, "Meicelase" (Meiji Seika Kaisha, Tokyo, Japan) derived from *Trichoderma viride*. The enzyme had 0.40 U/mg of filter paper degrading activity, 4.9 U/mg of CMC-Na degrading activity and 0.94 U/mg of cellobiase activity. Avicel (200 mg, dry weight) was incubated in 10 mL of a 0.1 M sodium acetate buffer (pH 4.8) with enzyme (0-400 mg) at 40 °C for 2 days. The reaction mixture was separated by filtration through sintered glass crucible (G-4) into the residue and filtrate. The residue was thoroughly washed with distilled water, then freeze-dried and weighed. The enzymatic susceptibility was calculated as the ratio of weight loss to initial sample weight and yield of reducing sugar. The control was incubated without enzyme. The amounts of reducing sugar in the filtrate were measured according to the Somogyi-Nelson's method. The neutral

sugar composition was determined as described in Chapter 2. Avicel was also treated with enzyme up to 10 days. In addition, *Halocynthia* cellulose and cotton linter pulp were treated up to 28 days.

(3) Observation by TEM.

Some of the freeze-dried residues were suspended in water or 50% EtOH. A drop from each suspension was deposited on a carbon-coated grid and observed with a TEM (JEM-2000EX, JEOL, Japan) with staining of 1.5% uranyl acetate for imaging. The results were recorded on Mitsubishi electron microscopic films (MEM).

(4) X-ray diffraction and electron diffraction.

X-ray diffraction sample disks were prepared by compression at 200 kgf/cm² under a vacuum. An X-ray diffractometer (JDX-8200, JEOL, Japan) generated at 50 kV and 120 mA. The crystal dimensions of three main equatorial reflections of cellulose, which were (1 $\bar{1}$ 0), (110) and (200) planes, were determined using Sherrer's equation [1918]. Using the Bragg's equation, the *d*-spacings of the (1 $\bar{1}$ 0), (110) and (200) planes were calculated from the 2θ of the X-ray diffraction profiles [Bragg, 1913]. The crystallinity indices (CrI) of the initial samples were calculated from X-ray profiles by the method of Knolle and Jayme [1965]. For electron diffraction, the samples prepared for TEM observation were used without any treatment or shadowed by gold.

(5) Solid-state CP-MAS ¹³C-NMR.

¹³C-NMR spectra were obtained with a GSX-400 (JEOL, Japan) operating at 50 MHz. Recycle time of pulse was 10 s. The spectra were accumulated ca. 100 times.

3. Results

(1) Features of Avicel residues after treatment with large quantity of cellulase.

The Avicel used was composed of 95% of glucose, 2.4% of xylose, and 2.4% of mannose residues. The neutral sugar composition of enzymatic hydrolyzates was dominantly glucose and a small amount of xylose (0.8-2.9%). The hydrolyzate treated with 25 mg to 300 mg of cellulase per 200 mg of Avicel contained 1.9-2.3% of cellobiose.

Fig. 3-1 shows the relationship between the hydrolysis rates (weight loss and yield of reducing sugar) of Avicel and the amounts of cellulase. The more the quantity of cellulase was used, the higher the reducing sugar yield and the weight loss were obtained. The weight loss was slightly higher than the reducing sugar yield. The difference was due to small amounts of cellobiose in the hydrolyzate.

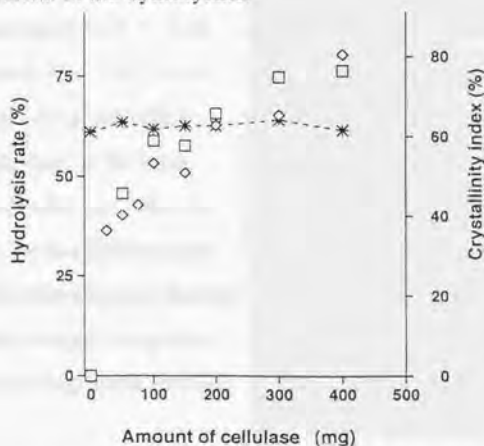


Figure 3-1. Relationships between hydrolysis rates (weight loss and reducing sugar yield) and amounts of cellulase.

Note: Avicel (200 mg in 10 mL of a 0.1 M acetate buffer at pH 4.8) was treated with 25 mg to 400 mg cellulase at 40°C for 48 h. Legend: □: weight loss, ◇: reducing sugar yield, +: crystallinity index (CrI) of hydrolysis residue.

Therefore, the weight loss was considered to permit an adequate evaluation of the enzymatic hydrolysis rate. The weight loss became 77% by use of the largest excess of cellulase (400 mg). The weight loss increased greatly with increasing the enzyme treated from 0 mg to 100 mg. However, the weight loss slightly increased in the residues treated with increasing the enzyme amount up to 400 mg.

The untreated Avicel contained large particles with several tens' μm in length and width, and fibrous small particles with a few μm in length (Fig. 3-2a). The large particles seemed to be too thick for the electron to pass through. The electron diffraction of the untreated Avicel could not be clearly obtained. Fig. 3-2b shows the changes of morphology and diffraction pattern in the residues of the treatment with 400 mg of cellulase. After enzymatic hydrolysis, the small fibrous particles disappeared and the electron density of the large particles became lower than that initial one and the length was less than $20 \mu\text{m}$.

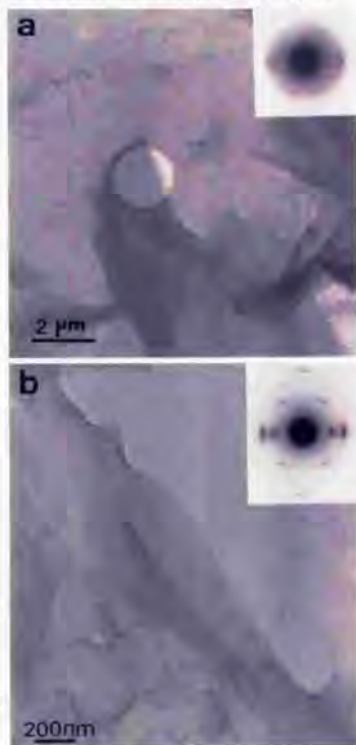


Figure 3-2. Electron micrographs and diffraction patterns (inset) of Avicel treated with cellulase; **a**: untreated; **b**: treated with of 400 mg.

The cellulose microfibrils in the large particles were observed to be tightly packed, and the outer parts of the particles were fibrillated. The arc of the diffraction pattern became narrow in both width and length being close to spot. The diffraction spots of the $(1\bar{1}0)$ and (110) planes were separated distinctly, and the other diffraction spots such as the (002) , (004) and (102) planes appeared clearly. Many diffraction spots were observed in the residues treated with 400 mg of cellulase (Fig. 3-2b).

The X-ray diffraction profiles in the residual Avicel are shown in Fig. 3-3. The heights of the (200) plane of the enzymatic hydrolysis residues decreased according with increasing the quantity of cellulase. The crystallinity index (CrI) of untreated Avicel and the enzymatically hydrolyzed residues were 61.1% and 65.4-67.2% (Fig. 3-1). The dimension of crystalline region at the (200) planes in untreated Avicel and the enzymatically hydrolyzed residues were 4.27 nm and 4.17-4.30 nm.

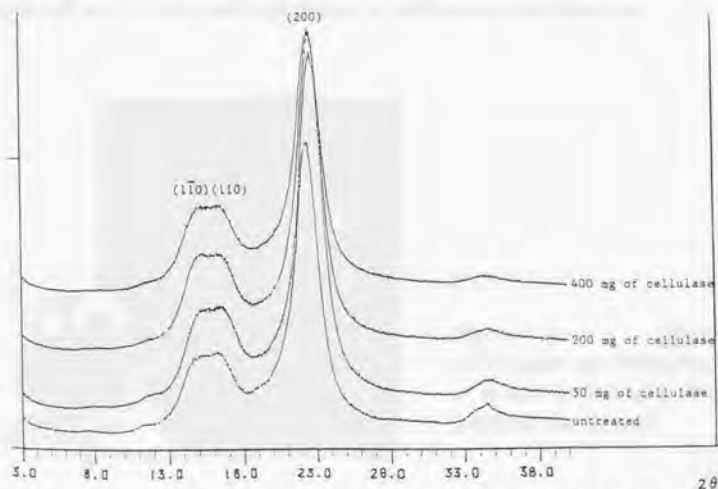


Figure 3-3. X-ray diffraction profiles of Avicel treated with various amounts of cellulase.

In the results of ^{13}C -NMR of the residual Avicel, the height of the peaks of C4 and C6 became higher than that of the untreated Avicel, and the peaks of C2, C3 and C5 were separated more clearly.

(2) Features of Avicel residues after cellulase treatment over a long period of time.

The weight loss and the rate of reducing sugar yield of Avicel treated with cellulase for 10 days was 95% and 97%, respectively. The neutral sugar composition of the enzymatic hydrolyzate was 69.1% of glucose, 9.6% of cellobiose and small portion of xylose.

The morphological change of the residual Avicel was essentially the same as observed in the Avicel residues after the treatment with 400 mg of cellulase. The large particles became thinner and shorter than the initial ones. The microfibrils aggregated tightly, was clearly observed in the residues, and was partly fibrillated in the outer part of the particles (Fig. 3-4). In the electron diffraction diagrams, each of the diffraction spots could be observed very clearly and high degree of diffraction was obtained.



Figure 3-4. Electron micrograph and diffraction pattern of Avicel treated with 50 mg of cellulase for 10 days.

The results of the X-ray diffraction analysis and solid state ^{13}C -NMR analyses were almost the same as those of the Avicel residue after the 400 mg of cellulase treatment. The CrI was 64%, and the crystallite width from the (200) peak was 4.43 nm. These data were considered to be identical with the untreated Avicel.

(3) Features of *Halocynthia* cellulose and cotton linter pulp residues after cellulase treatment over a long period of time.

Fig. 3-5 shows the weight loss of *Halocynthia* cellulose and cotton linter pulp with cellulase treatment for 3-28 days. The neutral sugar in the enzymatic hydrolyzate comprised dominantly glucose both for the *Halocynthia* cellulose and cotton linter pulp. The CrI in the enzymatic hydrolysis residues of *Halocynthia* cellulose decreased slightly with increasing the treated period, while that in the enzymatically hydrolyzed residues of cotton linter pulp changed little during the enzyme

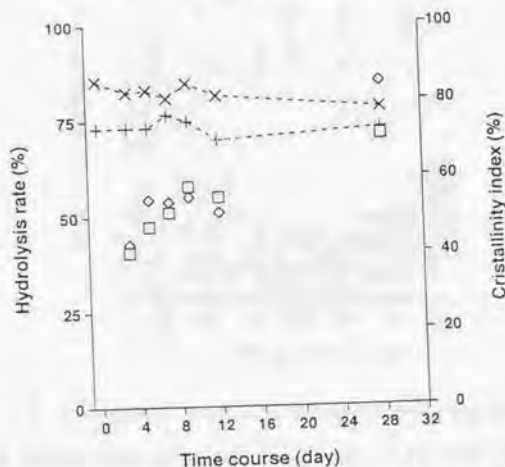


Figure 3-5. Changes of weight loss and crystallinity index during time course.
 Legend: Weight loss: *Halocynthia* cellulose (□) and cotton linter pulp (◇);
 crystallinity indexes: *Halocynthia* cellulose (x) and cotton linter pulp (+).

treatment. Fig. 3-6 shows the changes of the crystal dimensions in the time course of enzyme treatment. In the residues of *Halocynthia* cellulose and cotton linter pulp, the crystal dimensions at the $(1\bar{1}0)$, (110) and (200) planes did not change from the initial ones, except that the crystal dimension at the (200) plane of *Halocynthia* cellulose residues slightly decreased. In both the residues of the *Halocynthia* cellulose and cotton linter pulp, the d -spacings of the $(1\bar{1}0)$, (110) and (200) planes did not change from those of initial samples, either (0.593, 0.529, and 0.386 nm for *Halocynthia* cellulose; 0.591, 0.530 and 0.389 nm for cotton linter pulp).

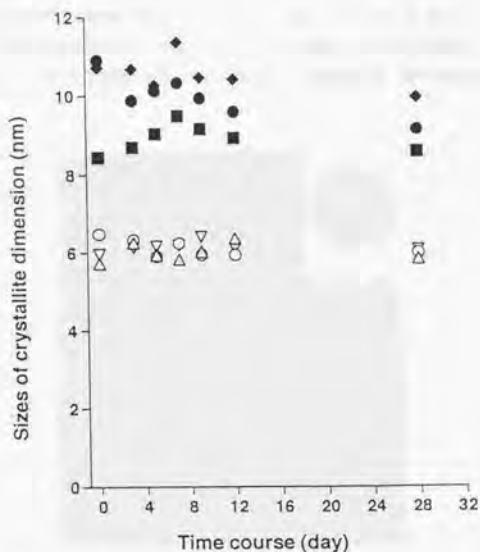


Figure 3-6. Changes of crystallite dimensions during time course.

Legend: *Halocynthia* cellulose: $(1\bar{1}0)$ (■), (110) (◆), and (200) (●); cotton linter pulp: $(1\bar{1}0)$ (△), (110) (▽), and (200) (○).

Fig. 3-7 shows the electron micrograph and diffraction patterns of the enzymatically hydrolyzed residue of *Halocynthia* cellulose with cellulase treatment for 28 days. While the microfibrils of the untreated *Halocynthia* cellulose were tightly packed in the form of the bundles, in the residual cellulose the bundles were untied and the microfibrils aggregated was separated into a single or a few microfibrils. These microfibrils of *Halocynthia* cellulose became thinner or fibrillated partly along to the axis with the enzyme treatment. In addition, the microfibrils were split from the ends to the subfibrils. The length did not change remarkably from those of the initial microfibrils. The electron diffraction diagram of the enzymatically treated *Halocynthia* cellulose is shown in Fig. 3-7. The outer part of the diffraction spots, which were observed in the untreated *Halocynthia* cellulose microfibrils, could not be obtained in the enzymatically hydrolyzed residue. The results were the same as those of cotton linter pulp residue after cellulase treatment for 28 days.



Figure 3-7. Electron micrograph and diffraction patterns of the hydrolysis residue of *Halocynthia* cellulose treated with cellulase for 28 days. Note: Fibrillation was observed partly (arrowheads).

4. Discussion

A most unique feature in the enzymatically hydrolyzed cotton-ramie type cellulose such as Avicel, *Halocynthia* and cotton cellulose was that the inherent crystalline properties such as crystallinity, dimensions of crystalline region, and *d*-spacing continued to be kept in the residues even if most of the celluloses were degraded. There were no remarkable changes in the CrIs and *d*-spacings calculated from the X-ray diffraction profiles in any enzymatically hydrolyzed residues. The increase of the CrI of the enzymatic hydrolysis residues has been reported about ramie [Hermans & Weidinger, 1949], cotton, Avicel, baggas pulp, straw pulp, and saw dust [Betrabet et al., 1974; Betrabet & Paralikar, 1977; 1978], and α -cellulose of southern pine [Caufield & Moore, 1974]. It was considered that these results were caused by the selective hydrolysis of the amorphous region in the cellulose samples, and that the enzymatically hydrolyzed residues should mainly contain crystalline region. The celluloses studied in Chapter 3 contained lower amorphous region than those in these reports. This should be a reason that the changes of CrIs were small.

A high degree of diffraction was obtained from the electron diffraction of the residual cellulose and the arcs of the diffraction spots decreased in their width and length. This indicated that the residual cellulose consisted of highly ordered cellulose molecular chains in cellulose microfibrils. The results were also confirmed by the results of the X-ray diffraction analysis and ^{13}C -NMR.

The size of the crystalline region of the cellulose has been considered to be one of factors influencing the enzymatic attack of cellulose [Fan et al., 1980; Walker & Wilson, 1991]. The decrease of the peak height of the (200) of X-ray diffraction diagram in the residual

cellulose, especially in *Halocynthia* cellulose, suggested that the (200) plane should be most sensitive to the enzymatic attack. This has also been reported in the enzymatic hydrolysis of bacterial and *Valonia* cellulose by Chanzy and Henrissat [1983b; 1984; 1985]. The enzymatic hydrolysis rate was 100% for Sugi holocellulose treated for 2 days (unpublished data), 97% for Avicel treated for 10 days, 85% of cotton linter pulp and 71% of *Halocynthia* cellulose treated for 28 days, respectively. Sugi holocellulose and Avicel were more susceptible than cotton linter pulp and *Halocynthia* cellulose. The difference seemed to be owing to both the crystallinity index (CrI) and the size of the crystalline regions. The CrI of Sugi holocellulose and Avicel was lower than that of cotton linter pulp and *Halocynthia* cellulose (Sugi holocellulose: 48.4% (unpublished data), Avicel: 61.1%, cotton linter pulp: 73.1%, and *Halocynthia* cellulose: 85.4%), and the dimension at the (200) plane were 2.8 nm for Sugi holocellulose (unpublished data), 4.41 nm for Avicel, 5.96 nm for cotton linter pulp, and 10.9 nm for *Halocynthia* cellulose. The ratio of the appearance of the cellulose molecular chains on the surface area depends on the dimensions of the crystalline region [Walker & Wilson, 1991]. The results obtained that the larger surface area of the crystal was the smaller enzymatic susceptibility was.

The aggregation of the cellulose microfibrils has also been considered to be one of factors affecting the enzymatic digestibility. Since Avicel was hydrolyzed by acid and air-dried in the manufacturing process, the cellulose microfibrils are highly ordered and tightly aggregated and has a high crystallinity [Akishima et al., 1992]. This should be the cause of difficulty for Avicel to hydrolyze with enzyme comparing with Sugi holocellulose. These are the same as the "white material", which introduced in the Chapter 2, and the microfibrils of the *Halocynthia* cellulose which were also tightly aggregated. In the cases of

Halocynthia cellulose, the crystallite dimensions were so large that the enzymatic hydrolysis process was slower than Avicel.

Therefore, the degradation process in such aggregated cellulose microfibril is speculated as follows: From the outer part of the particle, single or several cellulose microfibrils produced with cellulase by peeling. Then the ends of these microfibrils became thinner in the ends or were split from the ends to the subfibrils and digested immediately with cellulase. The "highly crystalline microfibril" treated by acid [Revol et al., 1992] had almost the same size as cellulose microfibril in the enzymatically hydrolyzed residue. This means that the single microfibril was probably yielded by peeling with the minimum enzyme aid. The "highly crystalline microfibril"s were also split from the ends to the subfibril by the enzymatic hydrolysis [Hayashi et al., 1994], as reported by White and Brown [1981; 1982], Chanzy and Henrissat [1983a; 1983b; 1984; 1985; 1986].

In conclusion, the aggregation of cellulose microfibrils was loosen with cellulase little by little from the surface contained the highly ordered cellulose microfibrils. The enzymatic degradation was accompanied with fibrillation on the surface of the crystals or with the formation of the subfibrils from the end, especially in the microfibril of *Halocynthia* cellulose, which has a large dimension. The inherent crystalline properties of cellulose microfibrils were kept until the celluloses were degraded completely. Their differences of degradation was explained in the cellulose microfibrils (cellulose I β) by their size and condition of the microfibrils' aggregation.

5. Summary

Avicel, cotton linter pulp, and *Halocynthia* sp. cellulose (cotton-ramie type cellulose: rich in cellulose I β) were extensively hydrolyzed with a cellulase prepared from *Trichoderma. viride* either using a large quantity of enzyme or treating it over a long period of time. The hydrolysis residues (weight loss : 77%) were examined by transmission electron microscopy (TEM), electron diffraction and X-ray diffraction, and solid state cross polarized magic angle spinning (CP-MAS) ^{13}C -NMR spectroscopy. TEM observation showed that the particles in the hydrolysis residue of Avicel were composed of tightly packed microfibrils. In electron diffraction diagrams of the residues, the $(1\bar{1}0)$ and (110) planes were separated distinctly, and the other diffraction spot such as the (002) , (004) and (102) planes appeared clearly. From the X-ray diagrams of the residues, the crystallinity index (CrI) of the hydrolysis residues was found to change little. These results suggested that the enzymatic hydrolysis residue of Avicel composed of highly ordered microfibrils. After the enzymatic hydrolysis, the microfibrils of *Halocynthia* cellulose and cotton linter pulp ultimately became thinner in the ends or was split to the subfibrils. Therefore, the aggregation of cellulose microfibrils was loosen with cellulase little by little from the surface. The enzymatic degradation was accompanied with fibrillation on the surface of the microcrystals in Avicel, whose dimensions were small, and with the formation of the subfibrils from the end in *Halocynthia* cellulose, which has large dimensions. The difference of degradation rate should be explained from the size and the aggregation of the microfibrils.

Keywords: Cellulose I β , Cellulase, Cellulose microfibril, Aggregation

Chapter 4. Enzymatic susceptibility of cellulose microfibrils of the algal-bacterial type and the cotton-ramie type

1. Introduction

The cellulase system from potent cellulolytic fungi such as *Trichoderma* species possesses endo-(1 → 4)-β-D-glucanases attacking randomly within the cellulose chain, exo-(1 → 4)-β-D-glucanases splitting either cellobiose or glucose from the non-reducing end of cellulose, and a β-D-glucosidase that converts cellobiose and other cello-oligosaccharides to glucose [Wood & McCrae, 1979; Eveleigh, 1985].

The enzymatic hydrolysis of cellulose, particularly hydrogen-bonded and ordered crystalline cellulose, is a very complex process. As the cellulose is insoluble, the cellulases must diffuse and fit themselves to the structural feature of the substrate. A number of investigators regarded the crystallinity, the surface accessibility and the particle size of cellulosic substrates as the major factors affecting enzyme hydrolysis [Walker & Wilson, 1991]. The relationship between the fine structural features and the digestibility in cellulosic materials should be clarified, not only for achieving effective glucose production, but also for better understanding of the reaction mechanism.

Marrinan and Mann [1956] have indicated the difference of the cellulose crystals. Recent investigations have revealed that native cellulose crystals are the composite of two different crystalline components, cellulose I_α and cellulose I_β, and that cellulose I_α is rich in the algal-bacterial type celluloses, whereas cellulose I_β is dominant in the cotton-ramie type celluloses. The following information has been also obtained: (1) Cellulose I_α and cellulose I_β should have different hydrogen-bondings system. The difference was first demonstrated by Raman spectroscopy [Atalla & VanderHart, 1984; VanderHart & Atalla, 1984; Weiley &

Atalla, 1987a; 1987b; Horii et al., 1987; Atalla & VanderHart, 1989] and also confirmed by FTIR spectroscopy [Michell, 1990; Sugiyama et al., 1991]. (2) Cellulose I_{α} can be transformed into cellulose I_{β} by hydrothermal annealing in the presence of NaOH, therefore cellulose I_{β} is thermodynamically more stable than cellulose I_{α} [Horii et al., 1987; Yamamoto et al., 1989; Sugiyama et al., 1990]. (3) Cellulose I_{β} from the tunic of *Halocynthia sp.* exist in a pure I_{β} phase [Belton et al., 1989]. (4) Cellulose I_{α} and cellulose I_{β} are characterized as crystals consisting of triclinic structure with one chain per unit cell and monoclinic structure with two chains per unit cell, respectively, and the theoretical density of the monoclinic unit cell is slightly larger than that of the triclinic unit cell [Sugiyama et al., 1991]. (5) Hackney et al. [1994] and Uhlin et al. [1995] also suggested the presence of superlattice-like structure, in which the cellulose I_{α} and cellulose I_{β} domains co-exist throughout the cross-section of each microfibril. (6) It is noteworthy that cellulose I_{β} is dominant in wood cell walls [Wada et al., 1994].

The accessibility of cellulose dimorphs (I_{α} / I_{β}) to chemicals as well as biochemical reactions has been so far less studied in comparison to their structural characterization. Atalla and VanderHart have reported the acid hydrolysis residue of highly crystalline cellulose from *Rhizoclonium heiroglyphicum* and *Cladophora gromerata* investigated by solid state CPMAS ^{13}C NMR spectroscopy, that in the *Rhizoclonium* cellulose I_{α} and cellulose I_{β} were equally susceptible to acid hydrolysis [1985], but in the *Cladophora* cellulose I_{α} was degraded more rapidly than cellulose I_{β} [1989]. Kim and Newman [1994] suggested from ^{13}C NMR analysis of Korean red pine in brown rot decay that cellulose I_{α} was preferentially degraded. Both results suggested that the cellulose I_{α} component is more susceptible to enzymatic attack, but that fact was not clearly established. In this chapter, the dimorphs in the microfibrils of various native celluloses

was quantitatively analyzed on the susceptibility of *Trichoderma viride* cellulase. For this, the enzymatic susceptibility was examined by the weight loss during the degradation process, and the hydrolysis residues were analyzed by FTIR spectroscopy and by electron diffraction.

2. Experimental

(1) Substrates.

Two types of substrates were used. One was (a) the algal-bacterial type cellulose that is rich in cellulose I α : bacterial (*Acetobacter xylinum*) cellulose gel, cell walls of *Valonia* sp. harvested from Wakayama, Japan, and *Cladophora* sp. collected in Chiba, Japan. The other was (b) the cotton-ramie type cellulose that is dominant in cellulose I β : tunic of *Halocynthia* sp. commercially obtained, cotton linter pulp (dp 3500), bleached softwood pulp (dp 750 and 1500), bleached hardwood pulp (dp 1500), and Avicel (PH-101, Asahi Chemical Co.). Purification for some of the samples was needed to remove non-cellulosic substances and homogenization was carried out to avoid the aggregation of cellulose microfibrils. The pellicles of bacterial cellulose were purified by boiling in 1% NaOH for 10 h under a stream of N₂ gas, then washing with distilled water [Kai & Xu, 1990], homogenization into small fragments and freeze-drying. The vesicles of *Valonia* sp. were purified by the procedure of Gardner and Blackwell [1974] and treated acid-mechanically by the method of Chanzy and Henrissat [1983a]. The tunic of *Halocynthia* sp. was repeatedly bleached in 0.3% sodium chlorite in an acetate buffer at pH 4.9. This sample was soaked in 5% KOH overnight and washed thoroughly with distilled water [Sugiyama et al., 1990], and then homogenized into small fragments and freeze-dried. Avicel was boiled in 2.5 N HCl for 15 min and thoroughly washed with distilled water.

(2) Enzymatic hydrolysis.

All the samples were hydrolyzed with a commercial enzyme preparation, "Meicelase" (Meiji Seika Kaisha., Tokyo, Japan) derived from *Trichoderma viride*. The enzyme had 0.40 U/mg of filter paper degrading activity, 4.9 U/mg of CMC-Na degrading activity and 0.94 U/mg of cellobiase activity. The substrate (200 mg) in 10 mL of 0.1 M sodium acetate buffer (pH 4.8) was incubated with enzyme (50 mg) at 40 °C for 2 days, except the bacterial cellulose. The bacterial cellulose was incubated for 0.5 and 1 h because this sample was quite degradable with the cellulase. The reaction mixture was separated by centrifugation into the residues and products. The precipitate was thoroughly washed with 0.1 N NaOH solution to remove the enzyme adsorbed on the surface of the residual cellulose microfibrils and washed distilled water, and then freeze-dried and weighed. The enzymatic susceptibility was calculated as the ratio of weight loss to the initial sample weight. The enzymatic treatment was repeated twice or more replacing cellulase solution until the samples were hydrolyzed about 80-90% from initial weight on the residues of the *Cladophora* and *Halocynthia* cellulose, which have almost the same crystal dimensions. This treatment was also repeated on the residues of *Valonia*.

(3) Hydrothermal treatment

Some bacterial cellulose was subjected to a hydrothermal treatment. The purified and homogenized cellulose sample was inserted into a glass ampule with a small amount of 0,1 N NaOH. This sample was sealed and placed in an autoclave at 260 °C for 30 min, then cooled in tap water. The annealed sample was washed thoroughly with distilled water and then freeze-dried. This sample was also treated with the cellulase in the same fashion. The samples before and after the hydrothermal treatment showed almost the same crystallinity.

(4) Observation by TEM

Some of the freeze-dried residues were suspended in water. A drop from each suspension was deposited on a carbon-coated grid and observed with the transmission electron microscope (TEM; JEM-2000EX, JEOL, Japan) with staining of 1.5% uranyl acetate for imaging. The results were recorded on Mitsubishi electron microscopic films (MEM).

(5) FTIR spectral analysis

FTIR spectra were obtained from the samples mounted on a potassium bromide disk using an FTIR instrument equipped with an ordinary microscopic accessory (FT/IR-7300+Micro 20, Janssen, Japan; Nicolet-Magna 550 FT-IR, France). The wave number range scanned was $3800\text{--}650\text{ cm}^{-1}$; 64-200 scans of 4 cm^{-1} resolution were signal averaged and stored.

(6) X-ray diffraction and electron diffraction

From the characterization of the cellulose I_{α} (triclinic) and cellulose I_{β} (monoclinic), $(1\bar{1}0)$, (110) and (200) planes in the two-chain monoclinic unit cell are, respectively, equivalent to (100) , (010) and (110) planes in the one-chain triclinic unit cell [Sugiyama et al., 1991]. Here, we used the monoclinic indices to represent the Millar's indices of the two crystal systems. X-ray diffraction profiles were obtained with a JDX-8200 (JEOL, Japan) instrument. The separation of peaks in X-ray profiles was carried out using a least-squares refinement program by the method of Wada et al. [1993]. The diffraction angle was calibrated for each run with titanium oxide ($d = 0.2487\text{ nm}$). The crystal dimensions of three main equatorial reflections of cellulose, which were $(1\bar{1}0)$, (110) and (200) planes respectively, were determined using Sherrer's equation [1918]. The crystallinity indices (CrI) of the initial samples were calculated from X-ray profiles by the method of Knolle and Jayme [1965]. The samples

prepared for electron diffraction were used without any treatment or shadowed by gold.

3. Results

Table 4-1 shows the changes of weight loss, crystal dimension and the ratio of cellulose $I\alpha$ and cellulose $I\beta$ by the 2 days of enzymatic hydrolysis. Only the bacterial cellulose was examined at short intervals of 0.5 and 1 h of enzymatic hydrolysis. The peaks of (1 $\bar{1}$ 0) and (110) planes from the profiles of Avicel and pulp samples could not be separated clearly, and the crystal dimensions of (1 $\bar{1}$ 0) and (110) planes were not calculated, either.

Table 4-1 The changes of weight loss, crystal dimension and ratio of $I\alpha/I\beta$ on various native celluloses before and after the enzymatic hydrolysis.

Sample (CrI (%))	Time course	Weight loss (%)	Crystallite dimension (nm)			Ratio of $I\alpha/I\beta$ (%)
			110	110	200	
Valonia (87)	0 day	0	14.8	16.9	23.0	34/66
	2	46	14.8	16.9	23.0	16/84
Cladophora (82)	0 day	0	11.0	9.2	14.3	54/46
	2	52	10.5	9.1	11.0	50/50
bacterial (69)	0 hr	0	6.2	6.4	6.3	44/56
	0.5	68	5.7	6.2	6.1	26/74
	1.0	97	6.3	5.9	5.3	10/90
Halocynthia (86)	0 day	0	7.9	8.7	10.0	
	2	38	8.0	8.5	9.6	
cotton linter (73)	0 day	0	5.8	6.5	6.0	
	2	44	6.3	6.3	6.1	
Avicel HCl (63)	0 day	0	-	-	4.4	
	2	40	-	-	4.7	
soft wood pulp (DP=1000) (61)	0 day	0	-	-	4.6	
	2	39	-	-	4.3	
soft wood pulp (DP=2100) (59)	0 day	0	-	-	4.6	
	2	37	-	-	4.7	
hard wood pulp (DP=900) (56)	0 day	0	-	-	3.9	
	2	37	-	-	4.1	

It was also noted that short microfibrils became prominent during the enzymatic hydrolysis from the TEM observation of the residual *Cladophora* cellulose (Fig. 4-1).

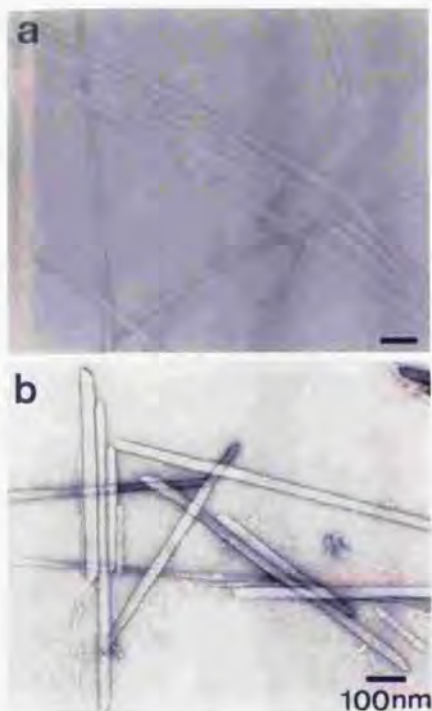


Fig. 4-1. The electron micrographs of the *Cladophora* cellulose microfibrils; (a) untreated, (b) hydrolyzed with cellulase for 2 days.

4. Discussion

The results of the weight loss in various cellulose samples suggested that the algal-bacterial type cellulose microfibrils seemed to be more susceptible to the enzymatic attack than the cotton-ramie type ones.

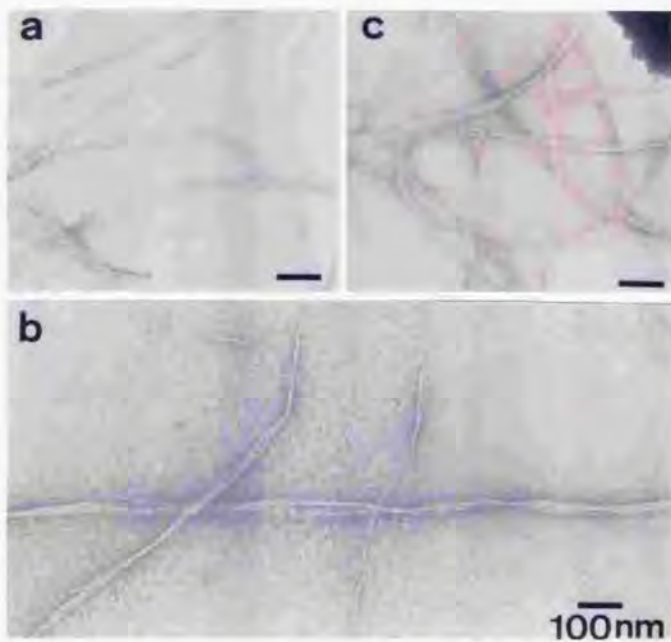


Fig. 4-2. The electron micrographs of the bacterial cellulose microfibrils; (a) untreated, (b) after hydrolysis with CBH I purified from the Meicelase, for 10 min and then treated with ultrasonic for 10 min, (c) after ultrasonic treatment for 20 min without enzymatic hydrolysis.

Interestingly, the bacterial cellulose was hydrolyzed with the enzymes quite easily. The morphological changes were compared in bacterial cellulose microfibril under different conditions: (a) control; (b) after hydrolysis for 10 min with CBH I purified from the Meicelase, which was a main component of the *T. viride* cellulase, and then ultrasonic treatment for 10 min; (c) ultrasonic treatment for 20 min. The results are shown in Fig. 4-2a-c. The untreated microfibrils were not fibrillated (Fig. 4-2a), but after the enzymatic hydrolysis the microfibrils

were fibrillated uniformly into bundles of thin subfibrils and some became short subfibrils (Fig. 4-2b). The microfibrils under only ultrasonic treatment were not different from the control sample, but partly fibrillated (Fig. 4-2c). White [1982] and Brown et al. [1983] have also reported the fibrillation of the ribbon of bacterial cellulose in the enzymatic degradation process. If the breakdown of the hydrogen bonding between subfibrils occurs by the enzyme, the resulting increase of the surface in the thinned subfibrils should be effective for following enzymatic attack. The rapid fibrillation during such a short incubation was not observed in the other cellulose samples. This might be the reason of the high degradability of the bacterial cellulose microfibrils and the bacterial cellulose should be a unique substrate for cellulase.

The CrI and surface area have been considered to be important factors for determining enzymatic susceptibility. Therefore, the CrI of cellulose substrates were determined before the enzymatic hydrolysis (Table 4-1). In the algal-bacterial type cellulose, the CrI of bacterial cellulose was 69%, *Cladophora*, 82%, and *Valonia*, 87%. The enzymatic susceptibility became higher in the order, bacterial cellulose, *Cladophora* cellulose, *Valonia* cellulose (Table 4-1). Thus there was a reasonable relationship between the CrI and the enzymatic susceptibility, namely the lower CrI of the sample was the more susceptible it was to enzymatic attack. In the cotton-ramie type cellulose, the CrI of *Halocynthia* cellulose was 86%, cotton linter pulp, 73%, acid treated Avicel, 63%, softwood pulp, 60%, and hardwood pulp, 56%. There was not a similar correlation in the cotton-ramie type between the enzymatic susceptibility and the CrI. As described in Chapter 3, the size of the cellulose crystallites and aggregation of cellulose microfibrils should play a major factor in determining the enzymatic susceptibility of the cotton-ramie type cellulose. Although the CrIs of the algal-bacterial cellulose were higher

han those of cotton-ramie type, and crystal dimension of the algal-bacterial type cellulose were greater than those of the cotton-ramie type, the algal-bacterial type cellulose was more susceptible than the cotton-ramie type cellulose.

The difference of crystalline dimorphs ($I\alpha/I\beta$) in the two types of cellulose may have an influence on the enzymatic action on the crystalline cellulose. Hydrothermal treatment transforms cellulose $I\alpha$ into cellulose $I\beta$ [Horii et al., 1987; Yamamoto et al., 1987; Sugiyama et al., 1990]. The effects of annealing on the enzymatic susceptibility of bacterial cellulose were studied. The morphological change of the annealed bacterial cellulose is shown in Fig. 4-3. The microfibrils were observed to shorten but not to form tight aggregation. The CrI was not changed after the annealing. After an 1h-enzymatic hydrolysis, the weight loss was 91% for the unannealed bacterial cellulose and 56% for the annealed sample, respectively. Bacterial cellulose was a highly degradable substrate, but the conversion of cellulose $I\alpha$ to cellulose $I\beta$ seemed to inhibit the enzymatic hydrolysis to some extent. The crystalline dimorphs ($I\alpha/I\beta$) may have much more influence on the enzymatic action on the crystalline cellulose, rather than the CrI and surface area.



Fig. 4-3. The electron micrograph of the bacterial cellulose after the hydrothermal treatment under NaOH.

The composite make-up of the residual cellulose was clarified with FTIR absorption and electron diffraction. In Figure 4-4, the IR spectrum around the region of 3600-2800 cm^{-1} of *Valonia* and *Halocynthia* cellulose are compared before and after the enzymatic hydrolysis. The absorption band near 3240 cm^{-1} is assigned to the cellulose I_{α} , whereas the absorption band near 3270 cm^{-1} is assigned to the cellulose I_{β} [Michell, 1990; Sugiyama et al., 1991a]. *Halocynthia* cellulose did not show any absorption at 3240 cm^{-1} at any rate. On the other hand, the absorption band at 3240 cm^{-1} in *Valonia* cellulose almost disappeared after 60h of enzymatic hydrolysis. This disappearance of the absorption band in *Cladophora* cellulose were also observed in the specimens after the enzyme hydrolysis. It is shown in Fig. 4-5 that the absorption band at about 3240 cm^{-1} in the unannealed bacterial cellulose remarkably decreased after the 1h of enzymatic hydrolysis (Fig. 4-5a), and that in annealed bacterial cellulose the absorption band at 3240 cm^{-1} disappeared, and the cellulase seemed to bring about little effect on the cellulose I_{β} crystalline phase (Fig. 4-5b).

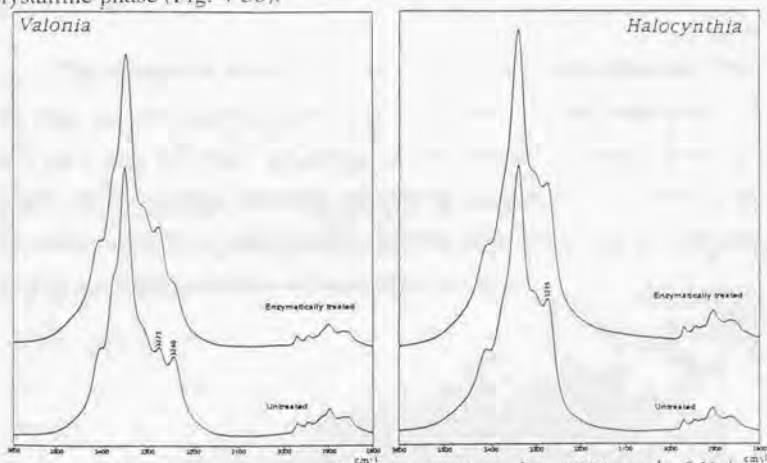


Fig. 4-4 FTIR spectra in the region from 3600 cm^{-1} to 2800 cm^{-1} of *Valonia* and *Halocynthia* celluloses. Note: the band near 3240 cm^{-1} is assigned as to cellulose I_{α} , the band near 3270 cm^{-1} is unique for cellulose I_{β} .

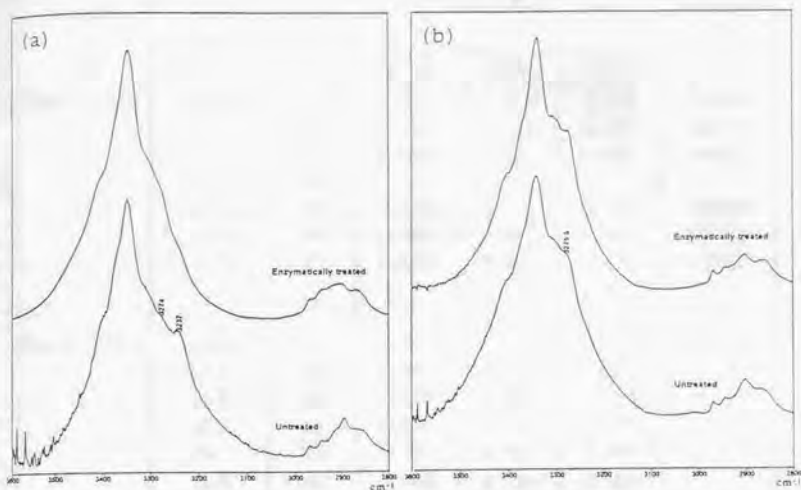


Fig. 4-5 FTIR spectra in the region from 3600 cm^{-1} to 2800 cm^{-1} of (a) unannealed and (b) annealed bacterial cellulose before and after enzymatic hydrolysis for 1 h.

The changes in the composition of cellulose I_{α} and cellulose I_{β} of the algal-bacterial type cellulose were calculated from the peak height of 750 cm^{-1} and 710 cm^{-1} according to the method of Yamamoto et al. [1994]. In the residual cellulose, cellulose I_{β} became rich (Table 4-1). In *Cladophora* cellulose, cellulose I_{β} was twice as much as that of cellulose I_{α} with increasing cellulase treatment (Table 4-2).

Table 4-2 The changes of weight loss, d -spacings and ratio of I_{α}/I_{β} of the residues of *Cladophora* and *Halocynthia* during the successional enzymatic hydrolysis.

sample	time course	weight loss (%)	d -spacing (nm)			ratio of I_{α}/I_{β} (%)
			(1 $\bar{1}$ 0)	(110)	(200)	
<i>Cladophora</i>	0 day		0.612	0.519	0.386	54/46
	2	52	0.599	0.523	0.387	50/50
	2+4	60	0.597	0.521	0.387	39/61
	2+4+2	69	-	-	-	
	2+4+2x2	75	0.599	0.522	0.387	36/64
	2+4+2x3	79	0.599	0.525	0.387	40/60
	2+4+2x4	82	0.602	0.526	0.388	37/63
<i>Halocynthia</i>	0 day		0.593	0.529	0.386	
	2x1	40	0.591	0.529	0.386	
	2x2	65	0.594	0.531	0.386	
	2x3	78	0.591	0.528	0.386	
	2x4	85	0.594	0.529	0.386	
	2x5	88	0.594	0.529	0.386	
	2x6	90	0.593	0.528	0.386	

The changes of the d -spacings of the residues of *Cladophora* and *Halocynthia* during the successive enzymatic hydrolysis are shown as dimension of (1 $\bar{1}$ 0), (110) and (200) planes in Table 4-2. The d -spacings from each crystalline phase have been reported: the I_{α} (triclinic) component; d_{100} = 0.621 nm, d_{010} = 0.528 nm, d_{110} = 0.397 nm and the I_{β} (monoclinic) component; $d_{1\bar{1}0}$ = 0.607 nm, d_{110} = 0.535 nm, d_{200} = 0.398 nm [Sugiyama et al., 1991b]. It is noted that d_{100} is larger than $d_{1\bar{1}0}$, and d_{010} is smaller than d_{110} . The d -spacings of the residues of the *Halocynthia* cellulose did not change during enzymatic degradation. The d_{100} ($d_{1\bar{1}0}$ in Table 4-2) of the residues of *Cladophora* cellulose became smaller, but the d_{010} (d_{110} in Table 4-2) became larger than the initial one. This was also observed in the residual cellulose of *Valonia*, so

that it was considered with respect to the d -spacings that the residual algal-bacterial type celluloses tended to become close to figures of the $I\beta$ phase in the advanced stages of enzymatic hydrolysis.

As shown in Fig. 4-4 and 4-5 and Table 4-2, the results of the FTIR absorption and electron diffraction diagrams indicate that the hydrolysis residues of the algal-bacterial type cellulose in the advanced stages of enzymatic hydrolysis were almost cellulose $I\beta$. It was suggested that the cellulose $I\alpha$ in the algal-bacterial cellulose microfibrils was hydrolyzed preferentially with cellulase, that is, the cellulose $I\beta$ was rather stable to the cellulase attack in comparison with the cellulose $I\alpha$. It was also considered that the preferential attack of the cellulase against the cellulose $I\alpha$ might be caused from the structural differences of the crystalline dimorphs ($I\alpha/I\beta$) such as the d -spacings, the theoretical density and the distribution of the two crystalline phases in the microfibril.

In the residual *Cladophora* cellulose, short microfibrils became prominent during the enzymatic hydrolysis (Fig. 4-1). When the bacterial cellulose was treated with *T. viride* CBH I and ultrasonic wave, some subfibrils cut into same length were observed in the resulting residues. Therefore, short microfibrils were thought to be formed during the enzymatic degradation from the algal-bacterial type cellulose. The formation of short microfibrils seemed to be related to the composition of cellulose dimorphs ($I\alpha/I\beta$) in the microfibril, and the findings was described in the other chapter. The results obtained were not preclude the presence of superlattice-like structure demonstrated by Atalla's group [Hackney et al, 1994; Uhlin et al., 1995]. It is also suggested that the domain composed mainly of cellulose $I\beta$ might exist in the cellulose microfibril of algal-bacterial type. The residual cellulose microfibrils of the cotton-ramie type became thinner and fibrillated with increasing the

enzyme treatment, but the formation of the short microfibrils was not observed.

The conclusions of this chapter are summarized as follows: (i) algal-bacterial type cellulose is more susceptible to the enzymatic attack than cotton-ramie type cellulose; (ii) cellulose I_{α} crystalline phase of the algal-bacterial type cellulose is degraded preferentially by *Trichoderma viride* cellulase and the residues become cellulose I_{β} phase dominant, and (iii) in the enzymatic degradation of algal-bacterial type cellulose, shortened microfibrils are observed. Further investigation is necessary to better understanding of the preferential degradation of cellulose I_{α} in the cellulose dimorphs.

5. Summary

Two types of substrates, the algal-bacterial type (rich in cellulose I_{α}) cellulose and the cotton-ramie type (dominant in cellulose I_{β}) cellulose, were degraded comparatively by *Trichoderma viride* cellulase. The algal-bacterial type cellulose microfibril was more susceptible than the cotton-ramie type. The residual cellulose microfibrils were observed by TEM and analyzed by FTIR and electron diffraction. It becomes clear that the residual cellulose of the algal-bacterial type cellulose was getting rich in the cellulose I_{β} with the lapse time of cellulase treatment. These results indicate that the cellulose I_{α} in the microfibril of the algal-bacterial type cellulose is hydrolyzed preferentially by the cellulase.

Keywords: Cellulose, algal-bacterial type; Cellulose, cotton-ramie type; Cellulase; Cellulose I_{α} ; Microfibril

Chapter 5. Selective degradation of the cellulose I_{α} component in *Cladophora* cellulose with *Trichoderma viride* cellulase

1. Introduction

The structural investigation of cellulose crystallite by solid-state CP/MAS ^{13}C NMR revealed spectral differences among samples of several cellulose origins [Atalla & VanderHart, 1984, VanderHart & Atalla, 1984, Horii, 1989; Yamamoto & Horii, 1993]. A crystalline model composed of cellulose I_{α} and cellulose I_{β} components was proposed, and it was reported that the algal-bacterial type celluloses are rich in cellulose I_{α} (triclinic), while cellulose I_{β} (monoclinic) is predominant in the cotton-ramie type celluloses. Atalla et al. suggested that these differences caused from the difference of the hydrogen-bonding pattern between cellulose I_{α} and I_{β} [Horii et al., 1984; Wiley & Atalla, 1987a; 1987b; Atalla & VanderHart, 1989]. It is investigated that the cellulose I_{α} is metastable and can be converted into I_{β} by hydrothermal treatment in the presence of NaOH [Sugiyama et al., 1990]. Sugiyama et al. [1991b] characterized these two crystalline structures: the triclinic structure with dimensions of $a = 0.674$ nm, $b = 0.593$ nm, $c = 1.036$ nm, $\alpha = 117^{\circ}$, $\beta = 114^{\circ}$, $\gamma = 81^{\circ}$, cell volume = 0.3395 nm 3 , and calculated density = 1.582; the monoclinic structure with dimensions of $a=0.801$ nm, $b=0.817$ nm, $c=1.036$ nm, $\alpha = \beta = 90^{\circ}$, γ (monoclinic angle) = 97.3° , cell volume = 0.6725 nm 3 , and calculated density = 1.599.

The mechanism of enzymatic degradation of crystalline cellulose is still poorly understood because of the complexity of the substrate: cellulose in nature is not water-soluble, fibrous and composed of both crystalline and amorphous regions. Wardrop and Jutte [1968], Chanzy and

Henrissat [1983a, 1983b; 1984] and Henrissat and Chanzy [1986] have observed that the hydrolyzed residue of the *Valonia* cellulose microcrystal becomes fibrillated or narrow after the treatment with *Trichoderma reesei* cellulase, and it was shortened by action of the cellulase from *Humicola insolens*. White and Brown [1981; 1982] also observed the fibrillation in the bacterial cellulose microfibril treated with cellulase derived from *T. viride*. No other detailed study has been reported on the enzymatic degradation of the crystals of the algal-bacterial type cellulose composed of two crystalline components.

In Chapter 4, it has been reported that the algal-bacterial type cellulose microfibril is more susceptible to cellulase attack than the cotton-ramie type cellulose, and the cellulose I_{α} in the algal-bacterial type cellulose microfibril is more selectively degraded than the cellulose I_{β} [Hayashi et al., 1994]. The substrate was a homogenized sample, which contained both crystalline and amorphous regions and their cellulose microfibrils aggregated tightly. Recently, Revol et al. have reported that the chiral nematic order structure is arranged by "highly crystalline microfibrils" [Revol et al., 1992]. They collected the highly-crystalline samples from the crystalline region of cellulose and suspended in water, where the highly crystalline cellulose dispersed one by one. If this sample is treated with cellulase, it is not needed to consider the influences of the amorphous region and of the aggregation of cellulose crystallites during enzymatic hydrolysis. Therefore, a suspension of cellulose crystallite (CC) from *Cladophora* sp., which is rich in cellulose I_{α} , was used as the substrate. Another aqueous suspension of CC of *Halocynthia* sp. which is exclusively the cellulose I_{β} component [Belton et al., 1989] was also used as a control substrate. The purpose in this chapter was to study the selective degradation of the cellulose I_{α} component by FTIR spectroscopy and by electron-diffraction analyses to characterize them.

2. Experimental

(1) Substrates

The substrates used were the suspensions of cellulose crystallites (CCs) of *Cladophora* sp. and *Halocynthia* sp. The purified sample of *Cladophora* sp. and bleached tunic of *Halocynthia* sp. were treated by 100 mL of 65% sulfuric acid (w/w). The treatment conditions were 25 °C for 30 min for the *Cladophora* sp. and 70 °C for 30 h for the *Halocynthia* sp. The obtained CCs were then washed with distilled water successively by centrifugation until a pH range of from 1 to 5 is achieved.

The crystallinity index (CrI) calculated from X-ray profiles of the purified samples before acid hydrolysis was 82% (*Cladophora* sp.) and 86% (*Halocynthia* sp.) [Hayashi et al., 1994], and the average crystallite sizes determined from (1 $\bar{1}$ 0) and (110)* planes by Scherrer's equation [1918] were as follows: 11 nm x 9 nm for *Cladophora* sp. and 8 nm x 9 nm for *Halocynthia* sp. The sizes of the two substrates were differed little.

(2) Enzymatic hydrolysis

The above samples were hydrolyzed with a commercial cellulase "Meicelase" (Meiji Seika Kaisha, Tokyo, Japan) derived from *Trichoderma viride* as described in Chapter 4. The cellulase was fractionated by ultrafiltration membranes. The fraction (2.5-5 mg) of higher molecular mass than 10 kDa was incubated with 5 mg of substrate in 5 mL of a 0.1 M sodium acetate buffer and incubated at 48 °C for 2 days. After the centrifugal separation of the reaction mixture into the residues and products, the residues were successively and thoroughly washed with 0.1 N NaOH and distilled water, and then freeze-dried. The

* : Throughout this study, indexing for major equatorial and meridional crystallographic planes are based on the monoclinic model [Sugiyama et al (1991b)]. However, the specific reflections are given by triclinic indexing by indicating (T) after millar indices.

enzymatic hydrolysis was repeated four times with the hydrolysis residues under the same conditions for removal of the susceptible portion. The enzymatic susceptibility was determined by ratio of the weight loss to the initial sample weight.

(3) Observation by TEM

The residues from two-days of enzymatic hydrolysis were examined under the transmission electron microscope (TEM; JEM-2000EX, JEOL). Some of the freeze-dried residues were suspended in water. Drops of the suspension were deposited on a carbon-coated grid. These were used without further treatment for electron diffraction, and negatively stained with 1.5% uranyl acetate for imaging. TEM was operated at an accelerating voltage of 100 kV or 200 kV for imaging, and of 200 kV for electron diffraction. The width of the CCs was measured from the electron micrographs of negatively-stained samples. In the micrographs their lengths were also compared with the number of CCs with both ends to the number of the CCs with one or no intact end. The diffraction diagrams were measured with a microdensitometer equipped with a microscopic accessory (3CS, Joice Loebler). From the profiles the half-width of the major 3 equatorial diffractions denoted as A₁, A₂ and A₃ were measured. The *d*-spacing was calculated from the diffraction profiles obtained by the densitometer.

(4) FTIR spectral analysis

Fourier transform infrared (FTIR) analyses were carried out using KBr discs containing hydrolyzed residues with a FTIR-8100M spectrometer equipped with a microscopic accessory (Shimadzu). All the FTIR spectra were recorded in the transmission mode with a resolution of 2 cm⁻¹ in the range 4000-650 cm⁻¹. The crystallinity indexes was calculated with the infrared ratios by the method of O'Connor et al.

[1958]. The ratio of absorption at 1429 cm^{-1} (CH_2 scissoring motion) and absorption at 893 cm^{-1} (vibrational mode involving C_1 of β -linked glucose) was used for CrI determination [Liang & Marchessault, 1959].

3. Results

The weight losses in the time course of each sample are shown in Table 5-1. Fig. 5-1 shows a linear relationship between the weight loss and the hydrolysis time; the slope of the *Cladophora* CC was steeper than that of the *Halocynthia* CC.

Table 5-1 The changes of weight loss, *d*-spacings of *Cladophora* and *Halocynthia* CCs and the change of the composition of I_{α} and I_{β} of *Cladophora* CC after enzymatic hydrolysis.

Sample	Time course (day)	Weight loss (%)	<i>d</i> -spacings (nm)		Composition of I_{α}/I_{β}	
			A1	A2	I_{α} (%)	I_{β} (%)
<i>Cladophora</i>	0	0	0.622	0.530	53	47
	2	20	-	-	50	50
	4	41	0.611	0.535	49	51
	6	59	0.590	0.535	39	61
	8	79	0.612	0.538	32	68
<i>Halocynthia</i>	0	0	0.605	0.537		
	2	13	-	-		
	4	27	0.606	0.537		
	6	35	0.592	0.537		
	8	46	0.605	0.536		

From the measurement of the negatively stained crystallites in electron micrographs, the original *Cladophora* CC and *Halocynthia* CC had 24-34 nm and 17-22 nm in width, respectively, and had variable lengths (500 nm to several μm). Fig. 5-2 shows the changes in the width of the residues of *Cladophora* and *Halocynthia* CCs that were measured from electron micrographs. In the residual *Halocynthia* CC, the width became much smaller by enzymatic hydrolysis, than that of the *Cladophora* CC decreased.

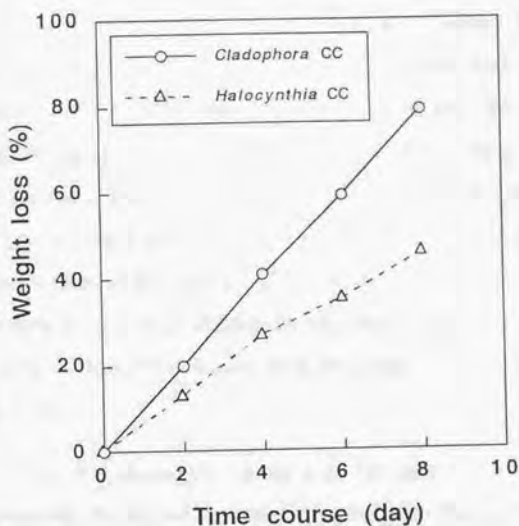


Fig. 5-1. Time course of the enzymatic hydrolysis of *Cladophora* CC and *Halocynthia* CC.

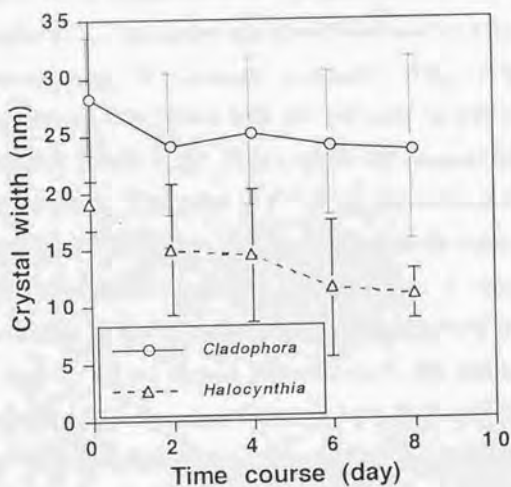


Fig. 5-2. The changes of the width of *Cladophora* CC and *Halocynthia* CC measured from electron micrographs in the residues after enzymatic hydrolysis.

Fig. 5-3 shows the *Cladophora* CC before (a) and after (b) enzymatic hydrolysis. The number of CCs with both intact ends to the number of CCs with one or no intact end was 86 to 449, while the numbers changed to 132 to 99 after 2 days' treatment. The length of CC after the enzymatic hydrolysis varied widely and the short CC with about 500 nm in length was frequently observed as shown in Fig. 5-3b. On the contrary, the *Halocynthia* CC did not change in length but became narrower in the width during the enzymatic hydrolysis. Some fibrillation was observed in the residues of *Halocynthia* CC treated with the cellulase (Fig. 5-4).

Fig. 5-5 shows the changes of IR spectra of *Cladophora* (a) and *Halocynthia* (b) in the enzymatic hydrolysis. Bands near 3240 cm^{-1} and near 750 cm^{-1} are characteristic of cellulose I_{α} component, whereas those near 3270 cm^{-1} and near 710 cm^{-1} denote cellulose I_{β} component [Michell, 1990; Sugiyama et al., 1991]. In the OH stretching region of the *Cladophora* CC, the absorption of the band near 3240 cm^{-1} decreased with increasing time of cellulase treatment (Fig. 5-5a). The original *Cladophora* CC comprises both the cellulose I_{α} and cellulose I_{β} crystal components [Wada et al., 1993], while the original *Halocynthia* CC has only cellulose I_{β} [Sugiyama et al., 1991], as confirmed by the FTIR data. The residue of *Cladophora* CC became rich in the cellulose I_{β} component. The second-derivative spectrum of the residues of *Cladophora* CC (Fig. 5-5c) gets close to that of the *Halocynthia* residues (Fig. 5-5d) near the 3350 cm^{-1} region. At the region $800\text{-}650\text{ cm}^{-1}$, the absorption at 750 cm^{-1} resulting from heavy-atom bending, both C-O and ring mode [Michell 1988; 1990] also decreased in the residual *Cladophora* CC. In Table 5-1 the changes in the composition of cellulose I_{α} and cellulose I_{β} are calculated from the peak height of 750 cm^{-1} and 710 cm^{-1} according to the method of Yamamoto et al. [1994]. The original *Cladophora* CC

consisted of 53% of the cellulose I α and 47% of the cellulose I β . After the enzymatic hydrolysis, the composition of the cellulose Ia changed to nearly half that of cellulose I β (Table 5-1). In response to the compositional changes, the absorption bands at about 3270 cm⁻¹ in *Halocynthia* CC were rendered observable by the enzymatic hydrolysis (Fig. 5-5b).

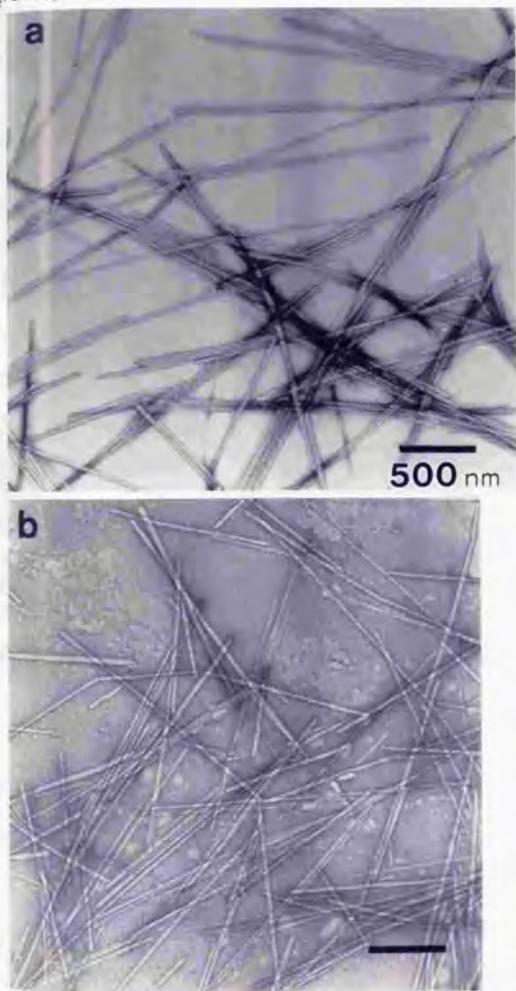


Fig. 5-3. The electron micrographs of *Cladophora* CC; a: intact; b: the residue after the 2 days of enzymatic hydrolysis.

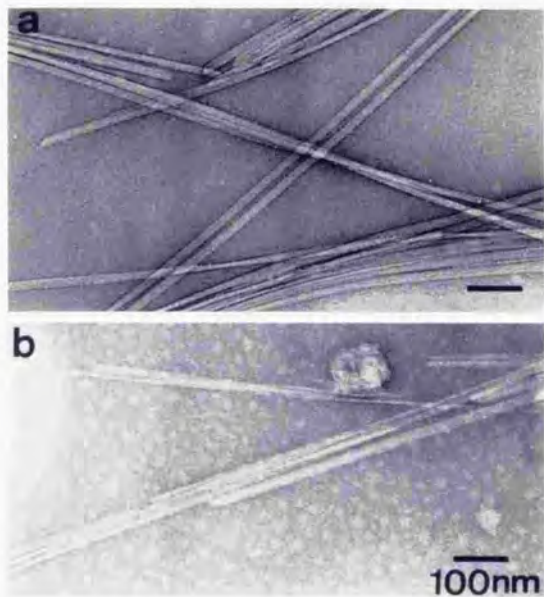


Fig. 5-4 The electron micrograph of *Halocynthia* CC; (a) untreated and (b) the residue treated with cellulase for 2 days.

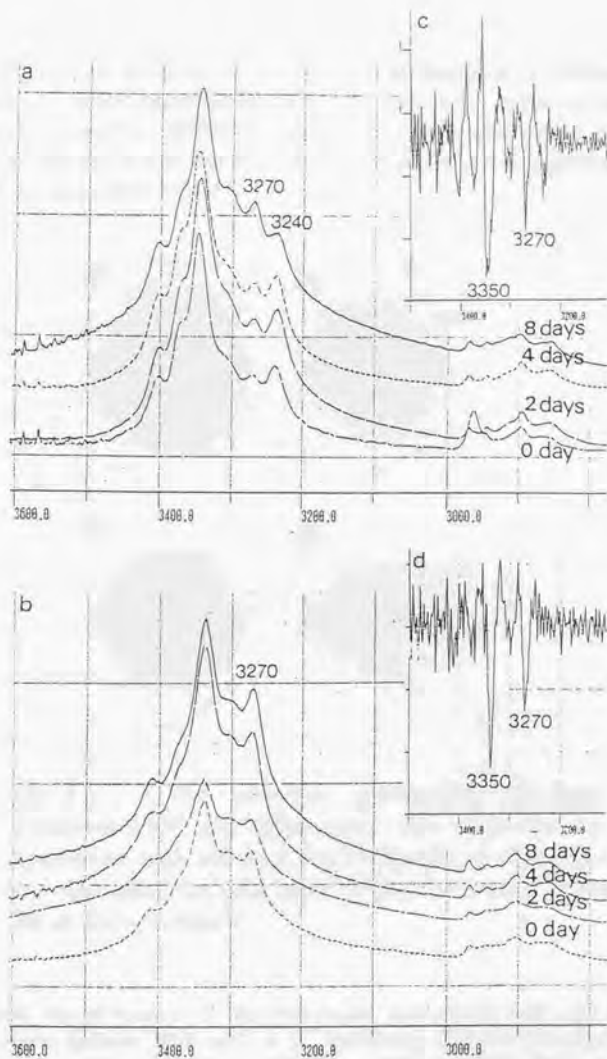


Fig. 5-5. FTIR spectra in the region from 3600 cm^{-1} to 2600 cm^{-1} of *Cladophora* CC (a) and *Halocynthia* CC (b) hydrolyzed with cellulase for 0, 2, 4, and 8 days, and the second-derivative spectra of the residues hydrolyzed for 8 days (c, d), respectively.

Fig. 5-6 shows the electron-diffraction diagrams of *Cladophora* and *Halocynthia* CCs before and after the enzymatic hydrolysis. In the residues of *Cladophora* CC, a triclinic diffraction spot of (03) plane disappeared, and the spot of the second-layer meridian reflection of (002) plane was observed clearer than that in the untreated sample.

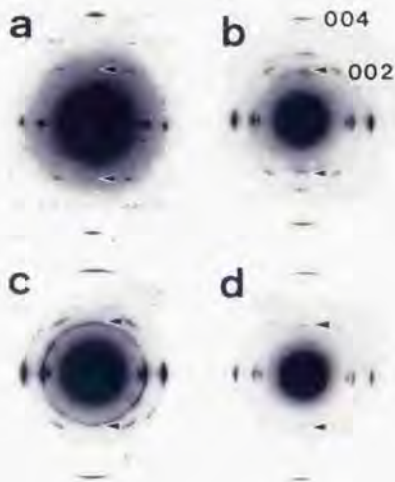


Fig. 5-6. The electron diffraction diagrams of *Cladophora* CC and *Halocynthia* CC; untreated (a) and hydrolyzed with cellulase for 8 days (b) of *Cladophora*CC, and untreated (c) and after 8 days-enzymatic hydrolysis (d) of *Halocynthia*CC.

From the geometry of the two-chain monoclinic unit cell and the one-chain triclinic unit cell, it is considered that in the algal-bacterial type cellulose whose cellulose crystal contains both a triclinic and monoclinic

system, the relative intensities of the meridional diffraction spots at the fourth layer line (004) should be more intense than those of the second layer (002) because the (002) in the triclinic system do not coincide with those in the monoclinic system as meridional lattice points [Sugiyama et al., 1991; Sugiyama, 1993]. For simplicity, we refer to the fourth- and second-layer meridional spots as (004) and (002) on the basis of the monoclinic system. The intensity ratio of (002)/(004) in the algal-bacterial type cellulose is below 0.1, and that of the cotton-ramie type cellulose is above 0.1 [Sugiyama et al., 1991b; Sugiyama, 1992; Wada et al., 1995]. Fig. 5-7 shows the changes of the intensity ratio of (002)/(004) of *Cladophora* and *Halocynthia* CCs during the enzyme treatment. The ratio of *Cladophora* CC was 0.06 before the enzymatic hydrolysis, whereas the

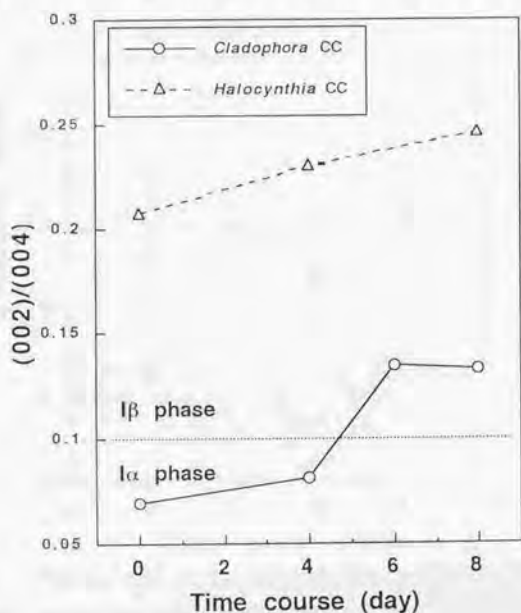


Fig. 5-7 The changes of the intensity ratio of (002)/(004) of *Cladophora* and *Halocynthia* CCs during enzymatic hydrolysis.

treatment made the value larger than 0.1. The value of *Halocynthia* CC, however, changed little. The d -spacing of the A1, (1 $\bar{1}$ 0) and A2, (110) spots of *Cladophora* CC changed into the dimension of typical cellulose I β by the enzymatic hydrolysis, whereas that of the *Halocynthia* crystallite did not change, even in the advanced stages of enzymatic hydrolysis (Table 5-1).

Fig. 5-8 shows the change of the infrared ratio, $a_{1429\text{ cm}^{-1}}/a_{893\text{ cm}^{-1}}$, which was a measure of crystallinity index by IR [Hayashi et al., 1994]. The crystallinity index shows gradual decrease in the residual *Cladophora* CC, but that of the residual *Halocynthia* CC increased remarkably.

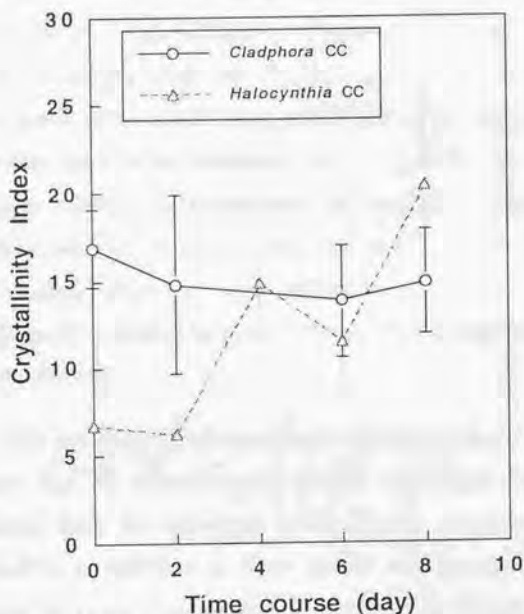


Fig. 5-8 The changes of the infrared ratio, $a_{1429\text{ cm}^{-1}}/a_{893\text{ cm}^{-1}}$, of the *Cladophora* and *Halocynthia* CCs after enzymatic hydrolysis.

4. Discussion

The CCs are less accessible to the enzyme than the cellulose sample from cell walls described in Chapter 4. Our results do not agree with Chanzy and Henrissat [1983a] who have studied the enzymatic susceptibility of *Valonia* cellulose pellicles and crystallites. The disagreement might be occurred because our samples contained exclusively highly-ordered cellulose chain molecules from the crystalline region of the cell walls. Nevertheless the *Valonia* sp. produces larger crystallites than either the *Cladophora* sp. and *Halocynthia* sp.

Two phenomena observed during the enzymatic hydrolysis of the *Cladophora* and *Halocynthia* CCs are (a) a constant rate of the weight loss and (b) a steeper slope for *Cladophora* than for *Halocynthia*. These observations indicate two facts; one is that both samples are completely free from amorphous cellulose as shown in the electron diffraction diagrams, and the other is that the *Cladophora* CC is more susceptible than the *Halocynthia* CC to the enzyme. The two CCs, even though with their quite similar features, are different in their crystal structure. Consequently, cellulose I_{α} is more susceptible to enzyme action compared with cellulose I_{β} .

The results of IR absorption and the d -spacings of the residual CCs indicate that the characteristics in the hydrolyzed residues might be explained from the difference of the crystal component. The ratio of cellulose I_{α} to cellulose I_{β} from the IR absorption confirmed that the cellulose I_{α} in the *Cladophora* CC was hydrolyzed more selectively with cellulase than the cellulose I_{β} . The electron-diffraction diagrams also supported the contention that the enzymatic action on *Cladophora* CC gave rise to selective removal of the cellulose I_{α} component in respect to the cellulose I_{β} component. The disappearance of diffraction spot $(\bar{1}03)(T)$

from the cellulose sample composed of cellulose I β was already confirmed by Sugiyama et al. [1991a]. This result was the same as that in Chapter 4.

The measurements of the sizes in the residual CCs suggested that the enzyme made to short the length of the *Cladophora* CC or to narrow the width of *Halocynthia* CC. Some fibrillation was observed in the residues of *Halocynthia* CC. The fibrillation was also observed in the residues of *Cladophora* CC that were treated repeatedly with cellulase and became rich in cellulose I β . In Chapter 3, we have already reported the thinned and fibrillated microfibrils that occur after the treatment with *T. viride* cellulase in the cotton-ramie type cellulose, in which cellulose I β is dominant. Therefore, the fibrillation seems to be associated with the region of the cellulose I β crystal component of the CCs.

The results of the FTIR analyses indicate a great deal about the supermolecular structure of the CCs. The untreated CCs have high crystallinity, thus, it was estimated that the ratio of absorption at 1429 cm^{-1} and at 893 cm^{-1} showed minute changes in those highly crystalline region even after the enzymatic hydrolysis. But there was a great difference between the residual *Cladophora* and *Halocynthia* CCs in the change of crystallinity index after the enzymatic treatment. The modest reduction in the crystallinity index of the *Cladophora* CC might reflect the selective degradation of the I α component. On the other hand, the increase in the crystallinity of the residual *Halocynthia* CC suggests that the CC contains a more highly-crystallized region. The increase of the peak height in the FTIR spectra of the hydrolyzed *Halocynthia* CC may also indicate the decrease of disordered chains of cellulose on the surface or within the crystallite. Partly-disordered chains have been proposed by Rowland and Howley [1988]. Verlhac et al. [1990] have compared the availability of the surface hydroxyl groups in *Valonia* and bacterial cellulose with those in cotton linter, and have found to be the high

surface-perfection in the *Valonia* and bacterial cellulose crystals but to be as accessible as in the fully disorganized surface in the cotton samples. Our results agreed with their findings. Further investigation is needed to clarify the causes of these phenomena concerning the morphological changes of the CCs.

It was concluded that the CC of algal-bacterial type is more susceptible than that of the cotton-ramie type to enzymatic attack, and cellulose I α component in the algal-bacterial type cellulose is much more selectively hydrolyzed than cellulose I β . In addition, shortened CCs are observed frequently in the residual *Cladophora* CC, whereas some fibrillation is observed in the residue of *Halocynthia* crystallite and repeatedly hydrolyzed *Cladophora* CC which comprised exclusively of cellulose I β . The fibrillation seems to be characteristic of the cellulose I β crystallite. FTIR analysis suggests the difference in the supermolecular structure as well as in the crystal component between the *Cladophora* and *Halocynthia* CCs.

5. Summary

The cellulose crystallite (CC) of *Cladophora* cellulose which is classified as algal-bacterial type was more susceptible to enzymatic attack than the CC of *Halocynthia* cellulose which is one of the cotton-ramie type cellulose. In *Cladophora* CC, the cellulose I α crystal component was more selectively degraded than the cellulose I β crystal component. The shortened CC was observed frequently in the residue of *Cladophora* CC. In addition, some fibrillation was observed in the residues of *Halocynthia* CC and repeatedly hydrolyzed *Cladophora* CC that richly contained cellulose I β . The both supermolecular structure of *Cladophora* and *Halocynthia* CCs should be estimated from these results, respectively.

Key words: Cellulose crystallite; *Cladophora* cellulose; *Halocynthia* cellulose; *Trichoderma* cellulase; Fibrillation; Cellulose I α

Chapter 6. Characterization of short microfibrils in native *Cladophora* cellulose produced by enzymatic hydrolysis.

1. Introduction

Atalla and VanderHart [1984] have reported that cellulose I is composed of two types of allomorphs, cellulose I α and cellulose I β , and later [VanderHart & Atalla, 1984; Wiley & Atalla, 1987a; 1987b; Horii et al., 1987; Atalla & VanderHart, 1989] it has been clarified that the algal-bacterial type cellulose richly contains cellulose I α while the cotton-ramie type cellulose is composed dominantly of cellulose I β . The presence of superlattice-like structure has also suggested in a cellulose microfibril, in which the cellulose I α and cellulose I β domains co-exist throughout the cross-section of each microfibril [Hackney et al., 1994, Uhlin et al., 1995]. As described in Chapter 4 and 5, it is indicated that cellulose I α crystalline phase is more susceptible to enzymatic hydrolysis than cellulose I β crystalline phase. The similar results were obtained in bacterial, *Cladophora* and *Valonia* celluloses regardless of the form of substrates such as cellulose pellicle, homogenized pieces and microfibrillated cellulose. It is also described in Chapter 4 and 5 that many shortened microcrystals with the almost same length are observed in the enzymatically hydrolyzed residues of algal-bacterial type cellulose.

To date, there is not such a report mentioning generation of the short fibers in these I α rich type celluloses. In this chapter, the short microcrystals are characterized minutely by electron microscopic observation, electron diffraction, X-ray diffraction, the size-exclusion chromatography and FTIR analyses. The results were discussed in terms of the enzymatic "leveling off degree of polymerization (LODP)" similarly observed in a dilute acid hydrolysis of cellulose microfibrils.

2. Experimental

(1) Substrates

The cell walls of *Cladophora* sp. and *Valonia* sp. were used. The former was collected in the sea at Chiba, Japan. The two cell walls were rich in cellulose I α crystalline phase. Prior to use as substrates, they were treated with 0.1 N aqueous NaOH at 100 °C and then with 0.05 N aqueous HCl at room temperature for overnight and rinsed thoroughly with distilled water. The *Cladophora* cellulose after homogenization and freeze-drying was treated with 66% sulfuric acid solution (w/w) at room temperature for 3 h under a strong stirring and then washed by centrifugation until the aqueous non-flocculating suspension of microcrystalline cellulose (CC), pH 5.0 was obtained. The *Valonia* cellulose was used without homogenization.

(2) Enzymatic hydrolysis

The enzyme used was "Meicelase" (Meiji Seika Co. Ltd.), a commercial product from *Trichoderma viride*. An exo-1,4- β -glucanase (CBH I) was isolated and purified from the enzyme product by multiple column chromatography equipped with anion and cation exchangers as described previously [Uemura et al., 1993].

Pieces of *Valonia* pellicle, homogenized *Cladophora* cellulose and its CC were hydrolyzed with Meicelase or CBH I, respectively. The enzymatic hydrolysis was performed under the following conditions: the three suspensions including the substrate (200 mg for *Cladophora* cellulose and 1-2 mg each for *Valonia* cellulose and *Cladophora* CC) and the enzyme (50-100 mg for *Cladophora* and 1-2 mg each for *Valonia* cellulose and *Cladophora* CC) in 10 and 5 mL of 0.1 M of sodium acetate buffer at pH 4.8 were incubated in water bath at 48 °C. After 2 or 3 days

of incubation, the precipitated residues was collected by centrifugation, washed with 0.1% NaOH solution and then distilled water, and dehydrated using a ethanol series to acetone for pellicle sample, and freeze-dried for the other samples. A piece of pellicle (6-8 μm in thick) was cut from the treated residues and mounted on a carbon-coated electron-microscope grid and provided for the optical analyses.

The reaction mixtures were separable into three portions in various stages of hydrolysis: precipitated residues, "floating residues", and supernatant. The "floating residues" was collected by centrifugation at greater g up to 18,000 after addition of three volumes of 99.5% ethanol. The precipitates were stored in 50% ethanol. The obtained "floating residues" were subjected to a mild acid treatment with 2.5 N HCl at 80 °C for 1 h in order to remove contaminants attached on the sample surface. The residues suspended in water. A few drops of the suspensions including cellulose were deposited on carbon-coated grids. The residues were also provided for observation with a transmission electron microscope (TEM) and/or a FTIR analysis after the residues were suspended in water and then dried.

The precipitated residues were repeatedly treated with crude cellulase until about 80% of the initial weight was hydrolyzed and the resulting precipitated and floating residues were collected in the same way.

(3) Acid hydrolysis

For comparison of enzymatically hydrolyzed residues and acid hydrolyzates, purified *Cladophora* cellulose and *Valonia* cellulose were treated with 1 N HCl in 100 °C for 3 h and 5 h. The residues were provided for the TEM observation, FTIR and SEC (size-exclusion chromatography) analyses.

(4) Determination of molecular weight

The "floating residues" of *Cladophora* cellulose after cellulase treatment for 2 and 12 days was treated at 0 °C with a mixture of nitric acid and phosphorus pentoxide for 30 min for preparation of the cellulose trinitrate for the SEC analysis. The product was separated and washed thoroughly with water. The average molecular mass weight (M_w) of the cellulose trinitrate from the enzymatic hydrolyzates was determined by SEC with tetrahydrofuran as eluent [Shibazaki et al., 1995]. The M_w of the cellulose trinitrate obtained from the acid hydrolysis residues was also measured.

(5) General Analysis

All the electron micrographs and electron diffraction diagrams were recorded with a JEM-2000EX (JEOL) operated at an accelerating voltage of 200 kV. The specimens were used with or without 1.5% uranyl acetate for imaging. Diffraction contrast images in bright or dark field were observed without any treatment. The images were recorded on Fuji electron microscopic films (FG), and the diffraction diagrams on Mitsubishi electron microscopic films (MEM). The electron diffraction diagrams were traced with a micro-densitometer (3CS, Joyce Loebel) to calculate d -spacings of the crystal structure.

FTIR spectra were obtained from the samples on the grid in the circular area of 100 μm in diameter using a Nicolet-Magna 550 FT-IR spectrometers equipped with a Nic Plan microscopic accessory. The wave number range scanned was 4000-650 cm^{-1} ; 64 scans of 4 cm^{-1} resolution were signal averaged and stored. The internal standard band at 2900 cm^{-1} which is assigned to C-H stretching in methyl and methylene groups in the crystalline region was commonly employed [Yamamoto et al., 1994]. An

X-ray diffractometer (JDX-8200, JEOL, Japan) generated at 50 kV and 120 mA to obtain a diffraction profile of the short microcrystal.

3. Results

Fig. 1 shows the weight loss of pellicle of *Valonia* cellulose, homogenized *Cladophora* cellulose and its microcrystalline cellulose (CC) during the treatment with crude cellulase. The enzymatic susceptibility depends more or less on the form of the samples as described in chapter 3. The pellicle of *Valonia* cellulose was degraded faster than the homogenized *Cladophora* cellulose regardless of the large dimensions of microfibril. This might be owing to the fibrillation of microfibril and the aggregation. In *Valonia* cellulose microfibril, some fibrillation was observed after the enzymatic hydrolysis [Wardrop & Jutte, 1968; Chanzy

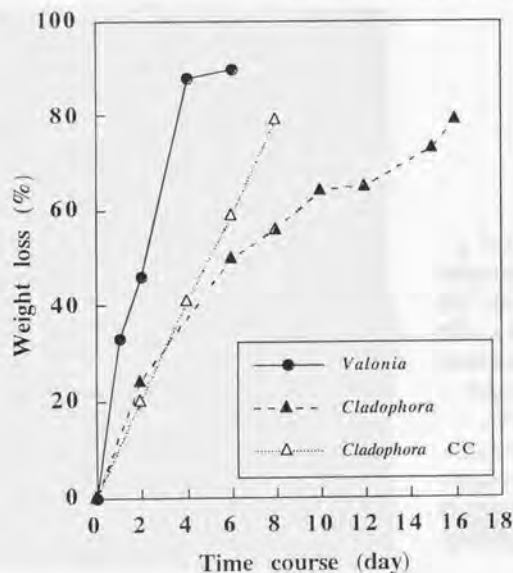


Fig. 6-1. Changes of the weight loss during the enzymatic hydrolysis of *Valonia*, *Cladophora* celluloses and *Cladophora* CC treated with crude cellulase.

& Henrissat, 1983a]. The weight loss of each sample by the CBH I was lower than that by the crude cellulase. The component enzymes in the crude cellulase might exhibit a synergistic effect on the hydrolysis of cellulose crystals.

Short microcrystals were observed in the floating residues from *Cladophora* CC as shown in Fig. 6-2. The short microcrystals were also observed in the floating residues of *Valonia* and *Cladophora* cellulose. The short microcrystals might be too small to obtain directly by centrifuging the reaction mixture. The major component in the floating residues was the short microcrystal and the short microcrystal was found not to be aggregated with each other. Gilkes et al. [1993] have reported that the flocculation of microcrystalline cellulose of bacterial cellulose inhibited by the surface coverage with the cellulose-binding domain. In fact, Fig. 6-2a shows that the aggregation in this system did not occur. Since the short microcrystals exhibited the small and clear reflected spots in the electron diffractograms, it was suggested that the cellulose chains in

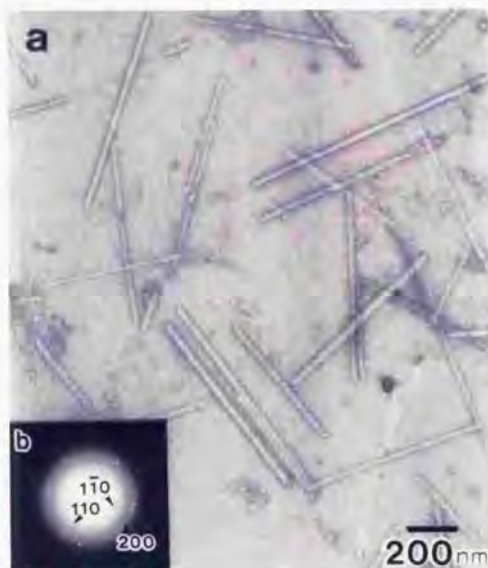


Fig. 6-2. Electron micrographs observed in the floating residues after 4 days CBH I treatment;

a: short microcrystals of *Cladophora* CC negatively stained, b: an electron diffraction diagram of the short microcrystals.

the microcrystals were highly ordered. The d -spacings [$(1\bar{1}0)=0.60$ nm, $(110)=0.54$ nm] of the short microcrystals agreed with the values for cellulose I β crystalline phase. This was also confirmed by a microscopic FTIR analysis. The results obtained suggested that the short microcrystals were composed dominantly of highly ordered cellulose I β crystalline phase (Fig. 6-3). The X-ray diffraction profile from the short microcrystal shows that the CrI is not changed from the initial one (Fig. 6-4).

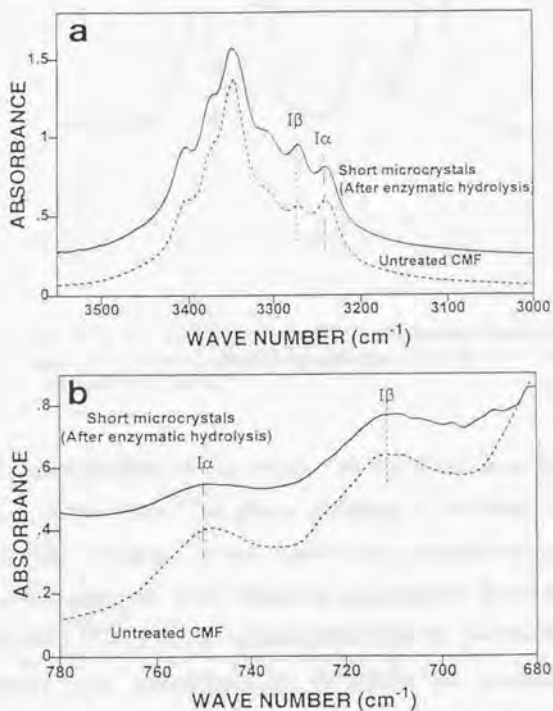


Fig. 6-3 FTIR spectra in the region from 3600 cm^{-1} to 2800 cm^{-1} of (a) untreated and (b) short microcrystals of *Cladophora* cellulose hydrolyzed with crude cellulase for 2 days.

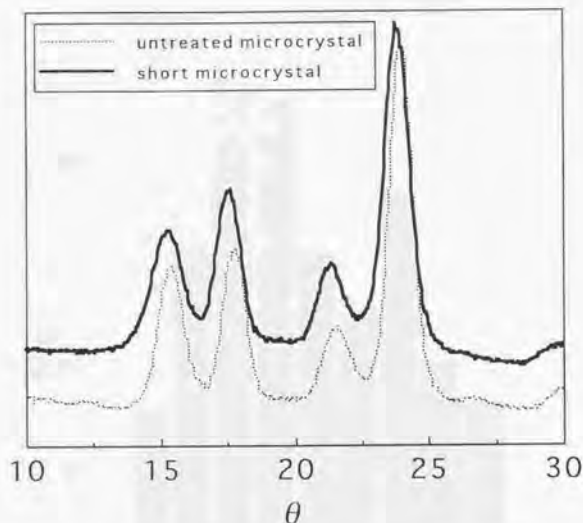


Fig. 6-4. X-ray diffraction profiles of untreated and short microcrystals of *Cladophora* cellulose treated with crude cellulase for 2 days.

The distribution of the length for the short microcrystals in the floating residues from *Cladophora* cellulose is evaluated graphically in Fig. 6-5. The frequency in this figure were obtained by counting each length of microcrystal in the electron micrographs. From the calculated statistic value ($=1.0$) of the apparent M_w/M_n for the microcrystals, the distribution was considered to be close to monodisperse. The microcrystals of 300-400 nm in length were observed most frequently. The value of M_w/M_n in the floating residues of *Valonia* cellulose was 1.2 and the average length was 450-500 nm.

The distribution of dp_w for the cellulose molecules in the short microcrystals was determined by SEC. The SEC chromatogram for the

short microfibrils from *Cladophora* cellulose after 12 days treatment with crude cellulase was shown in Table 6-1. The calculated dpw was about 690 and the dp distribution (dp_w/dp_n) was about 4.7.

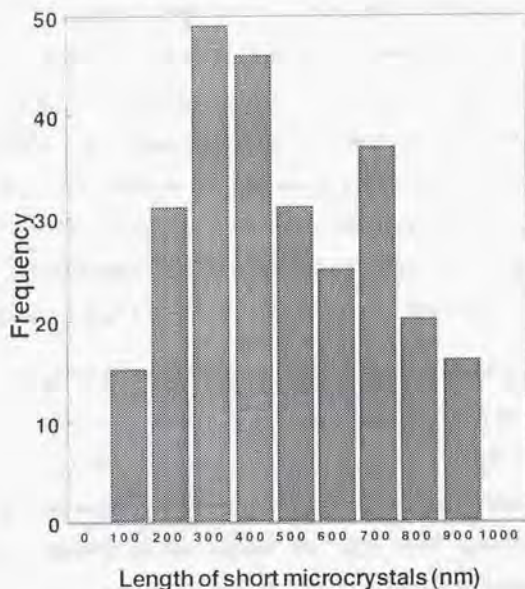


Fig. 6-5. Statistic frequency of the short microcrystals in the floating residues of *Cladophora* treated with the crude cellulase for 4 and 8 days and the CBH I for 2, 4, and 6 days.

Table 6-1 The changes in SEC chromatogram for the short microcrystals of *Cladophora* cellulose treated with crude cellulase for 12 days and the *Cladophora* cellulose after various acid hydrolysis time.

Sample Treatment	Untreated CMF	short microcrystals	Acid treated CMF			
			30 min	60 min	120 min	180 min
DPw	2870	690	3010	3150	4150	3130
DPw/DPn	9.6	4.7	25.3	21.8	19.1	10.0

4. Discussion

These results suggest the existence of highly ordered I β crystalline phase with a certain domain size of not less than 300-400 nm in the cellulose microfibrils of *Cladophora* cellulose and CC. The short microcrystals which had almost the same length of approximately 300-400 or 400-500 nm (depending on the species of the sample) with *d*-spacings of I β crystalline phase were also observed in the enzymatically hydrolyzed *Valonia* and bacterial cellulose. This indicated that I β crystalline phase had a certain domain size of 300-400 or 400-500 nm in the microfibril or CC.

The short microcrystals of I β phase from enzymatically hydrolyzed *Cladophora* samples were found to be composed of cellulose molecules with a *dp_w* (average degree of polymerization) of 690 which corresponds to 345 nm in molecular chain length. It is well known that the *dp* of cellulose falls rapidly to the LODP by mild acid hydrolysis. Acid hydrolysis causes continuously weight loss, whereas the further drop of the *dp* and the micelle dimensions remain unchanged [Battista, 1950; Fink et al., 1992]. Yachi et al. [1983] has reported that enzymatic hydrolysis of cellulose has not been recognized to alter the *dp* drastically although the LODP of native celluloses in acid hydrolysis is a constant value of about 200, except that of *Valonia* cellulose (LODP = 7000). On the other hand, enzymatic hydrolysis is not known to alter the *dp* of cellulose as well as acid hydrolysis. Recently, however, there have been a few reports concerning the decrease of the *dp* of cellulose by enzymatic hydrolysis. Hoshino et al. [1993] and Kanda et al. [1994] have reported that an endo-type cellulase lowered the *dp* of crystalline celluloses more drastically than exo-type cellulases, and that the endo-cellulase decreased the degree of crystallinity of celluloses as well. The LODP by enzymatic hydrolysis

has not been reported to date. Only the enzymatically hydrolyzed residue of *Cladophora* may have a LODP around 700 whereas the acid hydrolysis does not give LODP for the residue. This LODP by enzymatic hydrolysis in our system may be attributed to the selective degradation of I_{α} phase in the cellulose microfibril or crystallite. Fig. 6 shows the initial (a) and residual *Cladophora* CCs treated with cellulase (b, c) and acid (d). Short microcrystals are only observed in the enzymatically hydrolyzed residues but not in the acid hydrolyzed residue.

The short microcrystals from algal-bacterial type cellulose which is rich in cellulose I_{α} is not considered to be formed in the same manner as the short fiber from the enzymatic hydrolyzed cotton cellulose [Vaheer et al., 1939; Marsh, 1957; Halliwell, 1966; King, 1966; Halliwell & Riaz, 1970; Beldman et al., 1987; Din et al., 1991] which is I_{β} dominant. Henrissat and Chanzy [1986] reported that the formation of short fibers depends on the origin of the enzyme. However, we considered that this phenomenon may be explained by the distribution of the two crystal domains, cellulose I_{α} and cellulose I_{β} , in algal-bacterial type cellulose. Moreover, the width of the residual cellulose appeared not to be changed from that of the initial CC as shown in Fig. 6-6. This suggests that the enzymatic degradation may not proceed to the lateral direction, but to the longitudinal direction. Thus, cellulose I_{β} crystalline phase with a certain domain size may be crystal blocks which are intact to the lateral direction and the algal-bacterial type cellulose may release the short microcrystals with the preferential enzymatic attack to longitudinal I_{α} crystal blocks in the microfibril or CC. The cellulose microcrystals of *Microdictyon* which is classified as algal-bacterial type cellulose consists of cellulose I_{α} and I_{β} crystal blocks contiguously with about 500 nm in length [Sugiyama et al., 1991b; Horii, 1994]. The present results of the *Valonia* and *Cladophora* cellulose seemed to be similar to those of *Microdictyon* cellulose. In the

cellulose I α domains to the longitudinal direction, and consequently released the remaining cellulose I β domains as intact crystal blocks and the short microcrystals because of the limited susceptibility. In the case of the hydrolysis of I β -rich cotton-ramie type cellulose, fibrillation of the microcrystals was observed at the advanced stages of hydrolysis as described in chapter 7.

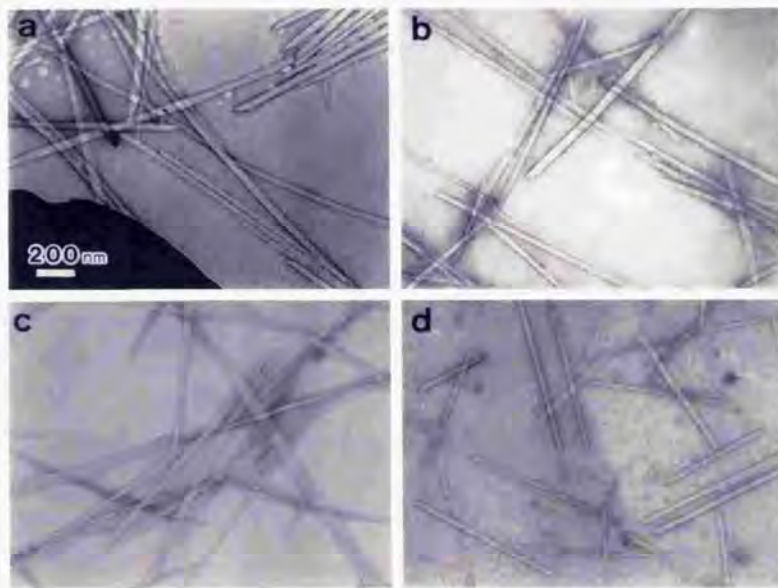


Fig. 6-6. Electron micrographs of the *Cladophora* CC negatively stained; (a) untreated CC, (b) after 2 days, and (c) after 8 days of enzymatic hydrolysis, and (d) after acid hydrolysis.

In the enzymatic hydrolysis of some algal-bacterial type celluloses, the short microcrystals from the cellulose I β domains was observed with the preferential degradation of cellulose I α domains. The short microcrystals possessed the d-spacings of cellulose I β crystalline phase and almost the same length of approximately 300-500 nm depending on the

microcrystals possessed the d -spacings of cellulose I β crystalline phase and almost the same length of approximately 300-500 nm depending on the cellulose sample. In addition, SEC analyses for the short microcrystals from *Cladophora* CC revealed that an average dpw of the cellulose molecules in the short microcrystals was 690. This value corresponded to 345 nm in the average longitudinal length of the short microcrystals. In conclusion, I β crystalline phase for cellulose microfibrils may be composed of highly ordered I β crystal blocks with a certain domain size (300-500 nm in length) (Fig. 6-7). In the I β crystal domains, every single molecular chain with almost the same length may be oriented parallel to the longitudinal direction from the head to the tail.

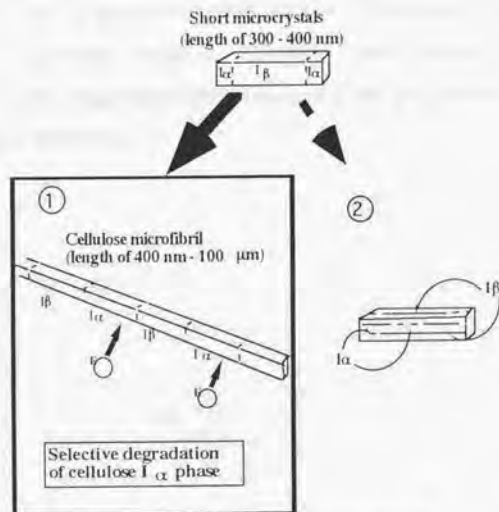


Fig. 6-7. A possible supermolecular structure for cellulose microfibrils with the I α /I β composite phases.

5. Summary

The residues after the enzymatic hydrolysis of algal-bacterial type celluloses were characterized by TEM and FTIR analyses. During the enzymatic hydrolysis, the cellulose I_{α} crystalline phase was preferentially degraded and the short microcrystals were observed in the floating residues. Electron microscopic observation, diffraction and FTIR analysis for the short microcrystals suggested the existence of highly ordered I_{β} crystalline domain of not less than 300-400 nm in length in the cellulose microfibrils of algal-bacterial type. In addition, the short microcrystals from *Cladophora* cellulose was found to be composed of cellulose molecules with a dpw (average degree of polymerization) of 690 which corresponds to 345 nm in molecular chain length. This result suggested that every single molecular chain in the short microcrystal may be oriented parallel to the longitudinal direction from the head to the tail of the cellulose I_{β} crystalline domain.

Chapter 7. Characterization of I β crystalline domain in native *Halocynthia* cellulose by analyzing the enzymatic hydrolysis residues

1. Introduction

The uniformity of microfibril size of 2-4 nm in width in the cellulose of plants and bacteria has been supposed by Frey-Wyssling et al. This hypothesis was confirmed by acid hydrolysis, enzymatic hydrolysis and strong ultrasonic treatment [Rånby & Ribí, 1950; Frey-Wyssling 1954; Harada & Goto, 1982]. The following three concepts were deduced; (1) all cellulose microfibrils contain uniform subunit of approximately 4 nm in width called "elementary fibril" [Frey-Wyssling 1954; Heyn, 1966; 1969], (2) 2-4 elementary fibril constitute a microfibril and the elementary fibrils are surrounded by "para-crystalline region" [Rånby & Ribí, 1950], (3) the elementary fibril coincides with the microfibril and the size of microfibril depends on the cellulose source [Balashov & Preston, 1955].

White and Brown [1981] have been proposed from the transmission electron microscopic observation of the enzymatic hydrolysis residue from bacterial cellulose and proposed that the weakest bonds in the composite ribbon may well be the hydrogen bonds between the subfibril bundles. Chanzy and Henrissat have also discussed that the cellulose microfibril in *Valonia* cellulose are held together by the loosen hydrogen bonds and that the cellulose chains within the crystals are linked by the strongest ones [Chanzy & Henrissat, 1983a]. Blackwell and Kolpak [1975; 1976] have suggested from the results of X-ray diffraction analysis and electron microscopy, and they suggested that gaps of 0.1 nm can be introduced into the perfect lattice of cellulose elementary fibrils without large scale changes in the equatorial intensity distribution and such gaps

are large enough to accommodate a layer of hydrogen-bonded water molecules.

The elementary fibril as smaller structural unit in the cellulose microfibril has been denied by Bourret et al. [1972] who used the technique of diffraction contrast electron microscopy in dark field mode in *Valonia* cellulose and by Sugiyama et al. [1985], Kuga et al. [1987] and Chanzy et al. [1985] studying the lattice imaging of cellulose microfibrils of *Valonia* sp., *Boergesenia forbesii* and bacterial cellulose, and *Halocynthia* sp. It is considered that the diffraction contrast and the lattice images directly show the single crystalline phase in the microfibrils.

Smaller unit in cellulose microfibril has also been recognized in studies on cellulose biosynthesis. Haigler et al. have observed from the study on the structure of cellulose microfibril biosynthesized by *Acetobacter xylinum* the extracellular ribbon consisting of small fibrils of 1.5 nm. Her group has proposed that the ribbon-like cellulose microfibril is assembled hierarchically from the ordered glucan aggregates at the cell surface and the polymerization and crystallization have time-limiting [Haigler & Benziman, 1982; Haigler, 1985]. Concerning the biosynthesis of the cellulose microfibril of the red algae, *Erythrocladia*, Tsekos [1996] has proposed that linear terminal complex (TC) synthesizes on fibrillar (mini-crystal) component which contains 12 glucan chains with dimensions 1.206 nm x 1.59 nm, and that the fibrillar component of one TC associates laterally to form a microfibril. Lee et al. [1994] have observed that the cellulose I synthesized from β -cellobiosyl fluoride by means of cellulase assembles by the aggregation and the alignment of glucan chains with the same polarity and then extends chain conformation, resulting in crystallization to form I β crystalline.

It was described in Chapter 6 that the short microcrystals as a uniform small unit were observed in the enzymatic hydrolysis residues from the algal-bacterial type celluloses. In this chapter, the possible supermolecular structure of crystalline domain was described through close observations of the enzymatic hydrolysis residues from *Halocynthia* cellulose.

2. Experimental

(1) Substrates

The substrate used was the cellulose crystallite (CC) of *Halocynthia* sp. The purified sample of *Halocynthia* sp. was treated with 100 mL of 65% sulfuric acid (w/w) at 70 °C for 30 h. The resulting CC was washed by suspending in distilled water and successively by centrifugation until achieving a pH ranging from 1 to 5. The original CC was a microfibril of about 20 nm in width and several μm in length and no aggregation was observed in the suspension.

(2) Enzymatic hydrolysis

The CC was hydrolyzed with a commercial cellulase "Meicelase" (Meiji Seika Kaisha, Tokyo, Japan) derived from *Trichoderma viride* as previously described [Hayashi et al., 1994]. An exo-(1 \rightarrow 4)- β -D-glucanase (cellobiohydrolase (CBH) 1) was isolated and purified by multiple column chromatography equipped with anion and cation exchangers as previously described [Uemura et al., 1993]. After the separation of the reaction mixture into the residues and supernatants by centrifugation, the residues were successively and thoroughly washed with 0.1 N NaOH and distilled water, and then freeze-dried. The cellulase treatment of the residues were repeated 4 times under the same conditions to remove the susceptible portion.

(3) Observation by TEM

The residues from 8-days of enzymatic hydrolysis were examined under the transmission electron microscope (TEM; JEM-2000EX, JEOL). Some of the freeze-dried residues were suspended in water. Drops of the suspension were deposited on a carbon-coated grid. This was used without any further treatment for electron diffraction, and negatively stained with 1.5% uranyl acetate for imaging. TEM was operated at an accelerating voltage of 200 kV for imaging and for electron diffraction. The micro-diffractograms from each sample were recorded on Imaging Plates (IPs) and analyzed by FDL 5000 (Fuji film Co.). The images of the same area were recorded on Mitsubishi electron microscopic films (MEM) in diffraction contrast. The length of the MCCs of the fibrillated regions were measured from the electron micrographs of negatively stained samples.

(4) FTIR spectral analysis

FTIR spectra were obtained from the samples mounted on a KBr disk using an ordinal microscopic accessory (Nicolet Nic Plan-Magna 550, France). The wave number range scanned was 4000 - 650 cm^{-1} ; 45 scans of 2 cm^{-1} resolution were signal averaged and stored.

3. Results

The hydrolysis rate is shown in Fig. 7-1. *Halocynthia* CC was more susceptible to the *Trichoderma viride* crude cellulase than the purified CBH I. Fig. 7-2 shows the morphological changes of the CC after the enzymatic hydrolysis. The initial CC was not fibrillated and showed uniform electron density. As described in Chapter 3, the residual CC became thinner and partly fibrillated when treated with the crude cellulase or the CBH I. Helical twisting was also observed in the CCs.

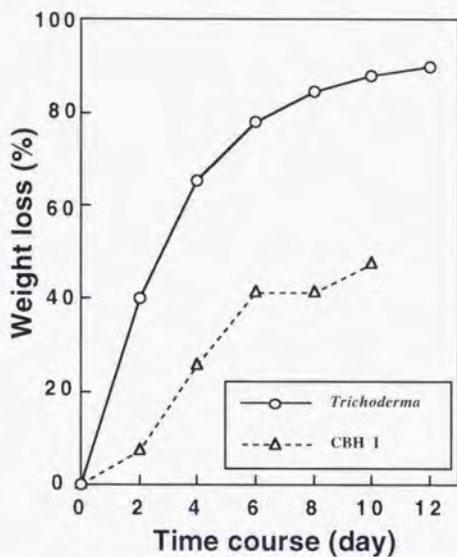


Figure 7-1. The changes of the weight loss of *Halocynthia* CC hydrolyzed with crude *Trichoderma* cellulase and CBH I.

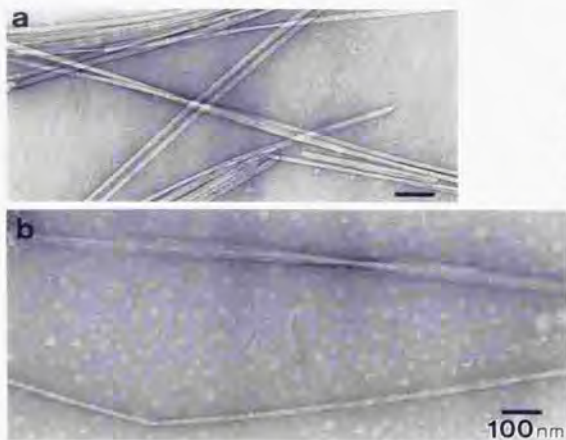


Figure 7-2. The electron micrographs of (a) untreated *Halocynthia* CC and (b) the residue hydrolyzed with crude cellulase for 8 days.

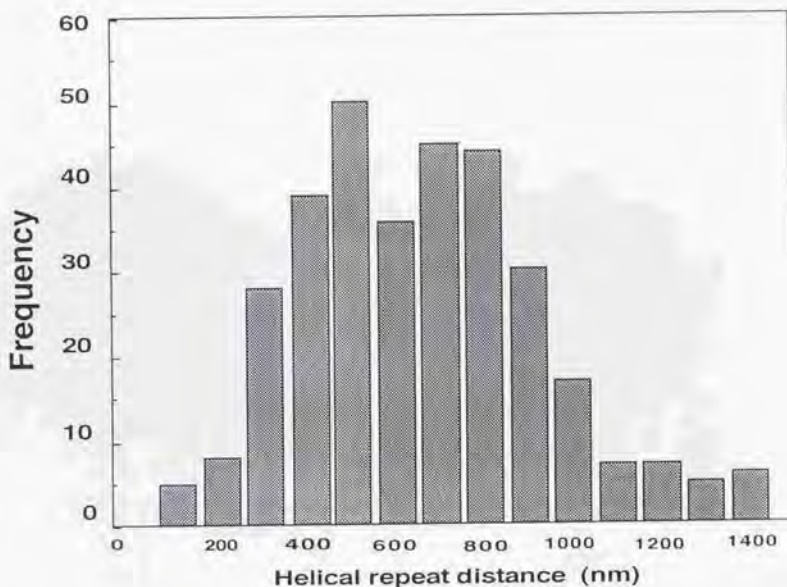


Figure 7-3. Static frequency of the helical repeat distance in the residues of *Halocynthia* CC treated with crude cellulase and CBH I.

The helical repeat distance in the residual CC was measured on electron micrographs and the result is shown in Fig. 7-3. The most frequently observed value was about 500-800 nm. The enzymatic hydrolysis residue was characterized by FTIR and electron micro-diffraction analyses. As described in Chapter 5, the crystallinity index of the *Halocynthia* CC increased with increasing enzymatic hydrolysis (Fig. 5-8). The result of the electron micro-diffraction analysis is shown in Fig. 7-4. The contrast of the diffraction from (200) plane, which shows only one spot for an untreated single CC, changed to a group of several spots in the CC after the enzymatic hydrolysis.

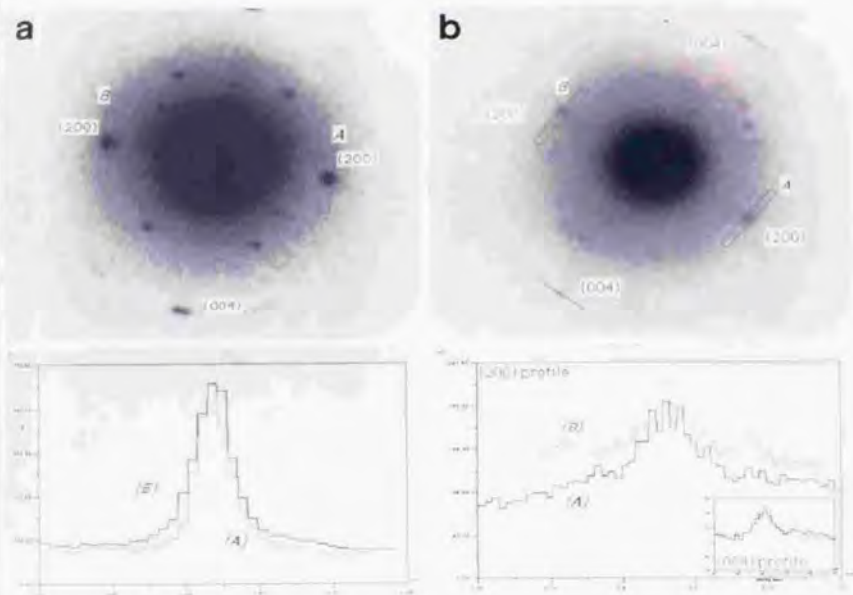


Figure 7-4. The electron diffraction diagrams recorded on IP from untreated *Halocynthia* CC (a) and the residual CC hydrolyzed with crude cellulase for 8 days (b) and their analysis.

In Figure 7-5, the FTIR spectrum around the region of 3600-2800 cm^{-1} of *Halocynthia* cellulose samples, which is the OH stretching region, is compared between before and after the enzymatic hydrolysis. The absorption band near 3270 cm^{-1} is assigned to the cellulose I β [Michell, 1990; Sugiyama et al., 1991a]. The width of the absorption band became slightly narrow after the enzymatic hydrolysis.

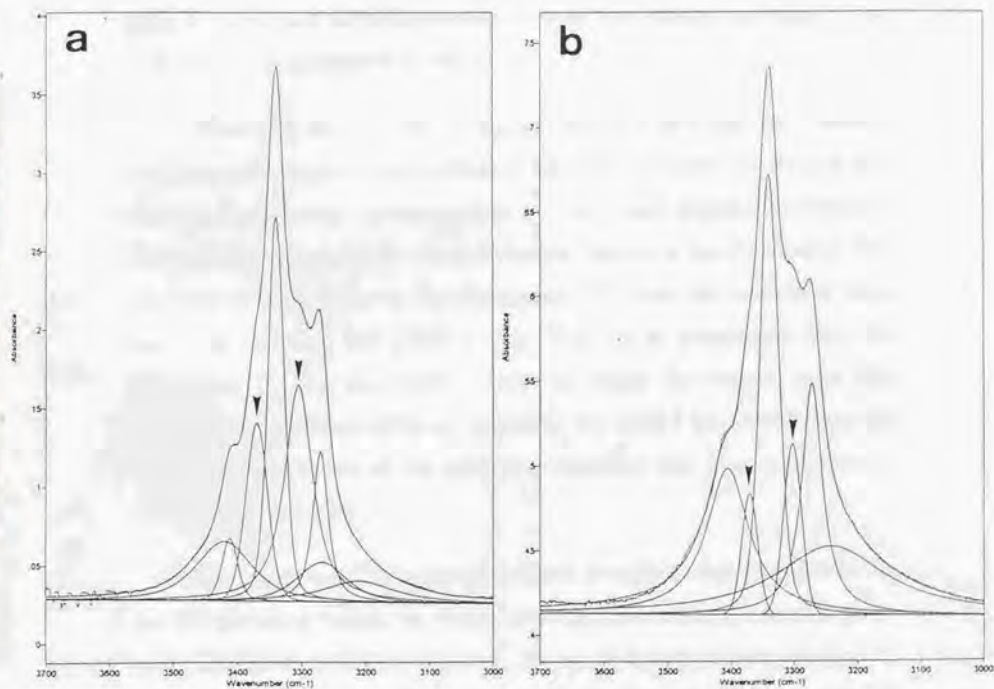


Figure 7-5. The changes of intensities of FTIR absorption from untreated *Halocynthia* CC and residual CC after 2 days of enzymatic treatment.

4. Discussion

The cellulose of *Halocynthia* sp., which is classified as the cottonramie type, contains dominantly cellulose I β . As shown in Fig. 7-2, the appearance of helical twisting of the subfibrils by the repetition of the enzymatic hydrolysis seemed to be characteristic of the residual CC. From the measurement of the length for the fibrillated regions, the length dispersion was about 1.2, which was considered as monodisperse, and the average helical repeat was about 500-800 nm (Fig. 7-3). These results suggest that the intact cellulose microfibrils of *Halocynthia* sp. contain the helix in nature and the helical repeat distance was double the domain size of the cellulose I β crystalline phase.

White and Brown [1981] suggested that the endo-glucanase attacks the glycosidic bonds on the surface of bacterial cellulose microfibril and thereby disrupted the organization of glucan chains required to maintain hydrogen bonding between the protofibrils. However, the fibrillation was observed in the residues of the *Halocynthia* CC after the treatments with the crude cellulase and CBH I (Fig. 7-2). It is considered that the fibrillation by the enzymatic hydrolysis might be caused from the structure of crystalline cellulose: probably, the CBH I first attacked to the weak hydrogen bonds of the cellulose crystallite and gave subfibrils to open up new surfaces.

The results of FTIR analysis seemed to support this hypothesis. In the OH stretching region, the behavior of absorption means the change of intra- and inter- hydrogen bonding. The peak height of two absorption bands (marked in Fig. 7-5) decreased and thereby the decrease of hydrogen bonding between the subfibrils in the residual CC was suggested.

The increase of crystallinity indexes of *Halocynthia* CC after repetitive enzymatic hydrolyses suggests that the enzyme possibly digests the disordered chains on the surface or within the subfibril of the CC. It is considered at present that the cellulose I β domain is accepted to be only a single phase [Belton et al., 1989]. However, from the TEM observation and the results of the FTIR analysis (Fig. 5-8) of the residual *Halocynthia* CC, the *Halocynthia* CC may not be a single phase but may contain more highly crystalline region.

Notably the fibrillation was not always observed in all the residual CC. The localized fibrillation might be explained by the adsorption of enzyme onto some of the surface of CC. Henrissat et al. [1988] have reported that the CBH I from *T. reesei* adsorbs specifically at the corners and/or the (110) face as the possible adsorption sites of cellulases on crystalline cellulose. Figure 7-6 shows the changes of the ratio of intensity at ($1\bar{1}0$), (110) and (200) planes to (004) plane in electron diffraction micrographs of the untreated and treated CCs. The intensity of (110) plane tended to decrease with time. The decrease was not so remarkable in X-ray diffraction diagram. Takai et al. [1983] and Chanzy et al. [1983a, 1984] have also observed the decrease of the (110) peak after the action of exo-cellulase on bacterial and *Valonia* cellulose. Comparison of intensity ratios between algal-bacterial type cellulose and cotton-ramie type cellulose indicated that the decrease in (110) plane intensity was more remarkably observed in the algal-bacterial type cellulose. This phenomenon might be explained by the specific uniplanar orientation of cellulose. It is considered that the ($1\bar{1}0$) plane was initially oriented in the *Halocynthia* CC, and after the enzymatic hydrolysis the specific uniplanar orientation was disrupted by fibrillation. When the residual CC was put on the grid parallel to ($1\bar{1}0$) plane, the fibrillation might be observed. Further investigation is necessary to confirm this hypothesis.

5. Summary

The cellulose of *Halocynthia* sp. is classified into the cotton-ramie type. *Halocynthia* cellulose and its micro crystalline cellulose was hydrolyzed with a crude *Trichoderma viride* cellulase or the cellobiohydrolase(CBH) I. The residual cellulose microfibrils became thinner and partly fibrillated. Helical twisting of the microfibrils were also observed. From the measurement of the length for the fibrillated regions, the length dispersion was about 1.2 which was considered as mono-disperse, and a helical repeat distance on the average was about 700 nm. These results suggest that the intact cellulose microfibrils of *Halocynthia* sp. contained the helix in nature and the helical repeat distance may be correlated with the domain size of the cellulose I β crystalline phase.

The cellulose I β domain in the *Halocynthia* cellulose microfibril has been accepted to be only a single phase by the diffraction contrast and the lattice images. From our observation, the untreated CC was not fibrillated and showed the uniform electron density, but the residual CC after the enzymatic hydrolysis was partly fibrillated and their crystallinity index became slightly higher than the untreated one. These facts may suggest that the cellulose I β domain is not a single phase but contains several subfibrils which seemed to be more highly crystallized.

General Conclusions

The influence of the crystalline structure on the susceptibility of cellulose to *Trichoderma viride* cellulase was examined. Not only the encrusting of cellulose microfibrils by lignin and the aggregation of cellulose microfibrils but also the crystal dimorphism (cellulose I α /I β) is considered to be one of the factors responsible for the susceptibility of crystalline cellulose. The results obtained are summarized as follows:

(1) In the xylem developing zones, cell walls of fibers, vessels and tracheids were lignified first at the cell corner regions of compound middle lamellae (CML) in the S₁ layer deposition stage. Then lignification extended successively in the entire CML, S₁, S₂ and S₃ layers. The unlignified parts of cell walls consisting of cellulose microfibrils and hemicellulose were degraded completely by the enzyme. CML became resistant against enzymatic attacks in the early stages of S₁ layer deposition. S₁, S₂ and S₃ layers became successively resistant in the following lignification stages. The cellulose microfibrils in the tracheid and vessel walls were not degraded by the enzyme after the completion of lignification, but those in the secondary walls of wood fiber were susceptible even after the complete lignification. The difference should be due to the kind of lignin and the encrusting structures in the tracheids, wood fibers and vessels. The network of condensed units of the guaiacyl lignin seemed to prevent the access of the enzyme to cellulose microfibril.

(2) Upon ozonization after steaming, the enzymatic susceptibility of the softwood (Sugi; *Cryptomeria japonica* D. Don) increased up to 67%. The susceptibility of wood meal was less than 3% for steaming, and 46% for ozonization. The solubility of hemicellulose and the cracks owing to steaming followed by fiberization resulted in the generation of the porous structure facilitating the penetration of ozone into the cell wall. When the

ozone-treated samples were subjected to enzymatic hydrolysis, a white material appeared as a hydrolysis residue, which was quite free from lignin and was identified as cellulose I. The white material might be formed by compact aggregation of the cellulose microfibrils in the cell wall as a result of removal of lignin and hemicelluloses during ozone treatment and steaming. The aggregation slowed down the enzymatic attack to the cellulose microfibrils.

(3) Avicel, cotton linter pulp, and *Halocynthia* sp. cellulose, (cotton-ramie type cellulose, rich in cellulose I β) were hydrolyzed extensively with a cellulase preparation from *T. viride* either using a large quantity of enzyme or treating it over a long period of time. TEM observation showed that the particles in the hydrolysis residue of Avicel were composed of tightly packed microfibrils. The microfibrils were thin, less than 20 μm in length, and partly fibrillated. The results from electron and X-ray diffraction analyses indicated that the residual Avicel consisted of highly ordered molecular chains of cellulose microfibrils. The residual *Halocynthia* cellulose microfibrils were also observed to become thinner in the ends or to be split to the subfibrils from the ends. The cellulose microfibrils were degraded little by little from the ends of the highly ordered microcrystal with cellulase. The enzymatic degradation was accompanied with fibrillation on the surface of the microcrystals in Avicel and with the formation of the subfibrils in *Halocynthia* cellulose. Their modes of degradation was explained from the size and packing of the microfibrils.

(4) The algal-bacterial type cellulose (rich in cellulose I α) and the cotton-ramie type cellulose (dominant in cellulose I β), were degraded completely by *T. viride* cellulase. The algal-bacterial type cellulose microfibril was more susceptible than the cotton-ramie type. The residue from the algal-bacterial type cellulose became enriched in cellulose I β component by the

cellulase hydrolysis. These results indicate that the cellulose I_{α} component in the microfibril of the algal-bacterial type cellulose is preferentially hydrolyzed by the cellulase.

(5) In cellulose crystallite (CC) of *Cladophora* sp., the algal-bacterial type, the cellulose I_{α} crystal component was more selectively degraded with *T. viride* cellulase than the cellulose I_{β} crystal component. The shortened CC was observed frequently in the residue of *Cladophora* CC. Some fibrillation was also observed in the *Halocynthia* CC and repeatedly hydrolyzed *Cladophora* CC residues which comprised exclusively cellulose I_{β} . These results suggest the difference of the supermolecular structure between both CCs.

(6) The short microcrystals observed in the enzymatic hydrolysis residue of *Cladophora* CC had almost the same length of approximately 300-400 nm. The results from electron diffraction and FTIR analyses suggested the existence of highly ordered crystalline domain, which contained mainly cellulose I_{β} , with a certain domain size of not less than 300-400 nm in the *Cladophora* cellulose microfibrils. In addition, the short microcrystals was found to be composed of cellulose molecules with a DPw (average degree of polymerization) of 690 which corresponds to 345 nm in molecular chain length. This agreement of the longitudinal length between the microcrystals and the molecular chain contained indicates that all molecular chains are straight and parallel to the longitudinal direction from the head to the tail of the I_{β} crystalline domain.

(7) *Halocynthia* cellulose and its cellulose crystallite (CC) was hydrolyzed with a crude *T. viride* cellulase or its CBH I. The residual cellulose microfibrils became thinner and partly fibrillated. Twisting of the microfibrils were also observed. From the measurement of the length for the fibrillated regions, the length dispersion was about 1.2 which was

considered as mono-disperse, and the helical repeat distance was about 700 nm on average. These results suggest that the intact cellulose microfibrils of *Halocynthia* sp. contain the helical structure in nature and the helical repeat distance might be double the domain size of the I β crystalline phase. The cellulose I β domain has been accepted to be only a single phase by the diffraction contrast and lattice imaging of the *Halocynthia* cellulose microfibril. The untreated CC was not fibrillated. However, the residual CC after the enzymatic hydrolysis was partly fibrillated and the crystallinity index of the residual CC became slightly higher than the untreated one. These facts suggest that the cellulose I β domain of the *Halocynthia* CC is not a single phase but contains several subfibrils.

The circumstances of cellulose microfibrils

In the cell wall

in wood

→ encrusting with lignin

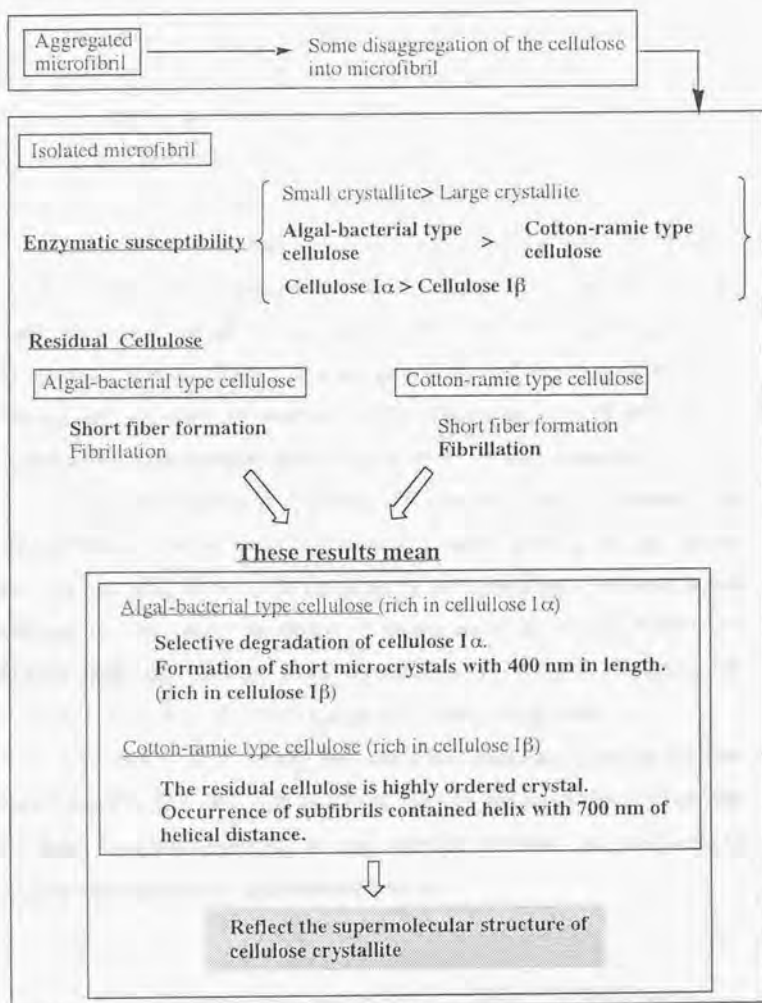
in *Valonia*, *Cladophora*, cotton,
Halocynthia and so on

→ aggregated

After chemical processing
(steaming and ozonization)

→ tightly aggregated after the treatment

After enzymatic treatment



Acknowledgment

This study has been carried out at Forestry and Forest Products Research Institute from 1986 to 1997, and at The University of Tokyo from May 1992 to February 1993. The author wishes to express her sincerest thanks to Professor Takeshi Okano, The University of Tokyo, for his kindest guidance and encouragement during the entire course of this study.

The author would like to express her sincere gratitude to Associate Professor Junji Sugiyama, Wood Research Institute, Kyoto University, who introduced her the existence of cellulose crystal component, cellulose I α /I β , and details of technique for electron diffraction, for his valuable and critical suggestions to continue this study.

The author would like to appreciate Dr. Mitsuro Ishihara, Forestry and Forest Products Research Institute, for his critical readings of the manuscripts and valuable suggestions. The author also appreciates Dr. Kazumasa Shimizu, FFPRI, for his persistent and kind encouragement. The author sincerely appreciates to Dr. Tetsuo Kondo, FFPRI, for his continuous encouragement and valuable criticism and discussion.

The author thanks Drs. Masahisa Wada and Hideki Shibazaki, The University of Tokyo, for their kind assistance with X-ray diffraction analysis and SEC. Thanks are extended to the members of Bioconversion Laboratory, the other members of Department of Wood Processing, FFPRI, and the members of Laboratory of Wood Physics, The University of Tokyo, for their kindness and encouragement.

The author also thanks the late Prof. Emeritus Hiroshi Harada, Prof. Emeritus Hiroshi Saiki and Prof. Minoru Fujita, Kyoto University, for their excellent guidance in the study of wooden cell wall and its components, especially cellulose microfibril.

Last but not least, the author sincerely thanks her parents, Yasuko and Wataru Araki, her children, Masayuki and Madoka Hayashi, and her husband, Tatsuyuki Hayashi, for their support and encouragement to continue this study.

REFERENCES

- Abuja, P.M., Pilz, I., Claeysens M., and Tomme, P., *Biochemical Biophysical Res. Comms.*, 156 (1988a) 180-185.
- Abuja, P.M., Schmuck, M., Pilz, I., Tomme, P., Claeysens, M., and Esterbauer, H., *European Biophysical J.*, 15 (1988b) 339-342.
- Akishima, Y., Isogai, A., Kuga, S., Onabe, F., and Usuda, M., *Carbohydrate Polymers*, 19 (1992) 11-15.
- Araki, N., Fujita, M., Saiki, H., and Harada, H., *Mokuzai Gakkaishi*, 28 (1982) 267-273.
- Araki, N., Fujita, M., Saiki, H., and Harada, H., *Mokuzai Gakkaishi*, 29 (1983) 491-499.
- Atalla R.H., and VanderHart, D.L., *Science*, 223 (1984) 283-285.
- Atalla, R.H., and Whitmore, R.E., *Biopolymers*, 24 (1985) 421-423.
- Atalla, R.H., and Vanderhart, D.L., in C.Schuerch (ed.), "*Cellulose and Wood-Chemistry and Technology*", John Wiley & Sons, Inc., 1989, pp. 169-188.
- Balashov, V., and Preston, R.D., *Nature*, 176 (1955) 64.
- Battista, O.A., *Ind. Eng. Chem.*, 42 (1950) 502-507.
- Beldman, G., Voragen, A.G.J., Rombouts, F.M., Searle-van Leewen, M.F., and Pilnik, W., *Biotech.Bioeng.*, 30 (1987) 251-257.
- Belton, P.S., Tanner, S.F., Cartier N., and Chanzy, H., *Macromolecules*, 22 (1989) 1615-1617.

- Betrabet, S.M., Khandeparker, V.G., and Patil, N.B., *Cellulose Chem. Technol.*, 8 (1974) 339-344.
- Betrabet, S.M., and Paralikar, K.M., *Cellulose Chem. Technol.*, 11 (1977) 615-625.
- Betrabet, S.M., and Paralikar, K.M., *Cellulose Chem. Technol.*, 12 (1978) 241-252.
- Bhikhabai, R., and Petterson, G., *Biochem. J.*, 22 (1984) 729-736.
- Blackwell, J., and Kolpak, F.J., *Macromolecules*, 8 (1975) 322-326.
- Blackwell, J., and Kolpak, F.J., *Appl. Polymer Symposium*, 28 (1976) 751-761.
- Bourret, A., Chanzy, H., and Lazaro, R., *Biopolymers*, 11 (1972) 893-898.
- Bragg, W.L., *Proc. Cambridge Phil. Soc.*, 17 (1913) 43.
- Brown Jr., R.M., Haigler, C.H., Suttie, J., White, A.R., Roberts, E., Smith, C., Itoh, T., and Cooper, K., *J. Appl. Polym. Sci. Appl. Polym. Sympos.*, 37 (1983) 33-78.
- Caufield, D.F., and Moore, W.E., *Wood Sci.*, 6 (1974) 375-379.
- Chanzy H., and Henrissat, B., *Carbohydrate Polymers*, 3 (1983a) 161-173.
- Chanzy, H., Henrissat, B., Vuong, R., and Schlein, M., *FEBS Lett.*, 153 (1983b) 113-118.
- Chanzy, H., Henrissat B., and Vuong, R., *FEBS Lett.*, 172 (1984) 193-197.
- Chanzy, H., Henrissat, B., and Vuong, R., *FEBS Lett.*, 184 (1985) 285-288.
- Converse, A.O., in Saddler J.N., (Ed.) "*Bioconversion of Forest and Agricultural Plant Residues*", C.A.B. International '93, 1993, pp. 93-106.

- Coughlan, M.P., *Biotech. Genetic Enz. Rev.*, 3 (1985) 39-109.
- Cowling, E.B., and Kirk, T.K., *Biotechnol. Bioeng. Symp.*, 6 (1976) 95-123.
- Din, N., Gilkes, N.R., Tekant, B., Miller Jr., R.C., Warren, R.A.J., and Kilburn, D.G., *Bio/Technology*, 9 (1991) 1096-1099.
- Divne, C., Ståhlberg, J., Reinikainen, T., Ruohonen, L., Pettersson, G., Knowles, J. K. C., Teeri T.T., and Jones, A., *Science*, 265 (1994) 524-528.
- Enari, T.-M. and Niku-Paavola, M.-J., *CRC Crit. Rev. Biotechnol.*, 5 (1987) 67-87.
- Eveleigh, D.E., in A.L.Demain and N. Solomon (eds.), "*Trichoderma In the Biology of Industrial Microorganisms*," Benjamin/Cummings Publishing Co., MenloPark, CA, USA, 1985, pp. 487-509.
- Fan, L.T., Lee, Y.H., and Beardmore, D.H., *Biotechnol. Bioeng.*, 22 (1980) 117-119.
- Fink, H.-P., Phillipp, B., Zschunke, C., and Hayn, M., *Acta Polym.*, 43 (1992) 270-274.
- Frey-Wyssling, A., *Science*, 119 (1954) 80-82
- Fujii, T., Harada, H. and Saiki, H., *Mokuzai Gakkaishi*, 27 (1981) 149-156.
- Fujii, T., Shimizu, K., Sudo, K. and Yamamoto K., *Mokuzai Gakkaishi*, 31 (1985) 366-374.
- Fujii, T., Shimizu, K., Sudo, S., Yamaguchi, A., *Mokuzai Gakkaishi*, 33 (1987) 400-407.
- Fujita, M., Saiki, H., Sakamoto, J., Araki N., and Harada, H., *Bull. Kyoto Univ. Forests*, 51 (1979) 247-256

Fujita, M., Hayashi, N., Hamada, K. and Harada, H., *Bull. Kyoto Univ. For.*, 59 (1987) 248-257.

Gardner, K.H., and Blackwell, J., *Biopolymers*, 13 (1974) 1975-2001.

Gilkes, N.R., Henrissat, B., Kilburn, D.G., Miller R.C., and Warren, R.A.J., *Microbiol. Revs.* 55 (1991) 303-315.

Gilkes, N.R., Jervis, E., Henrissat, B., Tekant, B., Miller Jr., R.C., Warren, R.A.J., and Kilburn, D.G., *J. Biol. Chem.*, 267 (1992) 6743-6749.

Gilkes, N.R., Chanzy, H., Kilburn, D.G., Miller Jr., R. C., Sugiyama, J., Warren, R.A.J., and Henrissat, B., *Int. J. Biol.Macromol.*, 15 (1993) 347-351.

Goyal, A., Ghosh, B., and Eveleigh, D., *Bioresource Technol.*, 36 (1991) 37-50.

Hackney, J.M., Atalla, R.H., and VanderHart, D.L., *Int. J. Biol. Macromol.*, 16(4) (1994) 215-218.

Haigler, C.H., and Benziman, M., in R.M. Brown Jr. (ed), "*Cellulose and Other Polymer Systems*", Plenum, 1982, pp. 273-296.

Haigler, C.H., in T.P. Nevell and S. H. Zeronian (eds.), "*Cellulose Chemistry and Its Applications*", Ellis Horwood Ltd., 1985, pp. 30-83.

Halliwell, G., *Biochem. J.*, 100 (1966) 315-320.

Halliwell, G., and Riaz, M., *Biochem.J.*, 116 (1970) 35-42.

Harada, H., and Goto, T., in R.M. Brown Jr. (ed.) "*Cellulose and Other Natural Polymer Systems*", Plenum, 1982, pp.383-401.

Hayashi N., Shimizu, K., and Hosoya, S., *Mokuzai Gakkaishi*, 35 (1989) 521-529.

- Hayashi, N., Ishihara, M., Shimizu, K., Sugiyama, J., and Okano, T., *Preprints of 94 Cellulose R & D* (1994) 101-106.
- Hayashi, N., Ishihara, M., and Shimizu, K., *Mokuzai Gakkaishi*, 41 (1995) 1132-1138; *Chem. Abstr.*, 124 (1996) 205311c.
- Henrissat B., and Chanzy, H., in R.A. Young and R.M. Rowell (eds.) "*Cellulose Structure, Modification and Hydrolysis*", 1986, pp. 337-347.
- Henrissat, B., Vigny, B., Buleon, A., and Perez, S., *FEBS Lett.*, 231 (1988) 177-182.
- Henrissat, B., Claeysens, M., Tomme, P., Lemsele, L., and Mornon, J. P., *Gene*, 81 (1989) 83-95.
- Henrissat, B., in "*Progress in Biotechnology, Vol. 7*" J. Visser, G. Beldman, M. A. Kusters-von Someren and A. G. J. Voragen (eds.), Amsterdam, Elsevier, (1992) pp. 97-110.
- Henrissat, B., and Bairoch, A., *Biochemical J.*, 293 (1993) 781-788.
- Henrissat, B., *Cellulose*, 1 (1994) 169-196.
- Hermans P.H., and Weidinger, A., *J. Polymer Sci.*, 4 (1949) 317-322.
- Hess, K., in "*Die Chemie der Zellulose and Ihrer Begleiter*" Akad. Verlagsges., Leipzig, 1928. in ref. "*The Polysaccharides vol. 2.*" ed. by G.O. Aspinnall.
- Heyn, A.N., *J. Cell Biol.*, 29 (1966) 191-197.
- Heyn, A.N., *J. Ultrastruct. Res.*, 26 (1969) 52.
- Honda, S., Takahashi, M., Nishimura, Y., Kakehi, and K., Ganno, S., *Anal. Biochem.*, 118 (1981) 162-167.

- Horii, F., Hirai A., and Kitamaru, R., *Macromolecules*, 20 (1987a) 2117-2120.
- Horii, F., Yamamoto, H., Kitamaru, R., Tanahashi, M., and Higuchi, T., *Macromolecules*, 20 (1987b) 2946-2949.
- Horii, F., in Pfeffer P.E., and Gerasimowicz W.V., (Eds.) "*Nuclear Magnetic Resonance in Agriculture*", CRC Press (1989) pp. 311-335.
- Horii, F., *Kagaku to Seibutu*, 32 (1994) 361-365.
- Hoshino, E., Sasaki, Y., Okazaki, M., Nishizawa, K., and Kanda, T., *J. Biochem.*, 114 (1993) 230-235.
- Hosoya, S., *Jpn TAPPI Journal*, 60 (1985) 1-9.
- Johansson, G., Ståhlberg, J., Lindeberg, G., Engstöm, Å., and Pettersson, G., *FEBS Lett.*, 243 (1989) 389-393.
- Joseleau, and J.- P., Martini, E., *Cellulose Chem. Technol.*, 15 (1981) 473-478.
- Kai, A., and Xu, P., *Polymer Journal*, 22(1990) 955-961.
- Kanda, T., Amano, Y., Shiroishi, M., and Hoshino, E., *Oyo Toshitsu kogaku*, 41 (1994) 273-282.
- Kaneko, H., Hosoya, S., Nakano, J., *Mokuzai Gakkaishi*, 25 (1979) 503-509.
- Kaneko, H., Hosoya, S., Nakano, J., *Mokuzai Gakkaishi*, 26 (1980) 752-758.
- Kaneko, H., Hosoya, S., Nakano, J., *Mokuzai Gakkaishi*, 27 (1981) 678-683.
- Kaneko, H., Hosoya, Iiyama, K., *J. Wood Chem. Technol.* 3 (1983) 399-411.
- Kerr, A.J. and Goring, D.A.I., *Cellulose Chem. Technol.*, 9 (1975) 563-573.
- Kim, Y.S., and Newman, R.H., *Holzforschung*, 49 (1994) 109-114.

- King, K.W., *Biochem. Biophys. Res. Comms.*, 24 (1966) 295-298.
- King, K.W., and Lee, T.H., *Arch. Biochem. Biophys.*, 120 (1967) 462.
- von Knolle H., and Jayme, G., *Das Papier*, 19(3) (1965) 106-111.
- Knowles, J., Lehtovaara, P., and Teeri, T.T., *Trends Biotechnol.*, 5 (1987) 255-261.
- Kraulis, P.J., Clore, G.M., Nilges, M., Jones, T.A., Pettersson, G., Knowles, J.K.C., and Gronenborn, A. M., *Biochemistry*, 28 (1989) 7241-7257.
- Kuga, S., and Brown, M.R., *Polymer Comm.*, 28 (1987) 311-314.
- Lee, J. H., M. Brown, R., Kuga, S., Shoda, S., and Kobayashi, S., *Proc. Natl. Acad. Sci. USA*, 91 (1994) 7425-8429.
- Liang C. Y., and Marchessault, R. H., *J. Polym. Sci.*, 39 (1959) 269-278.
- Linder, M., Mattinen, M.-T., Kontteli, M., Lindeverg, G., Ståhlberg, J., Drakenberg, T., Reinikainen, T., Pettersson, G., Annala, A., *Protein Science*, 4 (1995) 1056-1064.
- Marsh, P.B., Merola, G.V., and Simpson, M.E., *Text. Res. J.*, 23 (1953) 831-; 27 (1957) 913-916.
- Marsh, P.B., *Text. Res. J.*, 28 (1957) 913-916.
- Marrinan, J., and Mann, J., *J. Polym. Sci.*, 21 (1956) 301-311.
- Matsumura, Y., Sudo, K., and Shimizu, K., *Mokuzai Gakkaishi*, 11 (1977) 562-570.
- Michell, A. J., *Carbohydr. Res.*, 173 (1988) 185-195.
- Michell, A.J., *Carbohydr. Res.*, 197 (1990) 53-60.

Mizumoto, and K., Shimizu, K., *Abst. 36th Con. Jpn Wood Res. Soc.*, April, (1986) 215.

Neely, W. C., *Biotechnol. Bioeng.*, 26 (1984) 59-64.

O'Connor, R.T., DuPré, E.F., and Mitcham, D., *Textile Res. J.*, 28, (1958) 382-392.

Osawa, Z., Ervy, W. A., Sarkarnen, K. V., Carpenter, E., and Schurch, C., *Tappi*, 46 (1963) 84-88.

Pan, G., Chen, H. C. H., Chang, M., and Gratzl, J. S., *Ekman-Days 1981*, 2 (1981) 132.

Puri, V. P., *Biotechnol. Letters*, 5 (1983) 733-776.

Puri, S. C., and Anand, S. M., *Cellulose Chem. Technol.*, 20 (1986) 535-540.

Rånby, B.G., and Ribí, E., *Experimantia*, 6 (1950) 12.

Reese, E.T., Siu, R.G., and Levinson, H.S., *J. Bacteriol.*, 9 (1950) 485-497.

Reese E.T., and Gilligan, W., *Tex. Res. J.*, 24 (1954) 663-669.

Revol, J.-F., Bradford, H., Giasson, J., Marchessault, R.H., and Gray, D.G., *Int. J. Biol. Macromol.*, 14 (1992) 170-172.

Rivers, D.B., and Emert, G.H., *Biotechnol. Bioeng.*, 31 (1988) 278-281.

Rouvinene, J., Bergfors, T., Teere, T., Knowles, J.K.C., and Jones, T.A., *Science*, 249 (1990) 380-386.

Rowland, S. P., and Howley, P. S., *Text. Res. J.*, 58 (1988) 96-101.

Samejima M., *Mokuzai Hozon*, 21-22 (1995) 52-60.

- Schumuck, M., Pilz, I., Hayn, M., and Esterbauer, H., *Biotechnol. Lett.*, 8 (1986) 397-402.
- Senior, D.J., and Saddler, J.N., in "*Trichoderma reesei cellulases*", eds. by C.P. Kubicek, D.E. Eveleigh, H. Esterbauer, W. Steiner and E.M. Kubicek-Pranz, The Royal Soc. Chem, (1990) pp. 47-59.
- Sherrer, D. *Göttinger Nachrichtn.*, 2 (1918) 98.
- Shevale, I.G., and Sanada, J.C., *Canadian J. Microbiol.*, 25 (1979) 773.
- Shibasaki, H., Kuga, S., Onabe F., and Brown Jr., R.M., *Polymer*, 26 (1995) 4971-4976.
- Shimizu, K., Sudo, K., Nagasawa, S., and Ishihara, M., *Mokuzai Gakkaishi*, 29 (1983) 428-437.
- Shimizu, K. and Ishihara, M., *Res. Rep. Biomass Conversion Prog.*, 21 (1990) 43-61.
- Sinitzyn, A.P., Gusakov, A.V., and Vlasenko, E.Y., *Appl. Biochem. Biotechnol.*, 30 (1991) 43-59.
- Sinner, M., Simatupang, M. M., and Dietrichs, H. H., *Wood Sci. Technol.*, 9 (1975) 307-322.
- Sprey, B., and Bochem, H.-P., *FEMS Microbiol. Lett.*, 97 (1992) 113-117.
- Ståhlberg, J., Johansson, G., and Pettersson, G., *Bio/Technology*, 9 (1991) 286-290.
- Sudo, K., Matsumira, Y., and Simizu, K., *Mokuzai Gakkaishi*, 22 (1976) 670-676.
- Sudo, K., Shimizu, K., and Sakurai, K., *Holzforschung*, 39 (1985) 281-288.

- Sudo, K., Shimizu, K., Ishii, T., Fujii, T., Nagasawa, S., *Holzforschung*, 40 (1986) 339-345.
- Sugiyama, J., Harada, H., Fujiyoshi, and Ueda, N., *Planta*, 166 (1985) 161-168.
- Sugiyama, J., Okano, T., Yamamoto H., and Horii, F., *Macromolecules*, 23 (1990) 3196-3198.
- Sugiyama, J., Persson, J., and Chanzy, H., *Macromolecules*, 24 (1991a) 2461-2466.
- Sugiyama, J., Vuong, R., and Chanzy, H., *Macromolecules*, 24 (1991b) 4168-4175.
- Sugiyama, J., *Mokuzai Gakkaishi*, 38 (1992) 723-731; *Chem. Abstr.*, 119 (1993) 30185g.
- Takabe, K., Fujita M., and Harada, H., *Mokuzai Gakkaishi*, 27 (1981a) 249-255.
- Takabe, K., Fujita, M., Harada, H. and Saiki, H., *Mokuzai Gakkaishi*, 27 (1981b) 813-820.
- Takabe, K., Fujita M., and Harada, H., *Mokuzai Gakkaishi*, 29 (1983) 183-189.
- Takabe, K., Fujita M., and Harada, H., *Mokuzai Gakkaishi*, 30 (1984) 103-109.
- Takabe, K., Fujita M., and Harada, H., *Mokuzai Gakkaishi*, 32 (1986a) 763-769.
- Takabe, K., Fujita, M., Harada, H. and Saiki, H., *Res. Bull. Coll. Exp. Forest Hokkaido Univ.*, 43 (1986b) 783-788.
- Takai, M., Hayashi, J., Nishizawa K., and Kanda, T., *J. Appl. Polymer Sci.: Appl. Polymer Symp.*, 37 (1983) 345-361.

Tanahashi, M., Takeda, S., Aoki, T., Goto, T., Higuchi, T., and Hanai, S., *Wood Res.*, 69 (1983) 36-51.

Teeri, T.T., Lehtovaara, P., Kauppinen, S., Salovuori, I., and Knowles, J.K.C., *Gene*, 51 (1987) 43-52.

Teeri, T.T., *Tib Tech.*, 15 (1997) 160-167.

Terashima, N., Fukushima K., and Takabe K., *Holzforschung*, 40 (1986) 101-105.

Terashima, N., in N.G. Lewis and M.G. Paice (eds.) "*Plant Cell Wall Polymers*," ACS Sym. Ser., 399, 1988, pp. 148-159.

Terashima, N., Fukushima K., Sano, Y., and Takabe, K., *Holzforschung*, 42 (1988a) 347-350.

Terashima, N.; Fukushima, K., in N.G. Lewis and M.G. Paice (eds.) "*Plant Cell Wall Polymers*," ACS Sym. Ser., 399, 1988b, pp.160-168.

van Tilbeurgh, H., Tomme, P., Claeysens, M., Bhikhabhai, R., and Pettersson, G., *FEBS Lett.*, 204 (1986) 223-227.

Tomme, P., van Tilbeurgh, H., Pettersson, G., van Danne, J., Vandekerckhove, J., Teeri, T., and Claeysens, M., *European J. Biochem.*, 170 (1988) 575-581.

Tsekos, I., *Protoplasma*, 193 (1996) 10-32.

Uemura, S., Ishihara, M., Jellison, J., *Appl. Microbiol. Biotechnol.*, 39 (1993) 788-794.

Uhlir, K.I., Atalla, R.H., and Thompson, N.S., *Cellulose*, 2 (1995) 129-144.

Vaheri, M., Leisola, M., and Kauppinen, V., *Biotech. Lett.*, 1 (1979) 41.

- VanderHart D.L., and Atalla, R.H., *Macromolecules*, 17 (1984) 1472-1479.
- Verlhac, C., Dedier, J., and Chanzy, H., *J. Polym. Sci.:Part A*, 28 (1990) 1171-1177.
- Wada, M., Sugiyama, J., and Okano, T., *J. Appl. Polym. Sci.*, 49 (1993) 1491-1496.
- Wada, M., Sugiyama, J., and Okano, T., *Mokuzai Gakkaishi*, 40 (1994) 50-56; *Chem. Abstr.*, 123 (1995) 138855x.
- Wada, M., Sugiyama, J., and Okano, T., *Mokuzai Gakkaishi*, 41 (1995) 186-192; *Chem. Abstr.*, 123 (1995) 138855x.
- Walker L.P., and Wilson, D.B., *Bioresource and Technol.*, 36 (1991) 3-14.
- Wardrop, A. B., and Jutte, S. M., *Wood Sci. Technol.*, 2 (1968) 105-114.
- White, A.R., and Brown Jr., R. M., *Proc. Natl. Acad. Sci. USA*, 78 (1981) 1047-1051.
- White A.R., in R. M. Brown ed. "*Cellulose and Other Natural Polymer Systems*", Plenum, New York, 1982, pp. 489-509.
- Wiley, J.H., and Atalla, R.H., *Carbohydr. Res.*, 160 (1987) 113-129.
- Wiley, J.H., and Atalla, R.H., in R.H Atalla (ed) "*The Structures of Cellulose*", *ACS Symposium Series 340*, 1987, 152-168.
- Wood, T.M., and McCrae, S.I., *Biochemical J.*, 128 (1972) 1183-1192.
- Wood, T.C., and McCrae, S.I., *Adv. Chem. Ser.*, 181 (1979) 181-209.
- Wood, T.M., in M.P. Coughlan ed. "*Enzyme Systems for Lignocellulose Degradation*", 1989, 19-35.

Woodcock, S., Henrissat, B., and Sugiyama, J., *Biopolymers*, 36 (1995) 201-210.

Yachi, T., Hayashi, J., Takai, M., and Shimizu, Y., *J. Appl. Pol. Sci.; Appl. Polym. Symp.*, 37 (1983) 325-343.

Yamamoto, H., Horii, F., and Odani, H., *Macromolecules*, 22 (1989) 4132-4134.

Yamamoto H., and Horii, F., *Macromolecules*, 26 (1993) 1313-1317.

Yamamoto, H., Hirai, R., and Horii, F., *Proc. of '94 Cellulose R & D*, (1994) 43-44.

公表論文

- (1) 平成元年6月 木材学会誌 35(6), 521-529(1989)
Pretreatment of ozone for increasing the enzymatic susceptibility of autohydrolyzed softwoods
(志水一允、細谷修二と共著)
- (2) 平成5年5月 木材学会誌 39(5), 503-508(1993)
Enzymatic degradation of cell walls in the xylem developing zone
(藤井智之、志水一允と共著)
- (3) 平成7年12月 木材学会誌 41(12), 1132-1138 (1995)
高結晶性天然セルロースの酵素加水分解残渣の特徴
(石原光朗、志水一允と共著)
- (4) 平成10年 Carbohydrate Research 305(2), 216-269 (1997)
The enzymatic susceptibility of cellulose microfibrils of the algal-bacterial type and the cotton-ramie type
(杉山淳司、岡野 健、石原光朗と共著)
- (5) 平成10年 Carbohydrate Research 305(1), 109-116 (1997)
Selective degradation of cellulose I_α component in *Cladophora* cellulose with *Trichoderma viride* cellulase
(杉山淳司、岡野 健、石原光朗と共著)

